NASA/TM-2010-216127

Effects of Changing Center of Gravity on Shirtsleeve Human Performance in Reduced Gravity

Jason R. Norcross[1], Kurt G. Clowers[2], Tim Clark[2], Matthew S. Cowley[3], Lauren Harvill[3], Steven P. Chappell[1], Leah C. Stroud[4], Lena Desantis[3], William H. Paloski[5], Richard M. Morency[6], Jessica R. Vos[6], Michael L. Gernhardt[6]

[1]*Wyle Integrated Science & Engineering Group, Houston*
[2]*MEI Technologies, Inc., Houston*
[3]*Lockheed Martin, Houston*
[4]*Rice University, Houston*
[5]*University of Houston, Houston*
[6]*NASA Johnson Space Center, Houston*

National Aeronautics and
Space Administration

Johnson Space Center
Houston, TX 77058

July 2010

THE NASA STI PROGRAM OFFICE . . . IN PROFILE

Since its founding, NASA has been dedicated to the advancement of aeronautics and space science. The NASA Scientific and Technical Information (STI) Program Office plays a key part in helping NASA maintain this important role.

The NASA STI Program Office is operated by Langley Research Center, the lead center for NASA's scientific and technical information. The NASA STI Program Office provides access to the NASA STI Database, the largest collection of aeronautical and space science STI in the world. The Program Office is also NASA's institutional mechanism for disseminating the results of its research and development activities. These results are published by NASA in the NASA STI Report Series, which includes the following report types:

- TECHNICAL PUBLICATION. Reports of completed research or a major significant phase of research that present the results of NASA programs and include extensive data or theoretical analysis. Includes compilations of significant scientific and technical data and information deemed to be of continuing reference value. NASA's counterpart of peer-reviewed formal professional papers but has less stringent limitations on manuscript length and extent of graphic presentations.
- TECHNICAL MEMORANDUM. Scientific and technical findings that are preliminary or of specialized interest, eg, quick release reports, working papers, and bibliographies that contain minimal annotation. Does not contain extensive analysis.
- CONTRACTOR REPORT. Scientific and technical findings by NASA-sponsored contractors and grantees.
- CONFERENCE PUBLICATION. Collected papers from scientific and technical conferences, symposia, seminars, or other meetings sponsored or cosponsored by NASA.
- SPECIAL PUBLICATION. Scientific, technical, or historical information from NASA programs, projects, and mission, often concerned with subjects having substantial public interest.
- TECHNICAL TRANSLATION. English-language translations of foreign scientific and technical material pertinent to NASA's mission.

Specialized services that complement the STI Program Office's diverse offerings include creating custom thesauri, building customized databases, organizing and publishing research results . . . even providing videos.

For more information about the NASA STI Program Office, see the following:

- Access the NASA STI Program Home Page at http://www.sti.nasa.gov
- E-mail your question via the Internet to help@sti.nasa.gov
- Fax your question to the NASA Access Help Desk at (301) 621-0134
- Telephone the NASA Access Help Desk at (301) 621-0390
- Write to:
  NASA Access Help Desk
  NASA Center for AeroSpace Information
  7115 Standard
  Hanover, MD 21076-1320

NASA/TM-2010-216127

Effects of Changing Center of Gravity on Shirtsleeve Human Performance in Reduced Gravity

Jason R. Norcross[1], Kurt G. Clowers[2], Tim Clark[2], Matthew S. Cowley[3], Lauren Harvill[3], Steven P. Chappell[1], Leah C. Stroud[4], Lena Desantis[3], William H. Paloski[5], Richard M. Morency[6], Jessica R. Vos[6], Michael L. Gernhardt[6]

[1]*Wyle Integrated Science & Engineering Group, Houston*
[2]*MEI Technologies, Inc., Houston*
[3]*Lockheed Martin, Houston*
[4]*Rice University, Houston*
[5]*University of Houston, Houston*
[6]*NASA Johnson Space Center, Houston*

National Aeronautics and
Space Administration

Johnson Space Center
Houston, TX 77058

July 2010

Available from:

NASA Center for AeroSpace Information
7115 Standard Drive
Hanover, MD 21076-1320
301-621-0390

National Technical Information Service
5285 Port Royal Road
Springfield, VA 22161
703-605-6000

This report is also available in electronic form at http://ston.jsc.nasa.gov/collections/TRS/

Prepared by:

Jason Norcross (Wyle), Project Science Coordinator
EVA Physiology, Systems and Performance Project

2/11/10
Date

Technical Review by:

Kurt Clowers, Ph.D. (MEI Technologies), Lead Engineer
Anthropometry and Biomechanics Facility

2/11/10
Date

Lena Desantis (Lockheed-Martin), Senior Human Factors Design Engineer
Usability Testing and Analysis Facility

2/11/10
Date

John De Witt, Ph.D. (Wyle), Lead Biomechanist
Exercise Physiology and Countermeasures Project

2/11/10
Date

Heather Paul (NASA), Ventilation Subsystem Lead
Constellation Space Suit Element Portable Life Support Systems

2/19/10
Date

Jessica Vos (NASA), Integrated Test Lead
Constellation EVA Systems Project Office

2/22/10
Date

Approved by:

Michael Gernhardt, Ph.D. (NASA), Principal Investigator
EVA Physiology, Systems and Performance Project

2/12/10
Date

Richard Morency (NASA), Technical Monitor
Anthropometry and Biomechanics Facility

2/16/10
Date

Jeff Patrick (NASA), Testing and Facilities Manager
Constellation EVA Systems Project Office

4/21/10
Date

Contents

1	Executive Summary	1
2	Introduction	1
2.1	Test Objectives	2
3	Methods	2
3.1	Subjects	2
3.2	Hardware	4
3.2.1	Partial-gravity simulator (POGO)	4
3.2.2	Gimbal support structure with adjustable center-of-gravity rig	4
3.2.3	VacuMed oversized treadmill	6
3.2.4	PRO Balance Master®	6
3.3	Testing Configurations	7
3.3.1	Center-of-gravity locations	7
3.3.2	Offload profiles	10
3.3.3	Test configurations	10
3.5	Test Protocols	11
3.5.1	Level ambulation	11
3.5.2	Graded ambulation	11
3.5.3	Exploration tasks	11
3.5.4	Postural stability	12
3.6	Metabolic Data Collection and Analysis	12
3.7	Biomechanical Collection and Analysis	12
3.8	Subjective Data Collection and Analysis	14
3.9	Postural Stability Data Collection and Analysis	15
3.10	Imaging	15
4	Results and Discussion	15
4.1	Center-of-gravity Locations	15
4.2	Level Ambulation	17
4.2.1	Metabolic results and discussion	17
4.2.2	Biomechanics results and discussion	20
4.2.2.1	Kinetics	20
4.2.2.2	Temporal-spatial Characteristics	24
4.2.2.3	Electromyography	34
4.2.2.4	Subjective Results and Discussion	35
4.2.2.5	Rating of Perceived Exertion	35
4.2.2.6	Gravity Compensation and Performance Scale	36
4.2.2.7	Subjective Rating Changes from 30 to 150 Seconds	37
4.3	Graded Ambulation	37
4.3.1	Metabolic results and discussion	37
4.3.2	Biomechanics results and discussion	39
4.3.2.1	Kinetics	39
4.3.2.2	Temporal-spatial Characteristics	40
4.3.2.3	Kinematics	43
4.3.2.4	Electromyography	47
4.3.2.5	Subjective Results and Discussion	48

4.3.2.6 Subjective Rating Changes from 30 Seconds to 3 Minutes 50
4.4 Exploration Tasks 50
4.4.1 Biomechanics results and discussion 50
4.4.1.1 Strategy 50
4.4.1.2 Stability 56
4.4.1.3 Subjective Results and Discussion 63
4.5 Postural Stability Results and Discussion 64
4.5.1 Subject weight 64
4.5.2 Quiet stance performance 65
4.5.3 Response to postural perturbations 69
4.5.4 Subjective ratings 71

5 Discussion and General Conclusions 73
5.1 Level and Graded Ambulation 73
5.1.1 Metabolic rate 73
5.2.2 Kinetics 73
5.2.3 Temporal-spatial characteristics 76
5.2.4 Kinematics 76
5.2.4.1 Speed vs. Center-of-gravity Condition and Offloading Mechanics 76
5.2.4.2 Incline vs. Center-of-gravity Condition 78
5.2.5 Electromyography 78
5.2.6 Subjective ratings 79
5.3 Exploration Tasks 80
5.3.1 Strategy 80
5.3.2 Stability 81
5.3.3 Subjective ratings 82
5.4 Postural Stability 82
5.5 Study Limitations 83
5.6 Lessons Learned 84

6 Summary 85
6.1 Metabolic Rate 85
6.2 Biomechanics 85
6.3 Subjective Ratings 85
6.4 Postural Control 86

7 Works Cited 86

Appendix A: Biomechanics Definitions and Reference Frames 90

Appendix B: Subjective Ratings Scales 92
B.1 Gravity Compensation and Performance Scale 92
B.2 Borg Rating of Perceived Exertion Scale (RPE) 92
B.3 Corlett and Bishop Discomfort Scale 93
B.4 Bedford Thermal Scale 93
B.5 Thermal Preference 93

Appendix C: Treadmill Relative Velocity 94

Appendix D: List of Variables for Common Equations and Relationships 95
D.1 Linear Motion 95

D.2 Rotational Motion 95

Appendix E: Additional Electromyography Graphs 97
E.1 Changing Speed Conditions 97
E.2 Changing Incline Conditions 100

Appendix F: Test Termination Criteria 103
F.1 Test Termination Criteria for All Submaximal Testing 103
F.2 Test Termination Criteria for Postural Stability 103

Appendix G: Integrated Suit Test-3 Conductor Checklist 104
G.1 Constellation Program Extravehicular Activity Systems Test 3 – Shirtsleeve Test Session 1 Checklist 104
G.2 Constellation Program Extravehicular Activity Systems Test 3 – Shirtsleeve Test Session 2 Checklist 109
G.3 Constellation Program Extravehicular Activity Systems Test 3 – Postural Stability and Exploration Task Checklist 113

Figures

1 Subject population distribution for stature (cm) against the HSIR database 3
2 Subject population distribution for body mass (kg) against the HSIR database 3
3 Shirtsleeve harness (Amspec no. JV0100P) showing additional modifications to the leg straps 4
4 Gimbal support structure with adjustable CG rig (offset view) 5
5 Stinger interface to gimbal support structure and adjustable CG rig 5
6 CG rig adjustments for subject comfort and controllability 6
7 PRO Balance Master® system 7
8 Lateral view of each CG configuration 8
9 Anterior view of each CG configuration 9
10 Illustration of marker placements for the unsuited subject. The markers in orange were only used for a static recording and were removed before the trial began 13
11 Illustration of marker placements for the gimbal support structure and CG Rig 13
12 Individual subject differences in how the system CG varied from the subject CG 16
13 System CG relation to the gimbal axes of rotation for each individual subject 17
14 Metabolic rate for different CG conditions during shirt-sleeved ambulation on a level treadmill 18
15 Metabolic rate for different CG conditions during shirt-sleeved ambulation on a level treadmill 19
16 Individual metabolic rate responses to increasing speed on a level treadmill in 1-g and for different CG conditions during shirt-sleeved ambulation on a level treadmill at 1/6-g 19
17 Mean peak vertical GRF, normalized to subjects' 1-g body weight, for shirt-sleeved ambulation on a level treadmill at different speeds. All varied CG conditions were performed at simulated lunar gravity 20
18 CG excursion range (pelvis centroid) among conditions with respect to speed 21
19 The change in CG excursion range of the CG rig conditions compared to the unsuited 1-g condition with respect to speed 22
20 Sample of the vertical motions of the pelvis, taken at its centroid, as compared to the vertical motion of the center of the CG rig. (NOTE: The CG rig data points are shifted vertically by a static offset for graphing purposes.) 23
21 Plot of the CG rig (red) with a 6^{th}-order polynomial fit (black) showing the slower system oscillation during 36 s of ambulation 23
22 Mean stance time in seconds for shirt-sleeved ambulation on a level treadmill at different speeds. All varied CG conditions were performed at simulated lunar gravity 24
23 Percentage difference for stance time between varying CG conditions and the 1-g, no-rig condition as a function of speed 25
24 Mean step width for shirt-sleeved ambulation on a level treadmill at different speeds. All varied CG conditions were performed at simulated lunar gravity 26
25 Percentage difference in step width at different speeds between varying CG conditions at 1/6-g and the 1-g, no-rig condition 26
26 Change in step width among varying CG conditions and the 1-g, no-rig condition for tested ambulation speeds 27
27 Joint angles averaged over subjects and gait cycles, categorized by CG condition, and plotted against speed. Error bars represent the standard deviation of the subject averages 28
28 Torso joint angles averaged over subjects and gait cycles, categorized by CG condition, and plotted against speed. Error bars represent the standard deviation of the subject averages 29

29 Percentage change in ROM of each CG condition from the unsuited 1-g baseline plotted against speed 29
30 Ankle joint angle traces over one gait cycle for each CG condition. Each plot is at specific speed 30
31 Knee joint angle traces over one gait cycle for each CG condition. Each plot is at specific speed 31
32 Hip joint angle traces over one gait cycle for each CG condition. Each plot is at specific speed 31
33 Torso angle traces over one gait cycle for each CG condition. Each plot is at specific speed 32
34 End contact shown unsuited (left) and on the POGO with a rig (right). Yellow lines indicate the angle of the leg with respect to vertical 33
35 Initial contact shown unsuited (left) and on the POGO with a rig (right). Yellow lines indicate the angle of the leg with respect to vertical 33
36 Initial contact and end contact on the POGO at the standard deviation condition. Yellow lines indicate the angle of the leg with respect to vertical 34
37 Erector spinae muscle activity during a gait cycle at 1.7 $m \cdot s^{-1}$. The gray shading indicates the intensity of the contraction 35
38 RPE at different CG conditions during shirt-sleeved ambulation on a level treadmill 36
39 GCPS at different CG conditions during shirt-sleeved ambulation on a level treadmill 36
40 Change in subjective ratings from the 30-s mark to the 150-s mark in a 180-s level-ambulation trial (n = 173) 37
41 Metabolic rate for different CG conditions during shirt-sleeved ambulation on an inclined treadmill 38
42 Metabolic rate for different CG conditions during shirt-sleeved ambulation on an inclined treadmill 38
43 Individual metabolic rate responses to increasing grade on treadmill at 0.8 $m \cdot s^{-1}$ in 1-g and at different CG configurations at simulated lunar gravity 39
44 Mean peak vertical GRF, normalized to subjects' 1-g body weight for shirt-sleeved ambulation on a level treadmill (0%) and at surface grades of -10%, 10%, 20%, and 30%. An ambulation speed of 0.85 $m \cdot s^{-1}$ was used across all varying surface grade conditions. All varied CG conditions were performed at simulated lunar gravity 40
45 Mean stance time for all subjects and conditions tested across surface grades of -10 decline, 0% (level), and 10%, 20%, and 30% treadmill incline 41
46 Percentage difference for stance time between varying offloaded conditions and the 1-g, no-rig condition across surface grades of -10% decline, 0% (level), and 10%, 20%, and 30% treadmill incline 41
47 Mean step width (m) for all subjects and conditions tested across surface grades of -10% decline, 0% (level), and 10%, 20%, and 30% treadmill incline 42
48 Percentage difference for step width between varying offloaded conditions and the 1-g, no-rig condition across surface grades of -10% decline, 0% (level), and 10%, 20%, and 30% treadmill incline 42
49 Joint angles averaged over subjects and gait cycles, categorized by CG condition, and plotted against incline. Error bars represent the standard deviation of the subject averages 43
50 Joint angles averaged over subjects and gait cycles, categorized by CG condition, and plotted against incline. Error bars represent the standard deviation of the subject averages 44
51 Percentage change in ROM of each CG condition from the unsuited 1-g baseline plotted against incline 44
52 Ankle joint angle traces over one gait cycle for each CG condition. Each plot is at specific incline 45

53 Knee joint angle traces over one gait cycle for each CG condition. Each plot is at specific incline 46
54 Hip joint angle traces over one gait cycle for each CG condition. Each plot is at specific incline 46
55 Torso angle traces over one gait cycle for each CG condition. Each plot is at specific incline 47
56 Erector spinae muscle activity during a gait cycle. Gray shading indicates the intensity of the contraction 48
57 RPE at different CG conditions during graded ambulation on a treadmill at 0.8 $m \cdot s^{-1}$ 49
58 GCPS at different CG conditions during graded ambulation on a treadmill at 0.8 $m \cdot s^{-1}$ 49
59 Change in subjective ratings from the 30-s mark to the 150-s mark in a 180-s graded ambulation trial (n = 114) 50
60 Hand involvement by subjects to perform the rock pickup task for all tested conditions. DNC = did not complete 51
61 Percentage of performed rock pickup trials in which subjects demonstrated either stable or unstable foot placement on the force platforms, or did not complete the task. DNC = did not complete 53
62 Percentage of kneel-and-recover trials performed in which subjects either did not complete the task, stood up from the kneeling position, or jumped up from the kneeling position. DNC = did not complete 53
63 Effect of the CG rig ("CTSD" CG configuration, on right) on subject posture at the kneeling portion of the kneel-and-recover task when compared to 1-g, no-rig controls (on left). Backward lean of the trunk caused by the CG rig, combined with the offload of the subject by the POGO system, allowed subjects to more easily jump up than stand up in certain conditions 54
64 Percentage of performed shoveling trials in which subjects demonstrated either stable or unstable foot placement on the force platforms, or did not complete the task. DNC = did not complete 55
65 Visual comparison of interaction (circled) between CG rig and POGO gimbal. On the left, the horizontal bar of the CG rig is free from contact with POGO gimbal 56
66 Example plot of rock pickup COP trajectory 57
67 Average percentage of time the COP was outside of the BOS during the rock pickup task 58
68 Number of times the COP crossed to the outside of the BOS for the rock pickup task 59
69 Average area normalized to 1-g for the rock pickup task 59
70 Average total distance the COP traveled during the rock pickup task 60
71 Average percentage of time the COP was outside of the BOS during the shoveling task 61
72 Number of times the COP crossed to the outside of the BOS for the shoveling task 62
73 Average area normalized to 1-g for the shoveling task 62
74 Average total distance COP traveled during the shoveling task 63
75 RPE for short-term exploration tasks at different gravity/CG conditions 64
76 GCPS for short-term exploration tasks at different gravity/CG conditions 64
77 Subject weights measured during SOT 1 trials for each CG/offload configuration 65
78 Effects of the six CG/offload configurations on each subject's postural stability control performance during SOT 1 (top) and SOT 4 (bottom) trials, as assessed by EQ score. The shaded region represents the normal performance range (5^{th} to 95^{th} percentile) for a large group of test subjects 66
79 Effects of the six CG/offload configurations on each subject's postural stability control performance during SOT 1 (top) and SOT 4 (bottom) trials, as assessed by TTC_{min}. Note that one subject refused to attempt the CTSD and POGO conditions owing to a perceived instability 68

80 Effects of the six CG/offload configurations on each subject's postural stability control performance during SOT 1 (top) and SOT 4 (bottom) trials, as assessed by iTTC. Note that one subject refused to attempt the CTSD and POGO conditions owing to a perceived instability 69
81 Effects of the six CG/offload configurations on each subject's postural stability control performance during sudden TU (top) and TD (bottom) trials, as assessed by TTC_{min}. Six randomized perturbation trials (three TUs, three TDs) were performed at each CG-weight configuration. All trials are displayed in the figure 70
82 Effects of the six CG/offload configurations on each subject's postural stability control performance during sudden TU (top) and TD (bottom) trials, as assessed by iTTC. Six randomized perturbation trials (three TUs, three TDs) were performed at each CG/offload configuration. All trials are displayed in the figure 71
83 RPE for postural stability tasks at different CG/offload profiles 72
84 GCPS postural stability tasks at different CG/offload profiles 72
85 Illustration of a simplified diagram of the CG rig and subject mass-spring system 73
86 Figure 86. Simulation data of the previously mentioned mass-spring system. The blue line is the displacement of a sine wave that is driving the m_1 element (subject); the red line is the resulting displacement in the m_2 element (CG rig) 75
87 Model-predicted VO_2 (red) and -observed VO_2 (blue) with respect to RPE 79

A-1 Commonly used biomechanics nomenclature of the body planes, the types of joint motion, and the body-based directions 90
A-2 Designations for the ankle joint directional rotations 90
A-3 Convention for local reference frames as prescribed by the International Society of Biomechanics and used by the ABF (4). The Y-axis usually lies along the long axis of the segment 91
A-4 Flexion is termed as the decrease in the relative angle between two segments. Flexion/dorsiflexion of a joint will always be a positive rotation in this report 91

C-1 Visual representation of trajectory motion with a stationary reference frame 94
C-2 Visual representation of a trajectory with and without a moving reference frame. The blue line represents the relative trajectory from the ballistic velocities as seen from the moving coordinate system; the black line represents the trajectory as seen by an outside observer 94

E-1 Muscle activation of the erector spinae at $0.4 \bullet m \cdot s^{-1}$ for all CG configurations and with no rig at 1-g 97
E-2 Muscle activation of the erector spinae at $0.8 \bullet m \cdot s^{-1}$ for all CG configurations and with no rig at 1-g 97
E-3 Muscle activation of the erector spinae at $1.3 \bullet m \cdot s^{-1}$ for all CG configurations and with no rig at 1-g 98
E-4 Muscle activation of the erector spinae at $1.7 \bullet m \cdot s^{-1}$ for all CG configurations and with no rig at 1-g 98
E-5 Muscle activation of the erector spinae at $2.1 \bullet m \cdot s^{-1}$ for all CG configurations and with no rig at 1-g 99
E-6 Muscle activation of the erector spinae at $2.5 \bullet m \cdot s^{-1}$ for all CG configurations and with no rig at 1-g 99
E-7 Muscle activation of the erector spinae at -10% grade for all CG configurations and with no rig at 1-g 100
E-8 Muscle activation of the erector spinae at 0% grade for all CG configurations and with no rig at 1-g 100

E-9 Muscle activation of the erector spinae at 10% grade for all CG configurations and with no rig at 1-g 101
E-10 Muscle activation of the erector spinae at 20% grade for all CG configurations and with no rig at 1-g 101
E-11 Muscle activation of the erector spinae at 30% grade for all CG configurations and with no rig at 1-g 102

Tables

1	System CG Locations	7
2	Test Configurations	10
3	Test Day and CG Condition Order	11
4	Inertial Comparison Among an Average Human Male Standing, the Human Male Torso Segment Only, and the POGO Gimbal	24
5	Upper- and Lower-extremity Coordination – Rock Pickup Task	52

Acronyms

ABF	Anthropometry and Biomechanics Facility
AMTI	Advanced Mechanical Technology, Inc.
AP	anterior-posterior
BOS	base of support
BW	body weight
CDP	computerized dynamic posturography
CG	center of gravity
CO_2	carbon dioxide
COM	center of mass
COP	center of pressure
CTSD	Crew and Thermal Systems Division
DNC	did not complete
EMG	electromyography
EPSP	excitatory postsynaptic potential
EQ	equilibrium
EVA	extravehicular activity
EXL	Exercise Physiology Laboratory
GCPS	gravity compensation and performance scale
GRF	ground reaction force
HR	heart rate
HSIR	Human Systems Integration Requirements
IST	Integrated Suit Test
iTTC	integrated time to contact
JSC	Johnson Space Center
MCT	motor control test
MK III	Mark III
MVC	maximal voluntary contraction
NBL	Neutral Buoyancy Laboratory
NEEMO	NASA Extreme Environment Mission Operations
NIRS	near-infrared reflectance spectroscopy
p-p	peak-to-peak
PLSS	Portable Life Support System
ROM	range of motion
RPE	rating of perceived exertion
SOT	Sensory Organization Test
SVMF	Space Vehicle Mockup Facility
TD	toes down
TGAW	total gravity adjusted weight
TTC	time to contact
TTC_{min}	minimum time to contact
TU	toes up
UTAF	Usability Testing and Analysis Facility
V_E	expiratory volume
VO_2	oxygen consumption

1 Executive Summary

This test was a continuation of Integrated Suit Tests (ISTs)-1 and -2 (1) (2). The main objective of the test was to investigate the effects of varying center-of-gravity (CG) locations on human performance in the suited and shirtsleeve condition; however, due to facility limitations, only the shirtsleeve condition was evaluated. Although there were different performance results among CGs, the data analysis seems to indicate that many of the observed differences may have been the result of system dynamics, hardware setup, and/or testing methodology rather than a direct result of system CG location in relation to the subjects' CG.

Three of the CG configurations unexpectedly had almost identical metabolic values. One CG configuration led to significantly greater metabolic rates than all other configurations; however, this was likely due to system configuration issues and not because it was a poor CG location. Overall, the lack of variability among the other three CG configurations indicates that either there were no notable differences in human performance among these CG configurations, or other factors may have compromised the ability to effectively vary CG using an overhead suspension lunar gravity simulator. Possible solutions to this issue include improvements to the lunar analog facility and the gimbal support structure used to interface subjects to the facility for testing.

Metabolic and subjective results among CG conditions for ambulation were very similar and led to the same conclusions. Biomechanics results were more variable in interpretation. One important finding was a high degree of variability among subjects for both the exploration tasks and the postural control test. This highlights the need to test a greater number of subjects and to thoroughly characterize the subject pool so that aspects of the subjects' anthropometry, strength, and/or fitness can be analyzed to determine whether these underlying subject characteristics significantly affected their performance.

In addition to the standard end-of-trial determination of ratings of perceived exertion (RPEs) and the gravity compensation and performance scale (GCPS), subjects also provided these ratings at the 30-s mark shortly after each trial began. Results indicated that GCPS had less variability between the 30-s and end of trial measurements, with 82% of trials showing no change compared to 68% for RPE. The majority of RPE and GCPS results that did change increased by only one unit on the rating scale (26% for RPE, 12% for GCPS). Although not conclusive, this does show promise for using both of these ratings with non-steady-state tasks and in environments that preclude direct metabolic measurement.

The Space Vehicle Mockup Facility's (SVMF's) partial-gravity simulator, known as "POGO," provides a reasonable ground-based analog for testing postural stability during reduced-gravity loading; however, its mechanical couplings limit observations to a single plane of motion (sagittal), and its upward force vector may have a mechanical and/or physiologic (haptic) stabilizing influence on balance control that could reduce apparent instabilities, particularly in body sway displacement.

Postural stability appeared to be degraded during the simulated reduced-gravity loading conditions tested in this experiment, and the performance patterns suggest that somatosensory information may be degraded in hypogravity environments. We recommend that follow-up experiments be performed, probably during parabolic flight, to verify these findings without the potential mechanical-based confounding factors of the POGO system.

2 Introduction

Analysis of video from Apollo lunar surface extravehicular activities (EVAs) has demonstrated that astronauts experienced difficulty maintaining stability. This led to the hypothesis that spacesuit CG is an important parameter affecting human performance. To specifically evaluate the role of CG, tests have been performed at the Neutral Buoyancy Laboratory (NBL) and during NASA Extreme Environment Mission Operations (NEEMO). Initially, six configurations framed the boundaries of potential CG locations (high,

low, aft, forward, ideal, and the Crew and Thermal Systems Division [CTSD] 2005 "baseline" CG); these configurations were evaluated for their effect on ambulation and performance of exploration tasks. Based on crewmember GCPS ratings, these studies demonstrated that ideal and forward CGs were acceptable (3). The other CGs required moderate to considerable operator compensation, with the high and aft CGs being the least favorable. Subsequent NEEMO tests evaluated four additional CG configurations located within the region expected to contain the lunar spacesuit system CG. Preliminary unpublished results indicated that these CG locations were acceptable based on crew GCPS ratings.

Although it provides an insightful first look at the effect of CG on human performance in lunar gravity, the underwater environment does not permit several critical data parameters such as metabolic rate and biomechanics to be collected. The purpose of this study was to expand on the preliminary CG research from the underwater environments and evaluate the effects of varying CG on human performance in lunar gravity using the Johnson Space Center (JSC) SVMF partial-gravity offload system (i.e., POGO) with unsuited subjects.

2.1 Test Objectives

The primary objective of this study was to evaluate whether and how a change in system CG affects human performance metrics (eg, metabolic rate, biomechanics, subjective ratings, stability) in simulated lunar gravity during level-ground ambulation, inclined ambulation, exploration tasks, and postural testing.

It should be noted that this objective was to be tested in both the unsuited and the suited condition, but was only tested in the unsuited condition. The POGO, in its current configuration, could not offload the additional weight required to complete the test in the suited condition (with the Mark III technology demonstrator suit system as described in the IST-1 final report (1) and the new CG rig); therefore, the planned objectives for the suited condition were deleted from this test.

3 Methods

3.1 Subjects

The subjects tested were all male crewmembers recruited from a group of astronauts selected to support exploration EVA studies. At the time of subject selection, the suited portion of the test was expected to be completed; therefore, only those who had a known acceptable suit fit in the MKIII were considered for inclusion because of potential medical safety issues. At the time of testing, no available female astronauts properly fit in the MKIII suit.

Over the course of the study, a total of seven subjects participated with five of these subjects participating in all portions of the testing protocols. Of the two remaining subjects, one performed only the ambulation portion of the study and the other performed only the postural stability and exploration tasks. The means and standard deviations for the ambulation subject statistics are: mass 83.2 ± 8.7 (kg), height 181.8 ± 6.8 (cm), and age 50 ± 5 (yr). Figure 1 and Figure 2 show the population distribution of these test subjects compared to NASA's Human Systems Integration Requirements (HSIR) database for stature and mass. The means and standard deviations for postural stability and exploration tasks subject statistics are: mass 78.1 ± 7.4 (kg), height 179.5 ± 6.2 (cm), and age 49 ± 6 (yr). As shown, the distribution of the subjects for stature is skewed to the upper end of the database for both the male and the female distribution. The distribution of subjects for mass is relatively centered for the male distribution.

As stated, no female subjects participated in this study. It should also be noted that several research studies have shown that there are biomechanical differences between males and females, with one study showing interesting differences between males and females while carrying loads (4). Therefore, results and conclusions should be only considered valid for males.

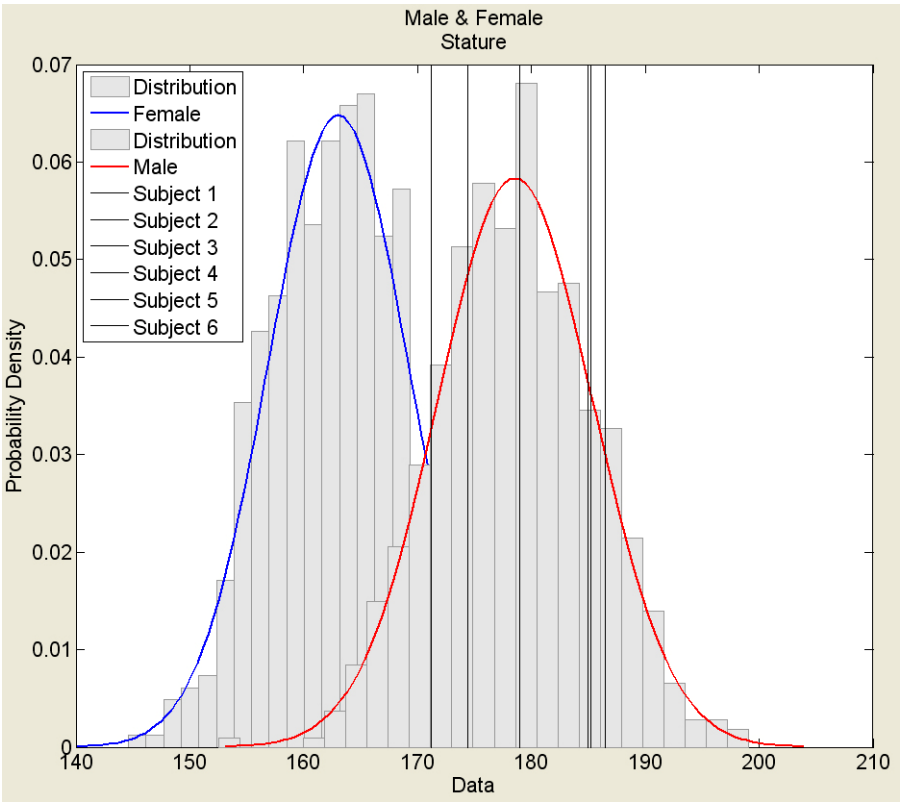

Figure 1. Subject population distribution for stature (cm) against the HSIR database.

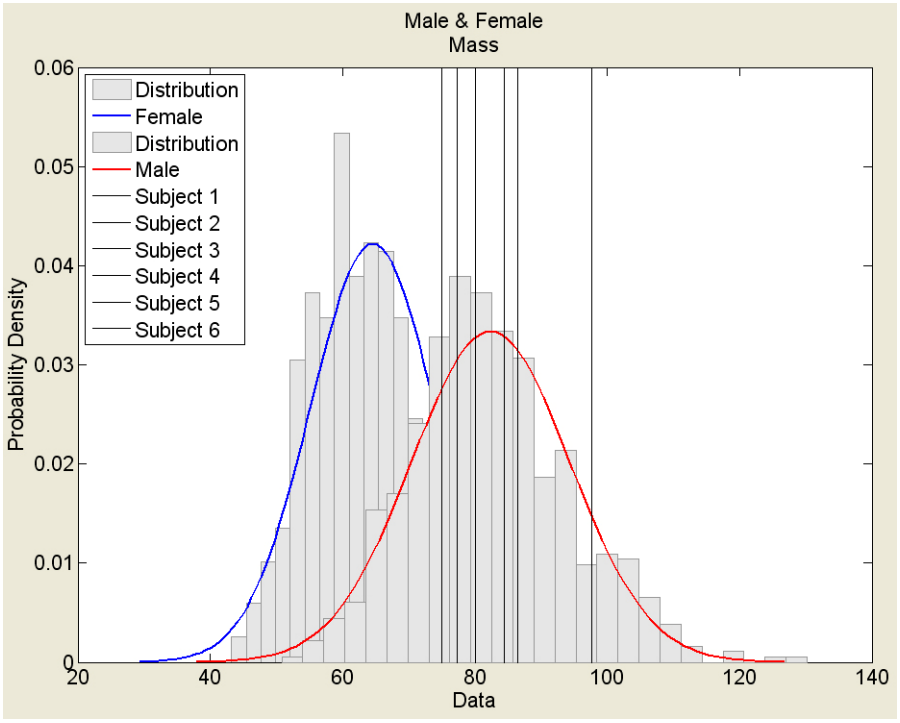

Figure 2. Subject population distribution for body mass (kg) against the HSIR database.

3.2 Hardware

3.2.1 Partial-gravity simulator (POGO)

All reduced-gravity simulations during IST-3 were performed using the SVMF POGO system. The POGO system was previously described in the EVA Walkback Test final report (5). The gimbal support structure also described in that paper was customized for specific IST-3 applications and will be discussed separately.

3.2.2 Gimbal support structure with adjustable center-of-gravity rig

The gimbal support structure has been described in the EVA Walkback Test and IST-1 Reports (1) (5). To alter the system CG, the gimbal support structure, previously only used for suited applications, was modified in two major ways. The first was a modification to support shirtsleeve subjects by attaching a harness (Amspec no. JV0100P, Van Nuys, Calif.), also know as a "jerk vest," to a flat metal plate rigidly connected to the gimbal. The leg straps of the harness were modified such that webbing was sewn to the leg straps, which pulled them together. This created a "seat" to improve comfort and remove an artifact of the leg straps that tended to pull subject's legs apart. Velcro® was also added to the leg straps to keep the straps securely tight during trials (Figure 3).

Figure 3. Shirtsleeve harness (Amspec no. JV0100P) showing additional modifications to the leg straps.

The second modification was the addition of an adjustable CG rig with support arms that allowed adjustment of system CG by the addition to and variable positioning of weights on the support arms. In addition to the movement of the weight support arms and the weights, the system CG was also adjustable by moving the "stinger" horizontally through the gimbal support structure or vertically through the connection to the adjustable CG rig. The gimbal support structure with adjustable CG rig is shown in Figure 4 with the stinger adjustments shown in more detail in Figure 5.

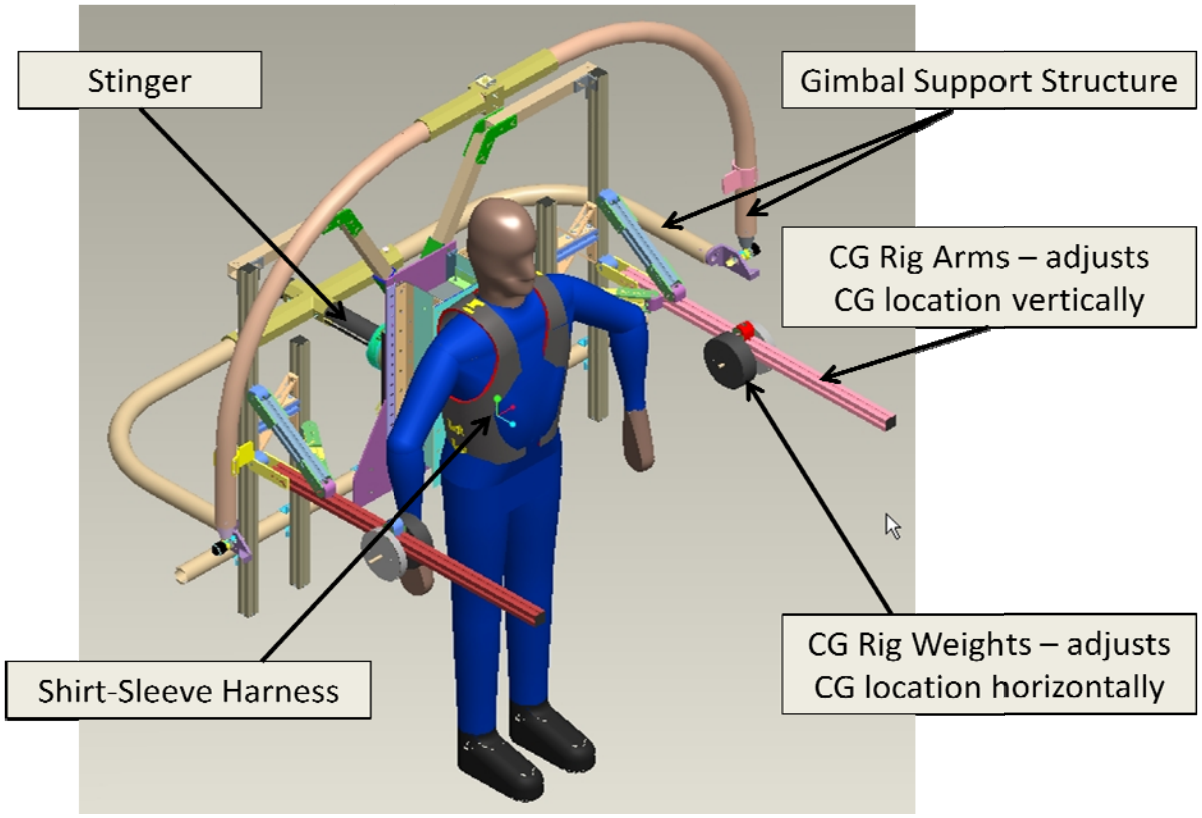

Figure 4. Gimbal support structure with adjustable CG rig (offset view).

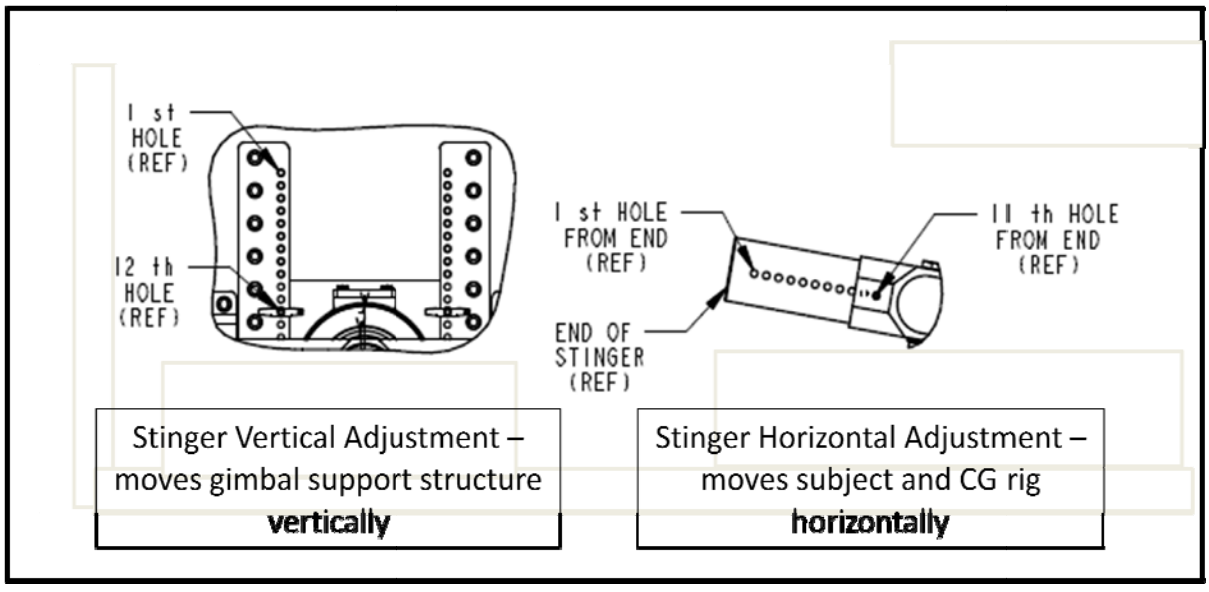

Figure 5. Stinger interface to gimbal support structure and adjustable CG rig.

Initial prototypes of the adjustable CG rig had the shirtsleeve harness attached directly to a metal plate that ended just above the gluteus maximus for the modeled subject with a height of 182.9 cm. On testing the harness, this location for the edge of the plate proved unsatisfactory because it rested painfully across the lower back, posing a safety risk. A portion of the bottom of the plate and plate support structure

was removed such that the bottom of the plate was now equivalent with the navel height. Rigid foam padding was then inserted in place of the previously existing plate so that the foam contacted the subject's lower back and top of the gluteus maximus. This rigid padding allowed for comfortable contact between the subject and the CG rig and provided a greater surface area of contact so that the subject's movements more easily translated into movement of the gimbal support structure and CG rig. These changes are shown in Figure 6.

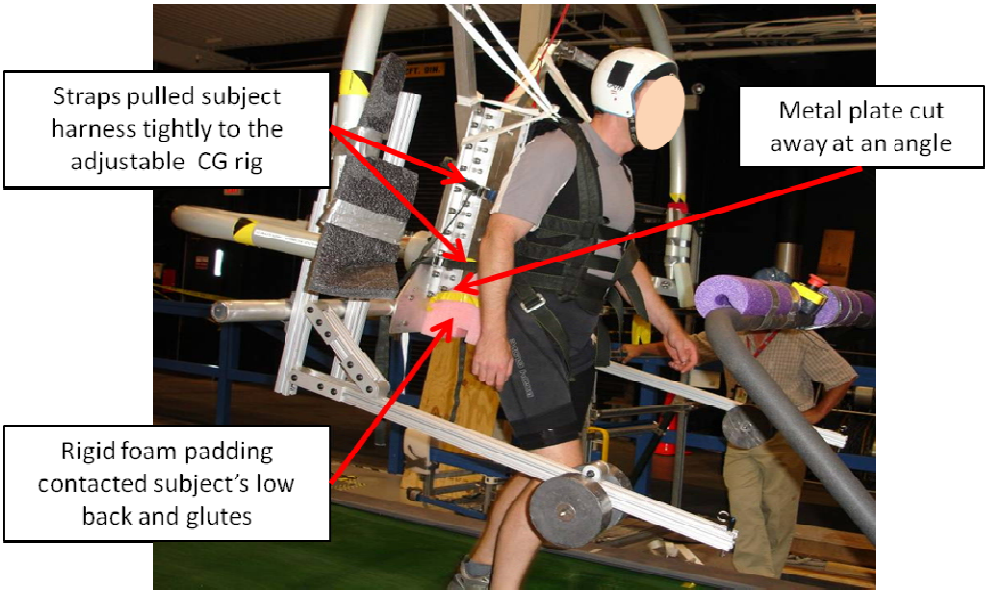

Figure 6. CG rig adjustments for subject comfort and controllability.

To keep the subject rigidly connected to the adjustable CG rig, hardware slid through the pickup points on the back of the shirtsleeve harness and bolted directly to the back plate of the adjustable CG rig. Adjustable straps were then connected to two different locations on each side of the shirtsleeve harness and the adjustable CG rig. These straps were pulled tight to allow the subject's movement to transfer directly into the gimbal rather than having the subject moving independently of the gimbal (Figure 6).

3.2.3 VacuMed oversized treadmill

The VacuMed large research treadmill (VacuMed, model no. 13610, Ventura, Calif.) was used for all treadmill testing. This treadmill was previously described in the IST-1 final report (1).

3.2.4 PRO Balance Master®

The PRO Balance Master® (Neurocom International, Inc., Clackamas, Ore.) provides objective assessment and retraining of the sensory and voluntary motor control of balance on either a stable or an unstable support surface (Figure 7). The system consists of a dual-force plate (18 in. × 18 in.), an electronic control module, and a computer. The dual-force plate measures the distribution of forces exerted by the feet against the support surfaces. The electronic control module consists of force transducer amplifiers, force plate servo controls, a platform-computer interface, and associated power supplies. The Balance Master® computer executes the test protocols, servo commands, and displays. The subject is placed atop the platform, and the subject's ankle joints are aligned with the rotational axis of the support surface. The platform, which is designed to provide sway referencing in the anterior-posterior (AP) direction, returns to a level starting position between trials.

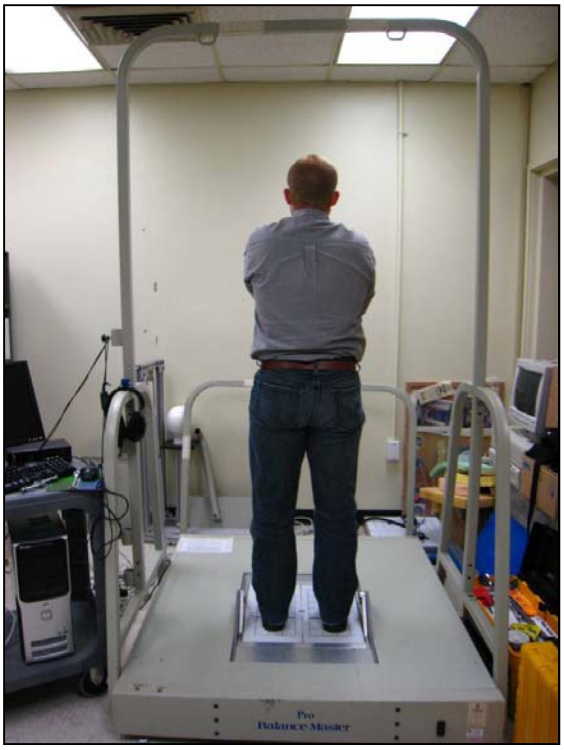

Figure 7. PRO Balance Master® system.

3.3 Testing Configurations

3.3.1 Center-of-gravity locations

Four different system CG locations were tested during IST-3. The CG locations will be defined throughout this report as the distance between the subject's CG and the overall system CG, which includes the subject, gimbal support structure, and adjustable CG rig. **Error! Reference source not found.** shows the amount the system CG was offset from the subject's CG. Negative values in the "Fore/Aft Offset" column indicate that the CG was behind the subject's CG. Positive values in the "High/Low Offset" column indicate that the CG was higher than the subject's CG. CG offsets were set using a 189.9-cm (72-in.), 81.6-kg (180-lb) male human computer model; therefore, CG offsets will vary slightly among subjects as their anthropometrics vary from the human computer model. Table 1 shows both the target offsets and the actual achieved offsets. Although achieved offsets were very close to the targeted offsets, there were slight differences due to the inability to adjust the spider vertical and horizontal adjustments by anything less than 1.27-cm (0.5-in.) increments.

Table 1. System CG Locations

CG Configuration	Target Fore/Aft Offset	Target High/Low Offset	Achieved Fore/Aft Offset	Achieved High/Low Offset
Perfect	0.0 cm	0.0 cm	0.2 cm	-0.2 cm
Backpack	-4.8 cm	1.0 cm	-4.9 cm	1.1 cm
CTSD	-7.6 cm	14.4 cm	-7.4 cm	13.7 cm
POGO	-11.2 cm	20.1 cm	-10.6 cm	20.1 cm

Figure 8 shows a lateral view of each CG configuration, and Figure 9 shows an anterior view of each CG configuration. Note the relationship of the subject to the gimbal axes of rotation, the height of the

horizontal arms of the CG rig, and the fore/aft distance of lead weights on the horizontal arms. As the subject moves forward of the gimbal axes of rotation and/or the weights are moved aft on the horizontal arms, the system CG is moved aft. As the gimbal is raised in relation to the subject or if the horizontal arms are elevated, the system CG is moved high.

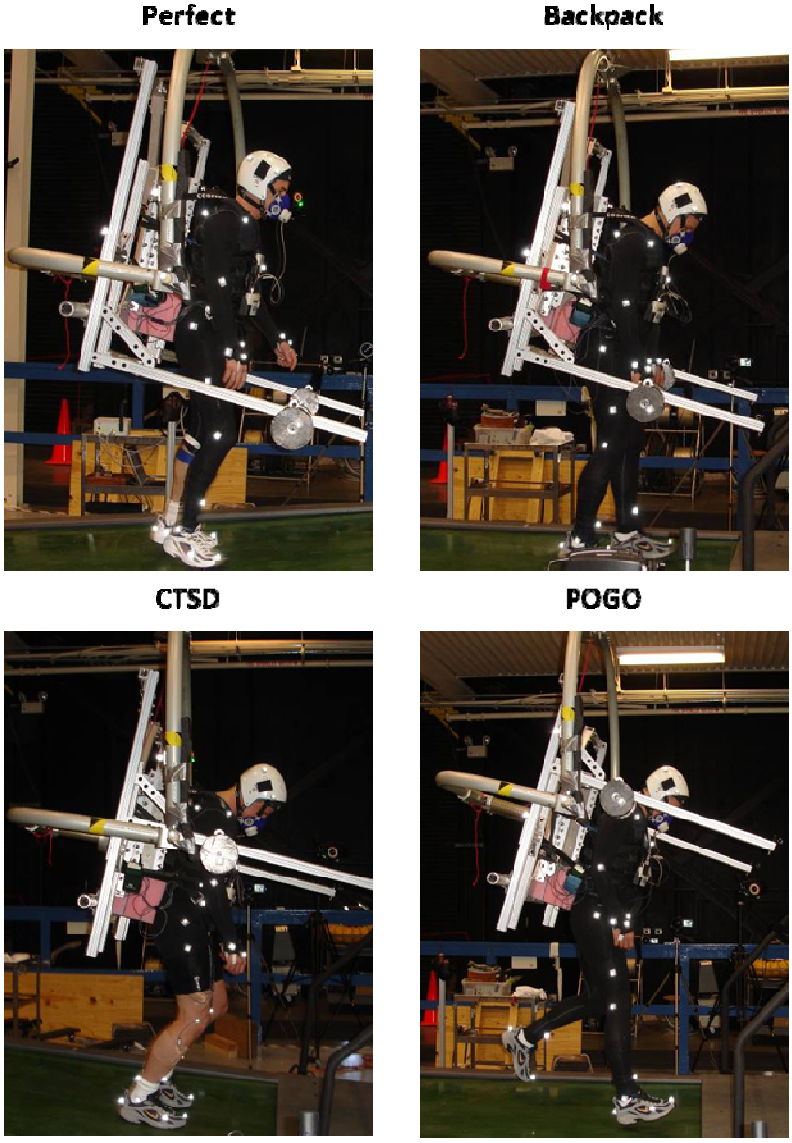

Figure 8. Lateral view of each CG configuration.

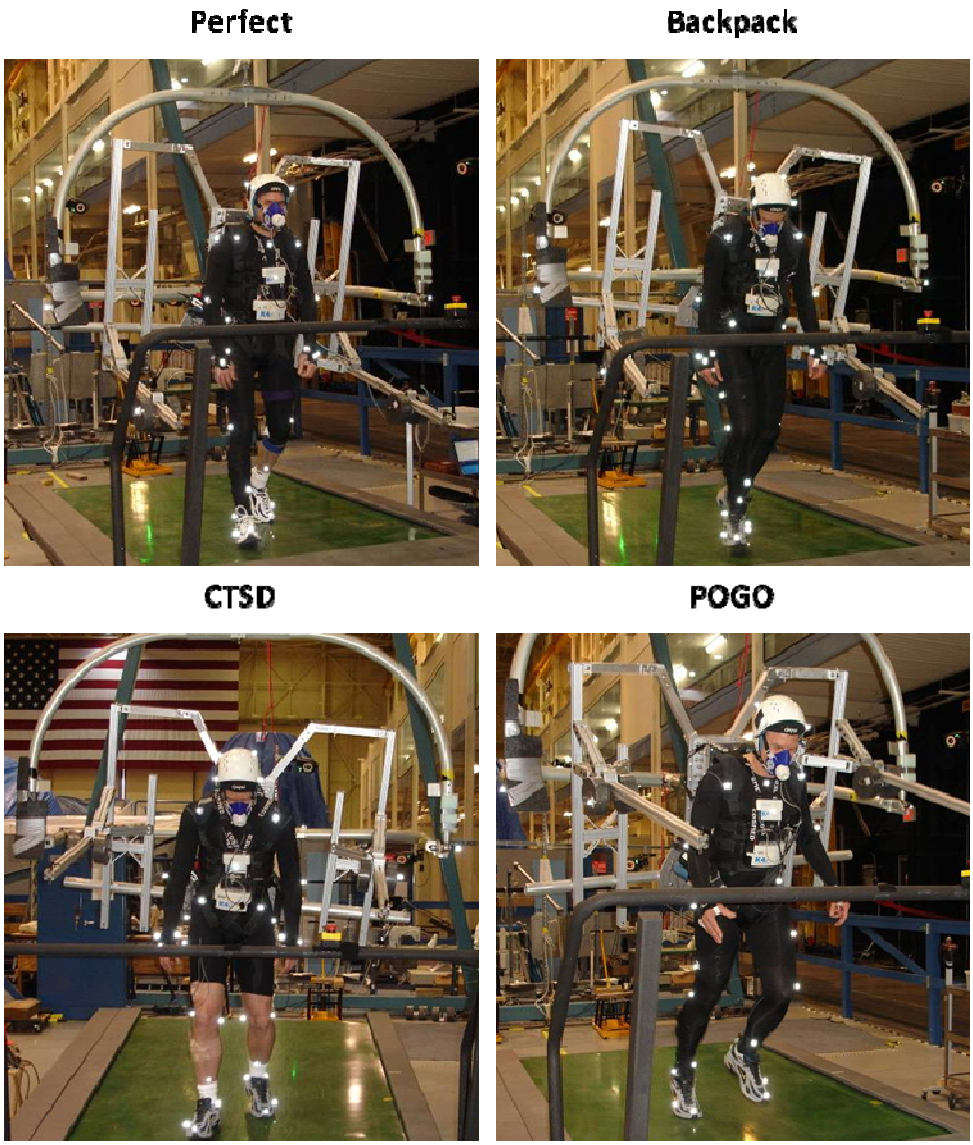

Figure 9. Anterior view of each CG configuration.

The perfect CG was chosen because it represents the ideal condition of adding significant mass to the subject in perfect proportion so that it does not alter the subject's own CG. The Backpack CG was chosen because it represented a potential option based on current suit and Portable Life Support System (PLSS) modeling. The CTSD CG was the CG of the suit and the PLSS as defined in 2005. The POGO CG was determined to be the system CG as tested during previous suit tests, including the EWT (5), IST-1 (1), and IST-2 (2).

In addition to achieving the correct CG offset from the system CG to the subject's CG, the system CG also needed to be collocated with the gimbal axes of rotation so as not to introduce any artificial rotational moments. The CG rig and subject were positioned so that the system CG was collocated as close as possible to the gimbal axes of rotation. Preliminary model calculations placed the system CG within 0.1 cm of the gimbal axes of rotation with the exception of the CTSD CG, which had the system CG 0.6 cm aft of the gimbal axes of rotation.

3.3.2 Offload profiles

Three different offload profiles were used during this study. The first profile involved no offload, with the subjects performing all tasks in 1-g with no CG rig and unconnected to the POGO (1-g). The second profile had the subject don the CG rig at the Perfect CG, but with the weight of the CG rig off-loaded so that the subject's total gravity adjusted weight (TGAW) was the same as the first profile, his 1-g body weight (1-g [Perfect]). TGAW, which is defined as the weight remaining on the ground, is the product of the total system mass and the offload level. The third profile had the subject don the CG rig before the total system mass (combined mass of the subject, gimbal, and CG rig) was offloaded to represent lunar gravity (1/6-g) (Perfect, Backpack, CTSD, POGO).

3.3.3 Test configurations

Six different CG/offload configurations were tested. They are described in Table 2, based on the reference subject's body mass of 81.6 kg. Each subject's actual TGAW varied slightly depending on respective differences from the reference subject.

Table 2. Test Configurations

Configuration Name	CG Fore/Aft Offset (cm)	CG High/Low Offset (cm)	Subject Mass (kg)	Gimbal/CG Rig Mass (kg)	Intended Offload	TGAW (N)	TGAW (lb)	Conditions Tested
1-g	N/A	N/A	81.6	0	1-g	800	180	All
1-g (Perfect)	0.2	-0.2	81.6	111	Weight of CG rig offloaded	800	180	Posture and exploration tasks
Perfect	0.2	-0.2	81.6	111	1/6-g	315	71	All
Backpack	-4.9	1.1	81.6	111	1/6-g	315	71	All
CTSD	-7.4	13.7	81.6	111	1/6-g	315	71	All
POGO	-10.6	20.1	81.6	111	1/6-g	315	71	All

3.4 Test Order

Initially, the test order was to have all subjects perform the tasks in the 1-g configuration followed immediately by the 1-g (Perfect) configuration. After trying to accomplish this with two subjects, it was determined that the 1-g (Perfect) configuration was too difficult for the treadmill tasks and incurred an unacceptable safety risk to the subject. Therefore, that configuration was not used for the remainder of the ambulation trials, although it was used for the exploration and postural stability tasks. It was also assumed that the high and aft CG configurations (CTSD and POGO) would be more difficult; so for each treadmill test day, the subject completed both the level and the incline conditions with either the CTSD or the POGO CG and either the Perfect or the Backpack. With the exception of placing the 1-g trial at the beginning for purposes of defining a baseline, all CG configurations were done in a balanced order to minimize possible learning and/or fatigue issues for the treadmill days. For each CG/offload configuration on the treadmill testing day, the level conditions were completed first and then the incline conditions were completed after a rest period. For the posture and exploration tasks test day, the order of the first three configurations was fixed as 1-g, 1-g (Perfect), and Perfect. The remaining CG configurations were completed in a balanced order. For the posture and exploration tasks days, the postural stability testing was done first immediately followed by the exploration tasks (Table 3).

Table 3. Test Day and CG Condition Order

	Sub 1	Sub 2		Sub 3	Sub 4	Sub 5	Sub 6
Day 1 - Treadmill	1-g	1-g	**Day 1 - Treadmill**	1-g	1-g	1-g	1-g
	1-g (Perfect)	1-g (Perfect)		CTSD	POGO	Backpack	POGO
Day 2 - Treadmill	Backpack	Perfect		Perfect	Perfect	POGO	Backpack
	CTSD	CTSD	**Day 2 - Treadmill**	Backpack	CTSD	Perfect	CTSD
Day 3 - Treadmill	Perfect	POGO		POGO	Backpack	CTSD	Perfect
	POGO	Backpack	**Day 3 - Posture and Exploration Tasks**	1-g	1-g	1-g	1-g
Day 4 – Posture and Exploration Tasks	1-g	1-g		1-g (Perfect)	1-g (Perfect)	1-g (Perfect)	1-g (Perfect)
	1-g (Perfect)	1-g (Perfect)		Perfect	Perfect	Perfect	Perfect
	Perfect	Perfect		POGO	Backpack	CTSD	Backpack
	CTSD	POGO		Backpack	POGO	Backpack	CTSD
	POGO	CTSD		CTSD	CTSD	POGO	POGO
	Backpack	Backpack					

3.5 Test Protocols

3.5.1 Level ambulation

All level ambulation was performed on a treadmill with the grade set to 0%. Treadmill speeds were 0.4, 0.8, 1.3, 1.7, 2.1, and 2.5 $m \cdot s^{-1}$. Time at each speed was 3 min. For each condition, subjects started at the lowest speed and proceeded continuously to the fastest speed.

3.5.2 Graded ambulation

All graded ambulation was performed on a treadmill with the speed set to 0.8 $m \cdot s^{-1}$. This speed, which was selected to overlap with one of the level-ambulation speeds, seemed a reasonable estimate of the speed that an astronaut might employ walking up and down slopes during a lunar EVA. Treadmill grades were -10%, 0%, 10%, 20%, and 30% incline. Time at each grade was 3 min. For each condition, subjects started at the decline and proceeded incrementally to the highest incline. Because of equipment calibration needs, a short break of approximately 1 to 2 min was required between each incline stage. Although the 0% incline stage was part of the graded ambulation data set, it was actually completed during level-ambulation data collection.

3.5.3 Exploration tasks

Subjects performed three distinct exploration tasks representing typical activities expected during lunar EVA operations. All tasks were short in duration, lasting only a few seconds. This was done intentionally to be able to compare results to a concurrent study using similar techniques during parabolic flight (6).

1. Rock pickup – Subjects stepped onto two force plates with one foot on each force plate and got into a steady position. They then bent down to pick up a 2.7-kg lead shot bag and then stood up completely. Subjects then returned the bag to the starting point, stood back up, and stepped off the force plates. To be consistent with previous studies, the bag was elevated on a surface 50 cm from the top of the force plates (2).
2. Shoveling – Subjects were provided a shovel before the beginning of this task. They then stepped onto two force plates with one foot on each force plate and got into a steady position. The subjects then proceeded to shovel a 2.7-kg lead shot bag from the 50-cm elevated surface before dumping

the bag on the floor. Once the single shovelful was transferred, subjects stepped off the force plates. To be consistent with previous studies, the bag was elevated on a surface 50 cm from the top of the force plates (2).

3. Kneel and recover – Subjects kneeled on one knee and returned to a standing position. Subjects always kneeled on the right knee.

3.5.4 Postural stability

Postural stability testing was performed with the subject standing quietly on a computerized dynamic posturography (CDP) system force plate (support surface) with arms folded across the chest. The subject was asked to maintain stable, upright stance under two 100-s-duration quiet stance conditions: Sensory Organization Test (SOT) 1, a standard clinical Romberg test condition with eyes open and fixed support surface; and SOT 4, a test identical to SOT 1 except that somatosensory inputs were distorted by sway-referencing (rotating about the ankle joint in direct proportion to the instantaneous center-of-mass sway angle) the support surface. Following the two quiet stance conditions, the subject was asked to maintain a stable, upright stance throughout a series of six 10-s duration motor control tests (MCTs), each challenging the posture control system with a sudden toes-up (TU) or toes-down (TD) rotation (840-ms rest, 8°/160 ms-perturbation, 9-s recovery). The six trials consisted of three TU trials and three TD trials presented according to a randomized schedule for each configuration.

3.6 Metabolic Data Collection and Analysis

During all ambulation testing, metabolic rate was determined from the continuous measurement of oxygen consumption (VO_2), carbon dioxide (CO_2) production, and expiratory volume (V_E) using an oronasal mask with the COSMED K4b2 (COSMED USA Inc., Chicago, Ill.). Heart rate was monitored from a chest strap monitor (Polar S810i, Lake Success, N.Y.).

The metabolic rates represent the highest 1-min average (VO_2) during each of the 3-min walking stages. Metabolic rate was defined as milliliter of oxygen consumed per kilogram of the subject's body mass, per minute ($mL \cdot kg^{-1} \cdot min^{-1}$). For all metabolic data, the best second-order polynomial fit was used for displaying trend lines.

Due to the limited sample size ($n = 6$), inferential statistics were not used; therefore, statistical significance was not calculated. For these analyses, a change in metabolic rate of 3.5 $mL \cdot kg^{-1} \cdot min^{-1}$ was chosen for practical significance. Rationale for this choice was described in the IST-1 final report (1).

3.7 Biomechanical Collection and Analysis

Four strain-gauge-type force plates (AMTI, Watertown, Mass.), which were mounted to the frame of the treadmill under the belt, recorded ground reaction force (GRF) during the ambulation trials. The GRFs recorded on the treadmill were normal (perpendicular) to the surface of the treadmill. Two additional force plates (AMTI, Watertown, Mass.) were used during the exploration task trials to record GRF and center of pressure (COP). During exploration tasks, the subjects would stand on top of the force plates while performing their task.

A Vicon MX motion capture system (Vicon, Oxford, England) was used to capture the kinematic data. Small retroreflective markers were placed on key landmarks of the body and on the CG rig and gimbal. Data were processed with a model custom made for use with the CG rig and gimbal. This new model provided additional flexibility and accuracy over previous models. The model used inverse kinematics and dynamics to calculate the output variables. The data processed with this model output kinematic, kinetic, and temporal-spatial information. For this report, we have used definitions, reference frames, and reference planes commonly employed in biomechanics and prescribed by the International Society of Biomechanics (7). Appendix A contains reference materials and graphical representations of the previously mentioned items.

The marker set used during the IST-3 testing was an unsuited marker set modified to be compatible with the CG Rig harness (Figure 10). Six of the markers, shown in orange in the figure, were only used for a pretrial static data capture and were removed before trials began. Ten additional markers were used on the CG rig and gimbal support structure to capture the motion data and location of the different rigid body sections (Figure 11).

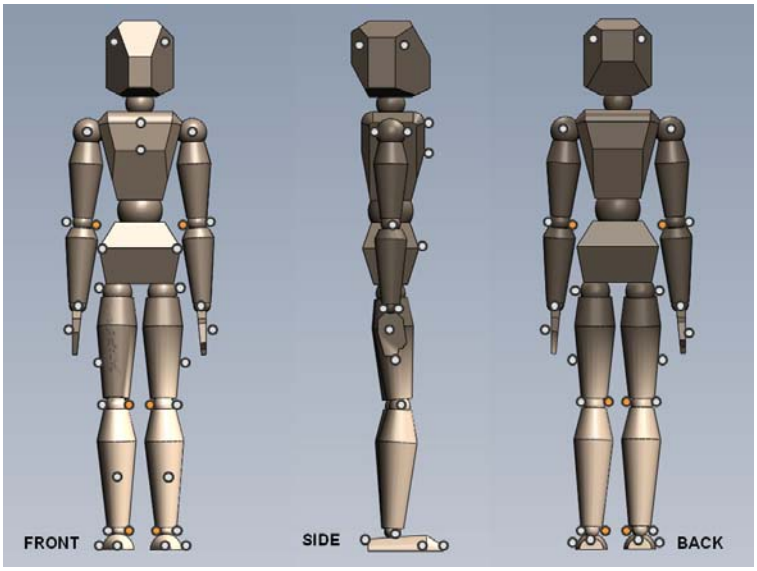

Figure 10. Illustration of marker placements for the unsuited subject. The markers in orange were only used for a static recording and were removed before the trial began.

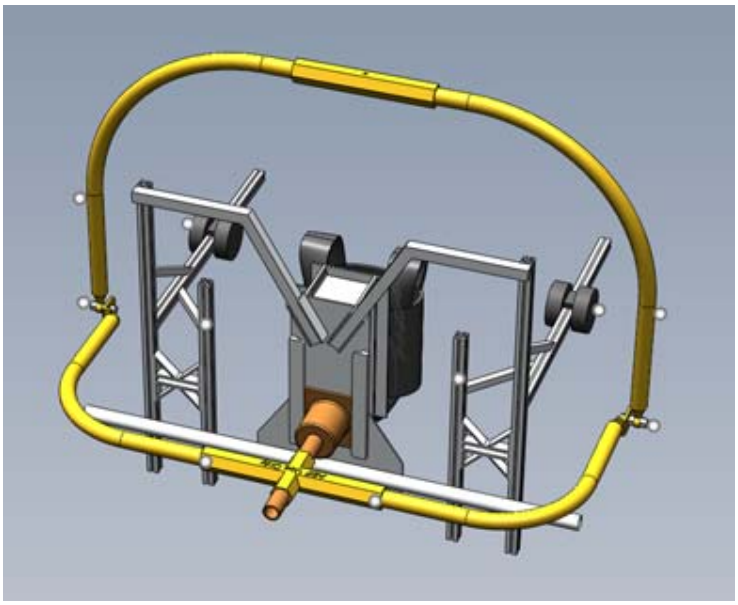

Figure 11. Illustration of marker placements for the gimbal support structure and CG Rig.

Electromyography (EMG) was collected with a Telemyo™ 2400 (Noraxon Inc., Scottsdale, Ariz.) wireless data collection system. The EMG signal was transmitted to the Vicon Nexus software and was recorded with the other data at a 1,000-Hz sampling rate. Processing of the data was done using custom code written with MATLAB software (The MathWorks™, Inc., Natick, Mass.). The EMG sampling sites

were rectus abdominis, erector spinae, rectus femoris, vastus lateralis, semitendinosus, anterior tibialis, and soleus muscles.

Subjects were prepped for electrode application before testing. Prepping included shaving the hair, removing dead skin cells, and using an alcohol swab to remove excess dirt for each application site. The surface electrodes were silver-silver chloride dual snap electrodes with a diameter of 1 cm each (Noraxon dual electrode; Noraxon Inc., Scottsdale, Ariz.). Each surface electrode was applied and secured with co-band. The subjects then wore spandex pants with the cables coming out at the waist for testing. The CG rig harness was placed on the subject in a manner that would not apply pressure or tension to the EMG electrodes or cables. All EMG electrodes were applied to the right side, and only the right foot was used for event markers.

All raw data were filtered with appropriate filtering algorithms. Because of data collection frequency differences, the 1,000-Hz data were either down-sampled to 100 Hz or expressed as time-independent variables.

3.8 Subjective Data Collection and Analysis

The following subjective ratings were recorded at various times throughout the test (additional information on each of these scales is included in Appendix B):

- RPE (8) was used to gauge how much effort subjects felt they must exert to complete each condition. The RPE was collected at 30 s into the trial and during the last 30 s of the ambulation trials. It was also collected immediately on completion of all postural stability and exploration tasks. With the small sample size, statistical significance was not tested but, rather, levels of practical significance were predefined. For these analyses, a change in RPE of 2 was chosen for practical significance. RPE changes of one unit are approximately at the level of practical significance for VO_2; but because RPE is a whole-number scale, it would take a change > 1 to see practically significant differences in metabolic rate.
- The GCPS was used to determine the level of compensation a person feels is necessary to maintain performance as compared to that person's performance unsuited in 1-g (5). GCPS was collected at 30 s and during the last 30 s of the ambulation trials. It was also collected immediately on completion of all postural stability and exploration tasks. GCPS, unlike RPE, is not a continuously linear scale. Therefore, changes in GCPS are more complicated to assign a simple level of practical significance. It is reasonable to define a range of GCPS in which changes within the range are of interest but would not be considered to be practically significant. Using this breakdown, we selected a GCPS category of 1 to 3 as "ideal," 4 as "acceptable," 5 to 6 as "modifications warranted," 7 to 9 as "modifications required," and 10 as "unable to complete task." A level of practical significance for GCPS is therefore one in which the value changes to a different category.
- The Corlett & Bishop body part discomfort scale was used to characterize discomfort at different body locations (9). Discomfort ratings were collected during the last 30 s of ambulation trials and at the completion of the postural stability testing and of the exploration tasks series.
- Thermal comfort and preference were assessed for two reasons: (a) to determine the thermal comfort of the subject and (b) to determine whether any changes were necessary to improve the thermal comfort of the subject during testing. Thermal comfort was assessed using the Bedford scale (10). Thermal comfort and preference were collected during the last 30 s of ambulation trials and at completion of the postural stability testing and of the exploration tasks series.

The addition of collecting GCPS and RPE at both the 30-s mark during ambulation and at the end was to begin to determine whether, and how, these ratings change over the course of time spent doing a constant activity as well as to be able to compare to results with a concurrent study using similar protocols during parabolic flight. In addition, GCPS will be used in conjunction with RPE to develop predictive models for metabolic rate with the intent to use these subjective factors in other lunar analog environments,

such as underwater analogs and parabolic flight, in which direct measures of metabolic rate are currently not possible. Discomfort and thermal comfort were both primarily used for test termination criteria as well as to provide feedback to the test team concerning test hardware, conditions, and length of trials. Discomfort and thermal data will not be presented or discussed in this report.

3.9 Postural Stability Data Collection and Analysis

The primary postural stability data for this experiment were obtained from GRFs sensed by load cell transducers mounted in the support surface and sampled at 100 Hz. Subject weight was determined at each test condition by averaging the summed values of the normal force transducers over the entire 100-s SOT 1 trial. During each trial, an instantaneous subject COP position was computed from analysis of the load distributions among the four normal force transducers at each sampling time. Instantaneous center-of-mass (COM) sway displacement in the sagittal plane (X_{cm}) was then estimated by low-pass filtering (f_c = 0.85 Hz) the AP component of the COP displacement data, and instantaneous COM sway velocity (V_{cm}) was estimated by digitally differentiating the sway displacement data. Peak-to-peak (p-p) displacements and velocities over each trial were obtained from these data series.

A dimensionless performance measure, the equilibrium (EQ) score, was computed using the first 20 s of data from each SOT trial for comparison with clinical norms. Assuming a single link inverted pendulum model having a longitudinal COM location proportional to the subject's height, instantaneous COM sway angles, θ, were estimated from instantaneous X_{cm} data. The AP p-p sway angle, θ_{pp} (in degrees), was then used to compute EQ = 100 × (1 – (θ_{pp}/12.5°)), where 12.5° is the theoretical maximum stable p-p sway displacement in the sagittal plane. Norms used for comparison in this study were obtained from the distribution of preflight performance scores garnered from more than 150 subjects previously tested in the JSC Neurosciences Laboratories.

More robust indicators of postural stability control were obtained by combining X_{cm} and V_{cm} data. Instantaneous time to contact (TTC) was defined as the amount of time it would take to reach the closest limit of stability (ie, fall) at any point in time during the trial. TTC was estimated throughout each trial by projecting the COM displacement from its current instantaneous AP position at its current instantaneous AP velocity until it intersected the limit of support represented by the maximum anterior or posterior aspect of the foot. The absolute minimum value of this data series over the trial, minimum time to contact (TTC_{min}), was used as an estimate of the greatest threat to postural stability during each trial. When loss of balance occurred, TTC_{min} was 0 s. An estimate of the average value of the threat to postural stability was obtained by numerically integrating the instantaneous TTC curve beneath an arbitrary ceiling set at TTC = 10 s. This parameter, integrated time to contact (iTTC), indicated the amount of time during the trial that the TTC was ≤10 s. Thus, lower TTC_{min} values and higher integrated TTC (iTTC) values indicate decreased performance. For the 100-s duration SOT trials, the minimum and maximum possible values for the iTTC were 0 s^2 and 1,000 s^2, respectively, while for the 10-s duration MCT trials, the minimum and maximum possible values were 0 s^2 and 90 s^2 (analysis was limited to the 9-s recovery period that followed the perturbation).

3.10 Imaging

Digital video was taken for each subject during every test condition. Audio was not captured consistently during the video recording. Whenever possible, digital photographs were taken of the subject from the front and side during each test condition.

4 Results and Discussion

4.1 Center-of-gravity Locations

CG locations for the system CG in relation to the subject and the gimbal axes of rotation were modeled before the test to provide the configuration of the CG rig for each condition, but these locations were

based on the standard subject model (182.9 cm, 81.6 kg). To determine how much variation occurred because of varied subject anthropometry, further analysis was performed using each individual subject's height and weight to modify the standard subject model on completion of the test sessions. Subjects were lined up in a consistent orientation (top of the shoulder lined up with the top of the back plate) to the gimbal support structure before the CG of the system and the relation of the system CG to the gimbal axes of rotation were recalculated. This recalculation proved valuable for another reason: Three of four CGs were well tolerated, but the CTSD CG was consistently the most difficult for all subjects to cope with. When performing tasks in this CG, many subjects described the feeling as similar to a "horse-collar" tackle in football (11) (12), with subjects feeling as though they were being pulled down and backwards from the base of the neck. Because these subjects did not experience this with any of the other conditions, the investigative team believed there was an error in the initial model calculations.

Figure 12 demonstrates the variability in how the system CG differed from the subject CG on an individual basis and with reference to the initial model calculations. In most cases, the system CG locations with respect to the individual subject CG were within 2 cm in any direction of the model calculations. For the Perfect and the Backpack CGs, the variation was primarily in the Y axis; but for the CTSD and the POGO CGs, the variation was in both the X and the Y axis.

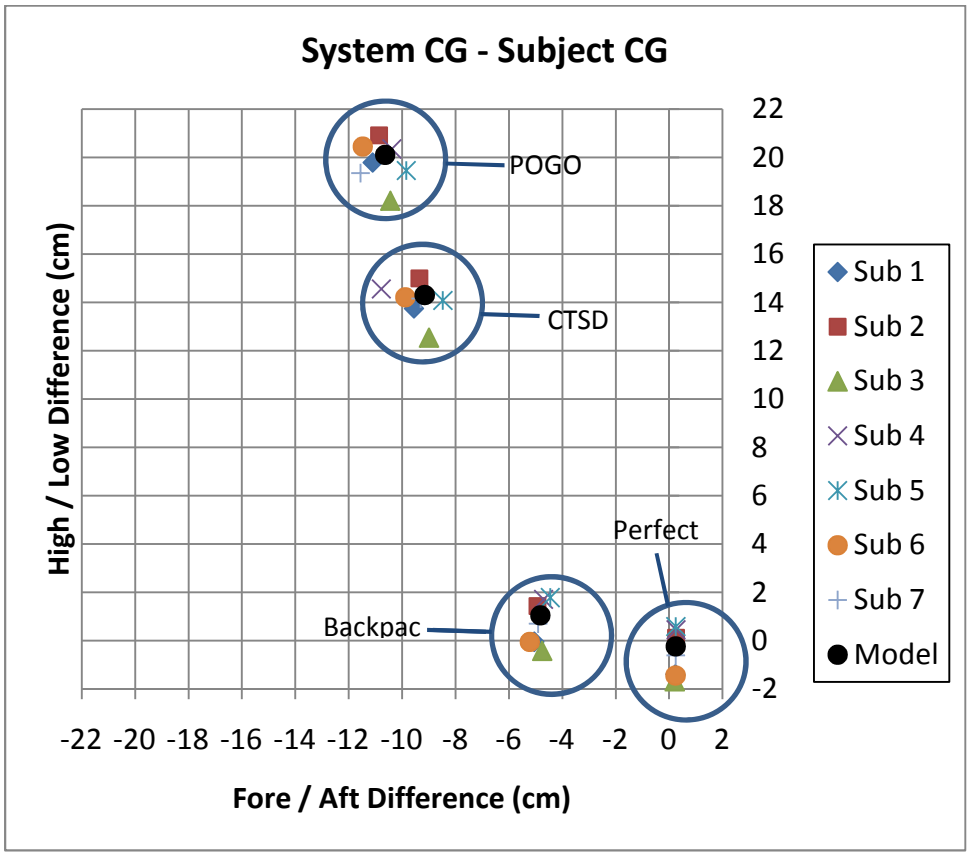

Figure 12. Individual subject differences in how the system CG varied from the subject CG.

Figure 13 shows the relationship of the system CG to the gimbal axes of rotation. Again, the variation in the Perfect and the Backpack CGs are primarily in the Y axis, and the CTSD and the POGO variation was in both the X and the Y axis. In previous studies, when subjects were allowed to freely choose how they are oriented into the gimbal, the system CG was typically aligned so that it was slightly (≤ 2.5 cm) forward and low of the gimbal axes of rotation (5) (1). This positioning is assumed to be the most advantageous to human performance. Given the orientation of the human body and the types of tasks performed

in this test, we expected small variations in the Y axis alone would not account for significant physiologic changes during upright-type tasks because the variation would still be in line with the lift vector and gravity. On the other hand, variations in the X axis could impact performance, especially during upright tasks, as the POGO and the gimbal system would impart rotational forces to line up the system CG with the lift and the gravitational forces in the vertical plane. Of the four CG locations, only the CTSD CG had an alignment that placed the system CG behind the gimbal axes of rotation, which would be consistent with the subjects' experience in which they felt they were being pulled down and backward.

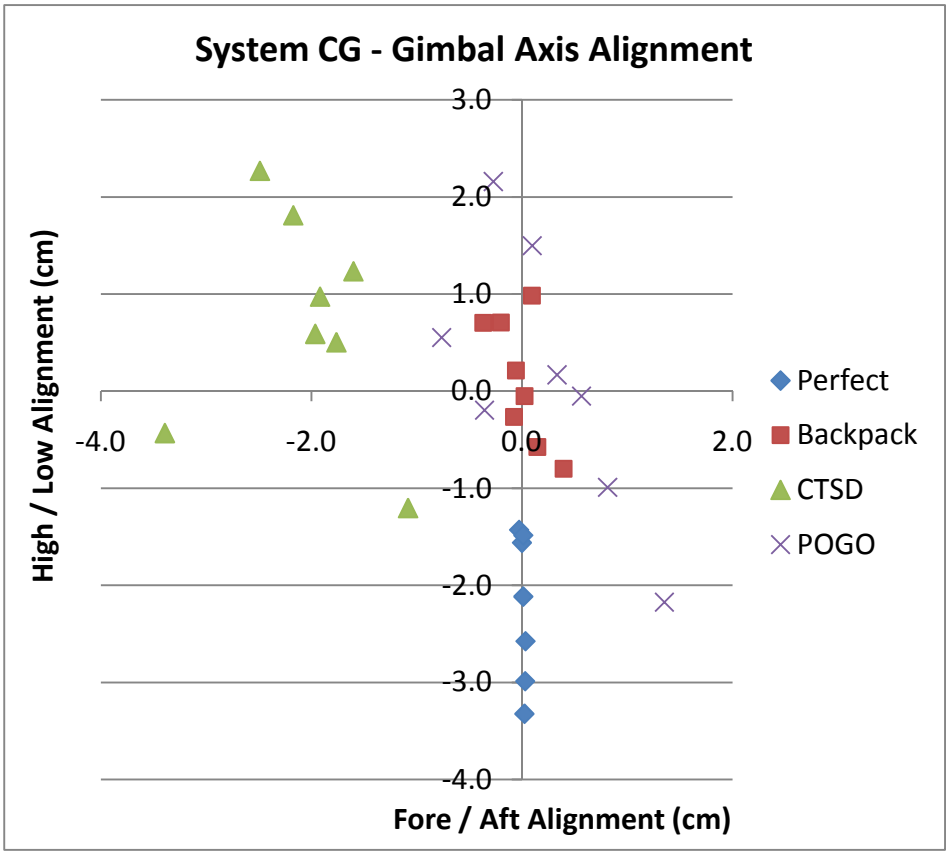

Figure 13. System CG relation to the gimbal axes of rotation for each individual subject.

4.2 Level Ambulation

Out of 180 trials, 174 were completed. All of the missing trials come from the CTSD CG condition. Half of the missing trials were not completed because the subject exceeded the maximum heart rate (HR), as described in Appendix F: Test Termination Criteria, during the prior trial. The other missing trials were not completed because of subject discomfort and an inability to position the subject properly in the rig.

4.2.1 Metabolic results and discussion

Metabolic rate was very similar for all varied CGs, except for CTSD, which had higher mean metabolic rates at all speeds (Figure 14). The baseline 1-g results were similar to the varied CG conditions while walking at speeds through 1.25 $m \cdot s^{-1}$. Baseline 1-g results were slightly greater than all but CTSD at 1.67 $m \cdot s^{-1}$, and were significantly greater (> 3.5 $mL \cdot min^{-1} \cdot kg^{-1}$) during the running speeds than all other CG conditions.

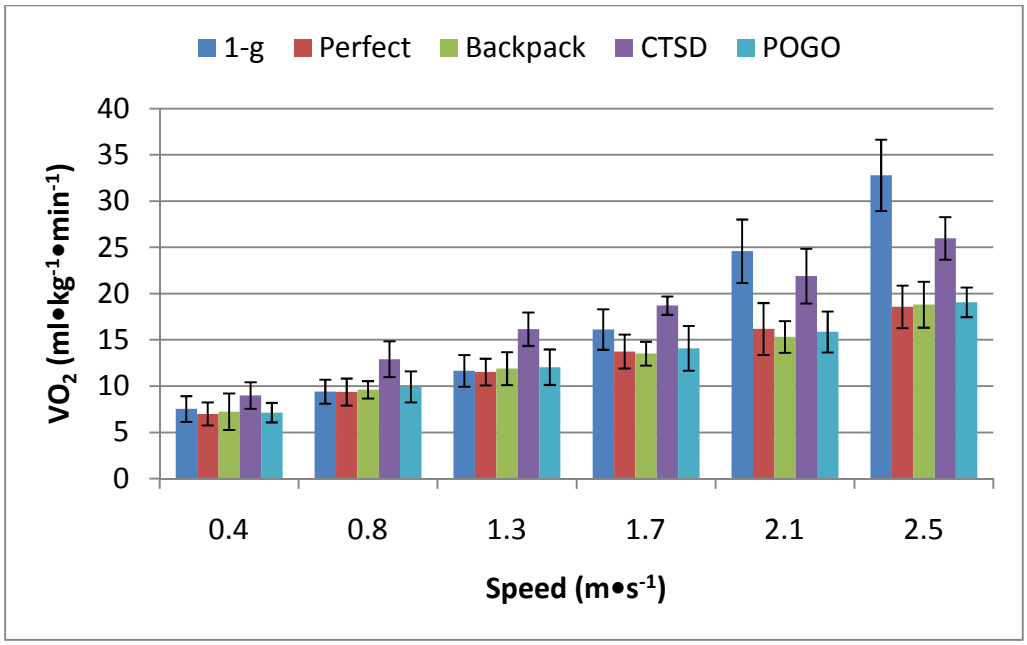

Figure 14. Metabolic rate for different CG conditions during shirt-sleeved ambulation on a level treadmill.

Figure 15 shows the nearly complete overlap of metabolic rate for the Perfect, Backpack, and POGO CG conditions, with the CTSD CG trending significantly higher on average. All of these were unexpected findings. Preliminary predictions were that the Perfect and Backpack CGs would lead to similar performance because they were closest to the 0,0 origin and that the CTSD and POGO CGs would lead to similar performance because they were both high and aft locations. To have the less high-and-aft CG (CTSD) of the two high-and-aft CGs (CTSD and POGO) lead to significantly higher metabolic rates was unexpected. Reasons for this poor performance were more likely related to the misalignment of the system CG with the gimbal axes of rotation than to the actual offset of the system CG from the subject's CG. Finally, all but the baseline 1-g data showed linear trends relating metabolic rate to speed.

Figure 16 shows similar metabolic responses for all subjects while walking and running on a level treadmill in 1-g and in simulated lunar gravity at the different CG configurations. For varied CG conditions, individual differences were not clearly evident for any CG other than the CTSD CG, with several subjects failing to complete all six speeds. Subjects were able to complete all trials at all other CG configurations.

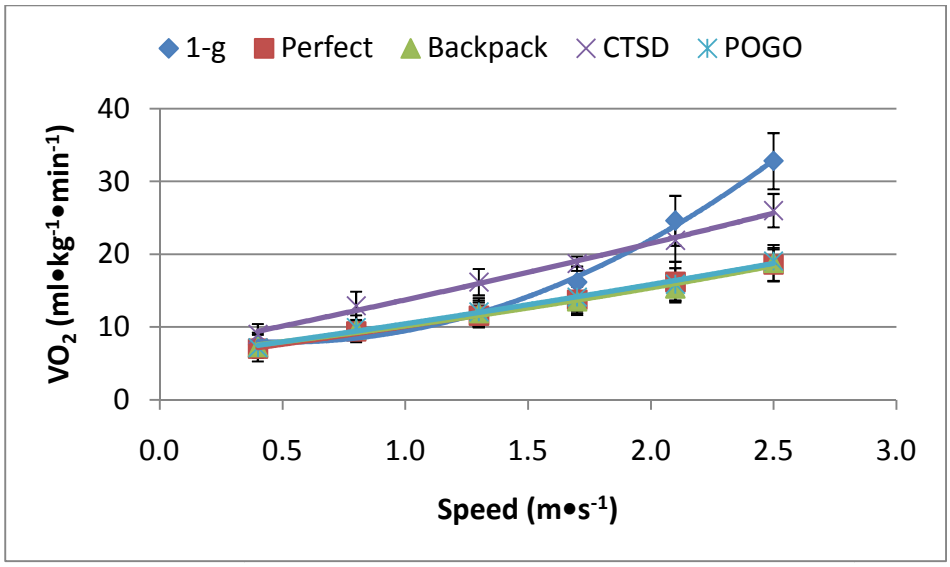

Figure 15. Metabolic rate for different CG conditions during shirt-sleeved ambulation on a level treadmill.

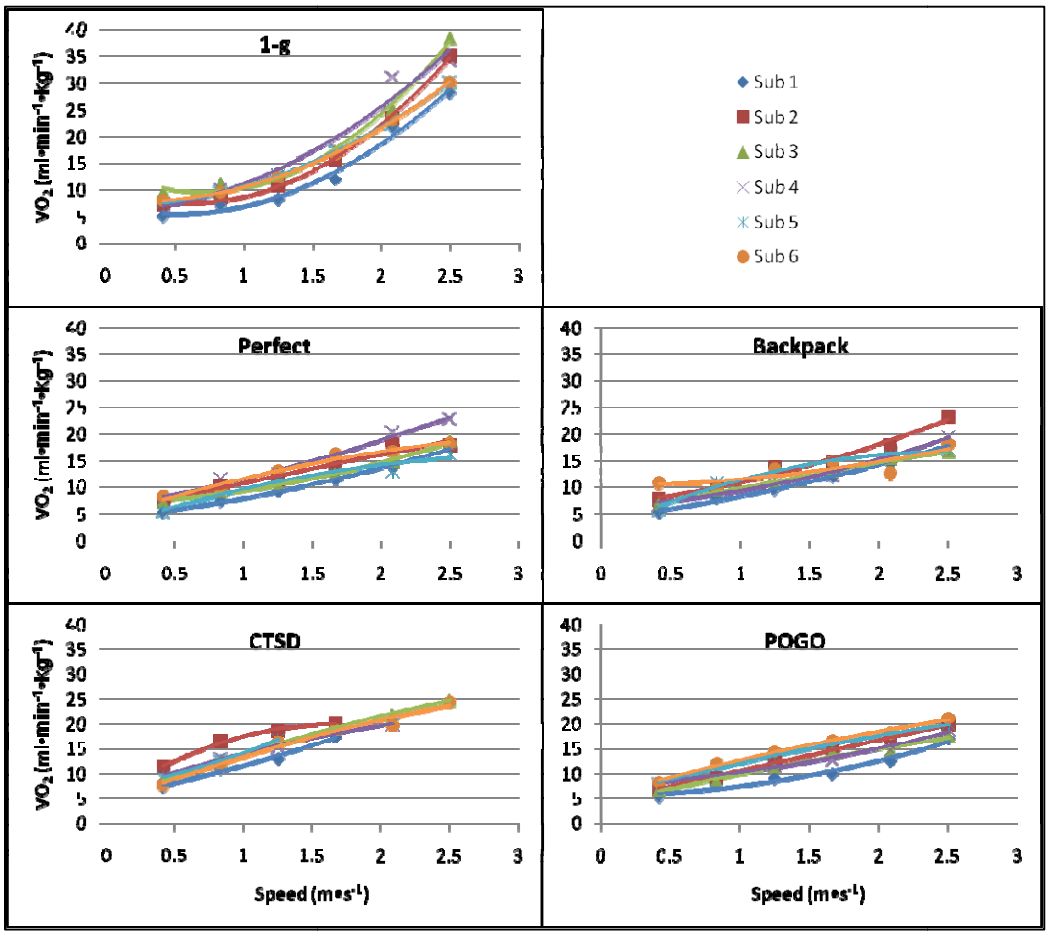

Figure 16. Individual metabolic rate responses to increasing speed on a level treadmill in 1-g and for different CG conditions during shirt-sleeved ambulation on a level treadmill at 1/6-g.

4.2.2 Biomechanics results and discussion

4.2.2.1 Kinetics

Kinetic analysis describes the methods the body uses to store, absorb, transfer, and expend energy. Studying these interactions, we can determine the nature of interactions between the human body and its environment. Normally, the body is a self-sustaining dynamic entity that receives no energy inputs from the surrounding environment. The POGO testing environment is not a passive environment and will impart some energy into the human body during ambulation. For this test, kinetics were measured via the GRF for the six crewmembers for all conditions completed.

In the current test, as with previous tests in the IST series, kinetic data were provided in the form of peak vertical GRF that represent the normal force acting on the subject when that subject is in contact with the walking surface (treadmill). Typically in literature as well as in these studies, GRF is represented as a function of body weight (BW). In the current study, GRF values for all tested conditions were normalized to the subject's 1-g BW. Normalization of the GRF data to subjects' respective BWs allows for a direct comparison to be made across subjects for the tested conditions.

Ground reaction force

In the current study, normalized peak vertical GRF for 1-g ambulation increased with an increase in ambulation speed (Figure 17). This follows expected trends seen in literature (13). As illustrated in Figure 17, a more notable increase is seen in normalized GRF values for the 1-g trials at 2.1 and 2.5 m•s^{-1} (ie, running trials). Conversely, normalized peak vertical GRF for all CG rig conditions appeared to plateau after subjects reached a 1.7-m•s^{-1} ambulation speed. This may indicate a less-prominent change in the adopted gait pattern at higher speeds, since subjects were offloaded to lunar gravity and did not need to develop as much propulsive force during gait.

Literature shows that peak vertical GRF during 1-g running registers roughly 2.5 times BW (13) (14). Results from the 1-g condition followed this, with normalized peak vertical GRF values ranging roughly between 2.3 and 2.6 times 1-g BW for the 2.5-m•s^{-1} running trial (Figure 17). Data from offloaded conditions reveal that GRF experienced by subjects in the CG rig ranged from approximately 0.5 times BW at a speed of 0.4 m•s^{-1} to approximately 1 BW at a speed of 2.5 m•s^{-1}. Minimal differences among varying CG conditions were observed for all subjects across all ambulation speeds (Figure 17).

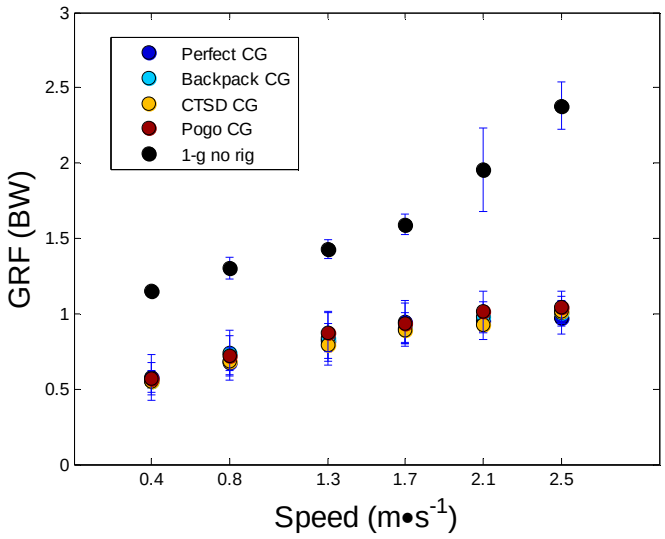

Figure 17. Mean peak vertical GRF, normalized to subjects' 1-g body weight, for shirt-sleeved ambulation on a level treadmill at different speeds. All varied CG conditions were performed at simulated lunar gravity.

Center-of-gravity excursion in the POGO test environment

Moving the body's CG is one of the main modes the body has of energy absorption, transfer, and expenditure. During walking and running, the body expels energy, propelling its CG up and forward, then absorbs energy as it comes back down and reacts with the ground (15). The faster a person walks or runs, the more energy that person puts into moving the CG. At first, a person would suppose that minimizing the CG excursion would improve the overall efficiency of the system, but, in reality, it has the just the opposite effect (16) (17). This is in part due to the human body's leg bones acting as a type of pole vault to help redirect the CG vector with little muscle work.

Figure 18 and Figure 19 display the ranges of CG excursion per condition and per treadmill speed as well as the percentage difference between the unsuited 1-g condition and the CG rig conditions. The excursion was only examined in the vertical direction and at roughly the same point (pelvis centroid) on all subjects. Dots represent the average of each subject's average over all cycles for the left foot. Error bars represent the standard deviation of those averages across subjects. The unsuited 1-g condition followed a near-linear progression from low to high speeds. The varied CG conditions followed a parabolic trend. The spread of the averages is fairly tight across the speed conditions. The middle speed (1.3 $m \cdot s^{-1}$) also seemed to be a common point of excursion range among all conditions.

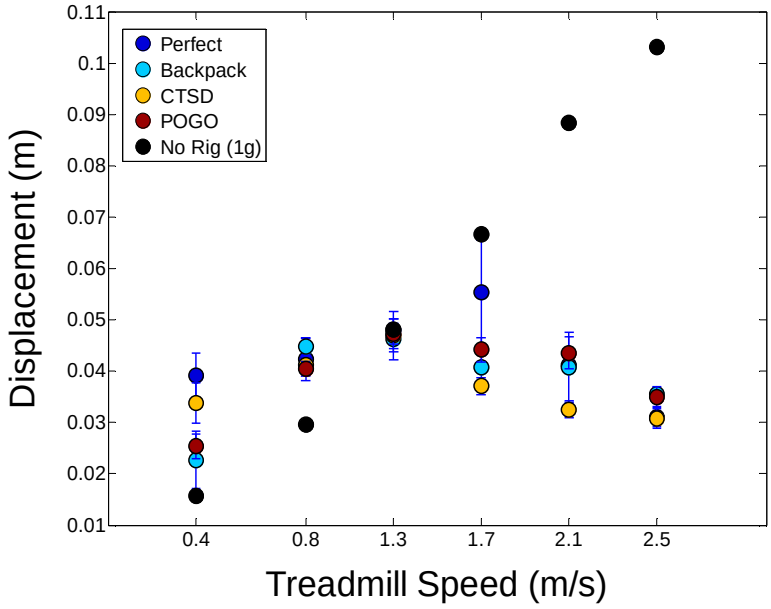

Figure 18. Average CG excursion range (pelvis centroid) among conditions with respect to speed.

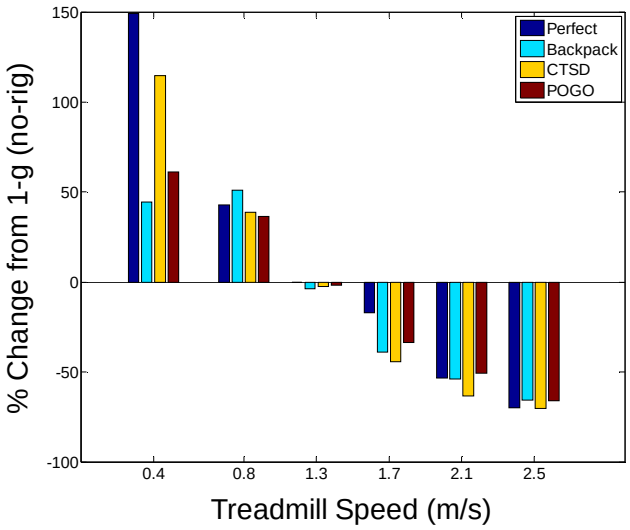

Figure 19. The change in CG excursion range of the CG rig conditions compared to the unsuited 1-g condition with respect to speed.

Examining the difference in excursion between the body and the CG rig can help determine the dynamics occurring between the mechanical system (POGO, gimbal, CG rig) and the human. In Figure 20, the pelvis centroid is plotted against the motion of the CG rig in a single sample of series of gait cycles. The actual displacements are shifted by a static offset so the two traces overlap. Excursions of the CG rig were larger than that of the body throughout trials. Two separate problems are shown in this graph. First, substantial displacement differences were seen between the peak and valley measurements for the subject and the CG rig. The variability of the difference between the CG rig and the subject CG would imply that the CG rig has significant freedom to move independently of the subject's body. Second, this independence allowed the subject and CG rig to become out of sync spatially and temporally. These differences occurred constantly between the CG rig and the body. Gait cycle averages also were not uniform in magnitude. The peaks and valleys are slightly out of phase from each other, with the body leading the CG rig by 5% to 10% of the gait cycle in this sample. This phenomenon comes from the large inertia of the gimbal and the CG rig system coupled to the POGO, causing the whole system mass (POGO, gimbal, CG rig, human body) to oscillate on a larger, slower scale on top of the smaller, quicker oscillations of the subject CG during the gait cycle (Figure 21). The nonuniform shape to the pelvis centroid peaks showed there were changes to the body dynamics near its peak excursion. This was most likely the result of dynamic collisions with the CG rig via the harness as a result of the phase difference.

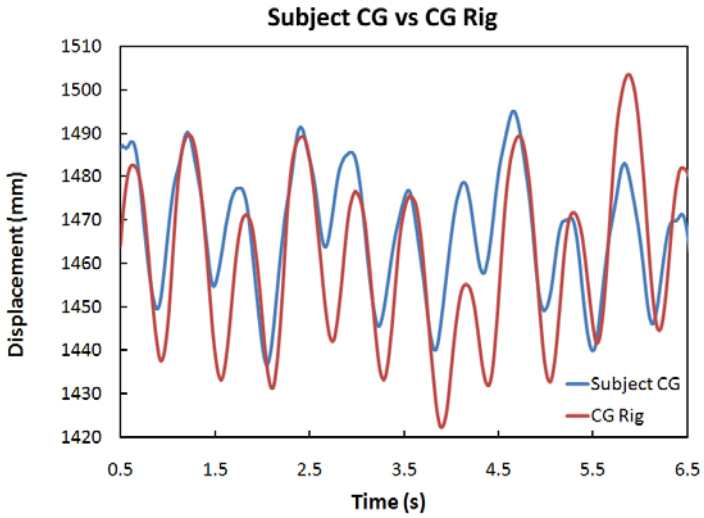

Figure 20. Sample of the vertical motions of the pelvis, taken at its centroid, as compared to the vertical motion of the center of the CG rig. (NOTE: The CG rig data points are shifted vertically by a static offset for graphing purposes.)

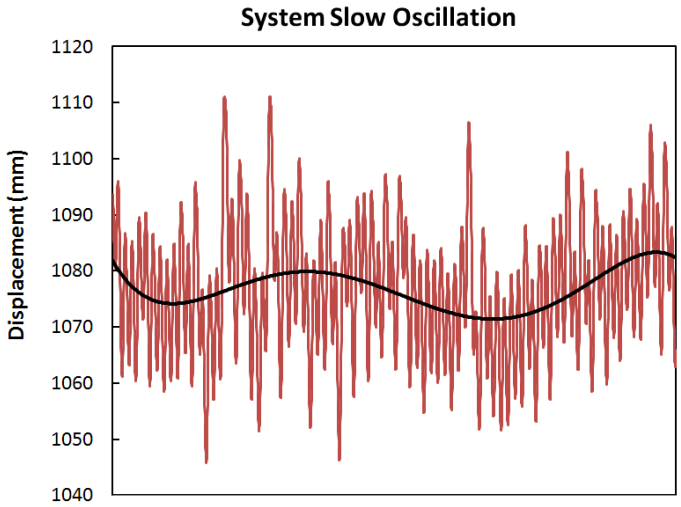

Figure 21. Plot of the CG rig (red) with a 6th-order polynomial fit (black) showing the slower system oscillation during 36 s of ambulation.

Inertial forces in the POGO test environment

Inertial forces are not often thought about as they do not exist until an object with mass begins to accelerate. The human body is constantly accelerating and decelerating during ambulation, although ambulation may be at a constant speed. Aside from the whole body CG accelerations, each body part (except for the head) is usually in some kind of dynamic motion. Therefore, each segment mass requires a small force to get it moving and then to slow it down again.

When ambulating in an environment such as that of the POGO, the gimbal has a substantial added inertia, as does the CG rig. In total, the CG rig and gimbal more than double the body's normal mass and add over 15 times the upper body's normal rotational inertia. As the body translates and rotates, the added mass and inertia become quite substantial, requiring the body to compensate and change normal dynamics

to limit the additional energy needed. Table 4 shows the inertial parameters of the human male standing and the human male torso segment against those of the current POGO gimbal. The principal axes for all three systems are located at the relative CG and are nearly coaxial to each other. The Ixx axis is anterior-posterior (frontal plane), the Iyy axis is medial-lateral (sagittal plane), and the Izz axis is superior-inferior (transverse plane).

Table 4 Inertial Comparison Among an Average Human Male Standing, the Human Male Torso Segment Only, and the POGO Gimbal

Moment of Inertia ($kg \cdot m^2$)	*Standing*	*Torso Only*	*POGO Gimbal*
Ixx (AP, through CG)	13.40	1.62	0.03
Iyy (ML, through CG)	11.89	1.08	3.95
Izz (SI, through CG)	1.72	0.38	14.54

4.2.2.2 Temporal-spatial Characteristics

Temporal-spatial characteristics pertain to a series of parameters that can be measured during ambulation that helps to differentiate changes in gait strategy or compensation for changing conditions. Primarily, these characteristics include timing of specific characteristics of gait (eg, time between initial contacts) or the spatial distances in which these characteristics occur (eg, linear distance between the feet at the initial contact).

Stance time

Stance time refers to the amount of time during the gait cycle that the foot is in contact with the walking surface. In the current study, subjects exhibited a consistent decrease in mean stance time with increased ambulation speed (Figure 22). Additionally, the variability observed across conditions notably decreased with increased speed.

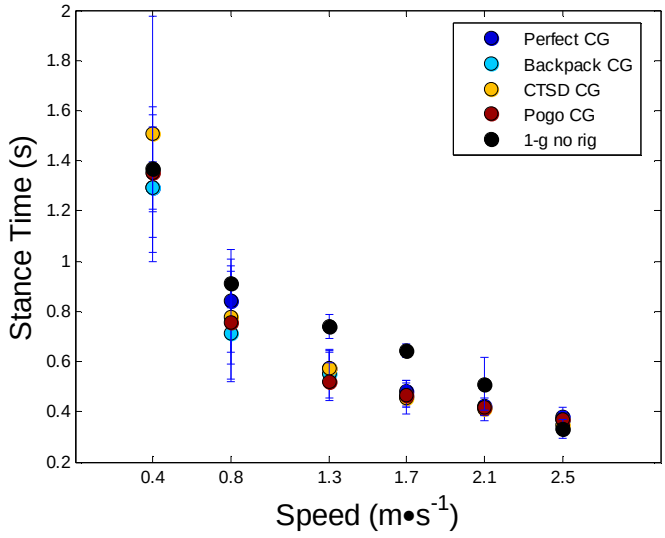

Figure 22. Mean stance time in seconds for shirt-sleeved ambulation on a level treadmill at different speeds. All varied CG conditions were performed at simulated lunar gravity.

Figure 23 illustrates the variation observed between the various CG conditions and the 1-g, no-rig condition. A notable variation in stance time values was observed at an ambulation speed of 0.4 $m \cdot s^{-1}$, possibly because ambulating at such a slow speed elicited the adoption of inconsistent gait patterns by

subjects. The largest percentage difference for all CG conditions, except for that of the "POGO CG," was observed at the 1.7 m•s^{-1} speed (~ -25% to -28% difference from 1-g) that may indicate inconsistent gait patterns adopted by subjects at this speed while attached to the CG rig and being offloaded to simulated lunar gravity. As seen in the GRF data, stance time for the CG conditions plateaus at the faster speeds, whereas the 1-g stance time does not.

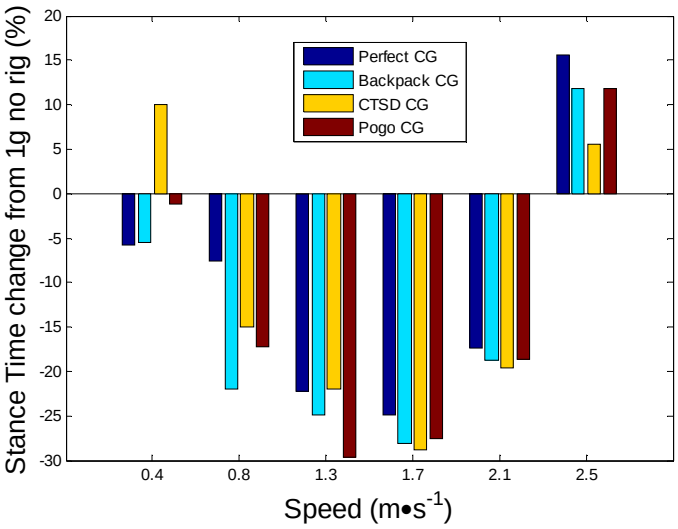

Figure 23. Percentage difference for stance time between varying CG conditions and the 1-g, no-rig condition as a function of speed.

Step width

Step width refers to the medial-lateral distance between the left and the right foot during the support phase of the gait cycle (ie, the portion of the gait cycle in which the foot is in contact with the walking surface). This metric can be used to provide an indication of stability during gait, with wider step widths suggesting greater amounts of effort to maintain stability.

Mean-step width decreased modestly with increased ambulation speed (Figure 24). Mean-step width for the 1-g condition was consistently lower than mean-step width for the varying CG rig conditions, with the exception of the 1.7 and 2.1 m•s^{-1} speeds. These results suggest a greater amount of stability during ambulation under 1-g conditions.. This is also demonstrated by notable percentage differences between offloaded conditions and the 1-g condition (Figure 25).

The lowest mean-step width for all conditions occurred at the fastest ambulation speed (2.5 m•s^{-1}), suggesting an increased amount of stability during stance at this speed. This may be because the stance time at this speed is considerably lower than at slower ambulation speeds (Figure 24). Additionally, subjects were less prone to making minor adjustments during each step/stride to maintain posture and forward progression at the faster gait speeds than at the slower gait speeds.

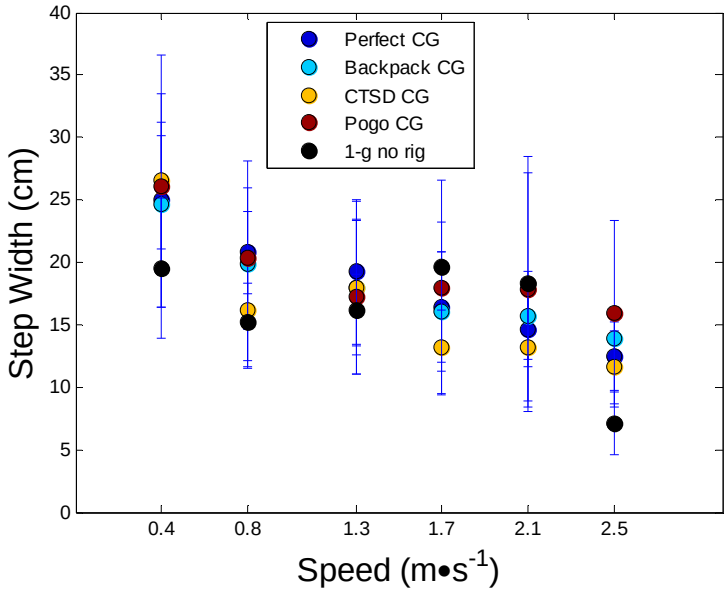

Figure 24. Mean step width for shirt-sleeved ambulation on a level treadmill at different speeds. All varied CG conditions were performed at simulated lunar gravity.

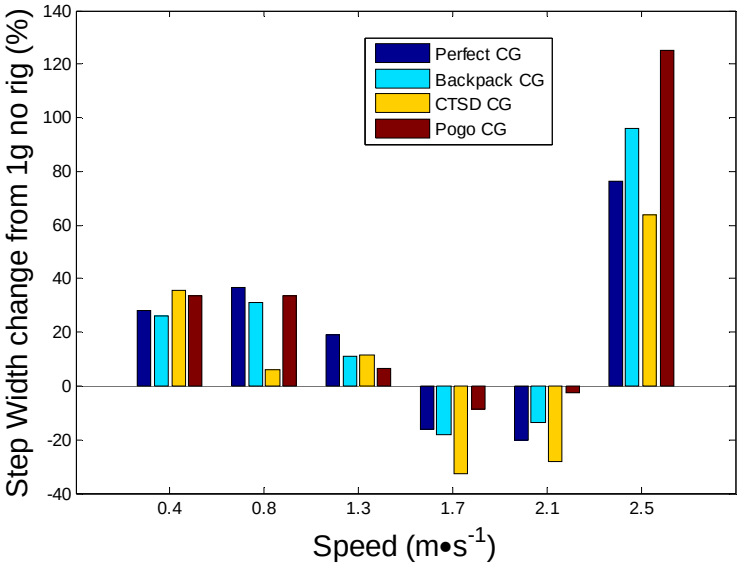

Figure 25. Percentage difference in step width at different speeds between varying CG conditions at 1/6-g and the 1-g, no-rig condition.

Mean-step width was examined using line plots to compare varying CG rig conditions to the 1-g, no-rig condition. Differences were calculated using three-dimensional trajectories of feet markers from motion capture data. It should be noted that differences exist between the following data and those presented in earlier figures (Figure 26). The reason for this involves the method used to determine and calculate step width. For instance, Figure 24 and Figure 25 represent data that involve plotting of marker trajectory only. However, on review of video footage, it was noted that several subjects adopted an off-balance gait when performing ambulation tasks. Therefore, the results provided in the main body of the report reflect calculations that addressed this off-balance gait by accounting for the asymmetrical orientation of the

pelvis. The Figure 26 plots, while calculated differently than preceding figures, still provide relevant data for examination of the effect of offloading and added mass on step width for an unsuited subject.

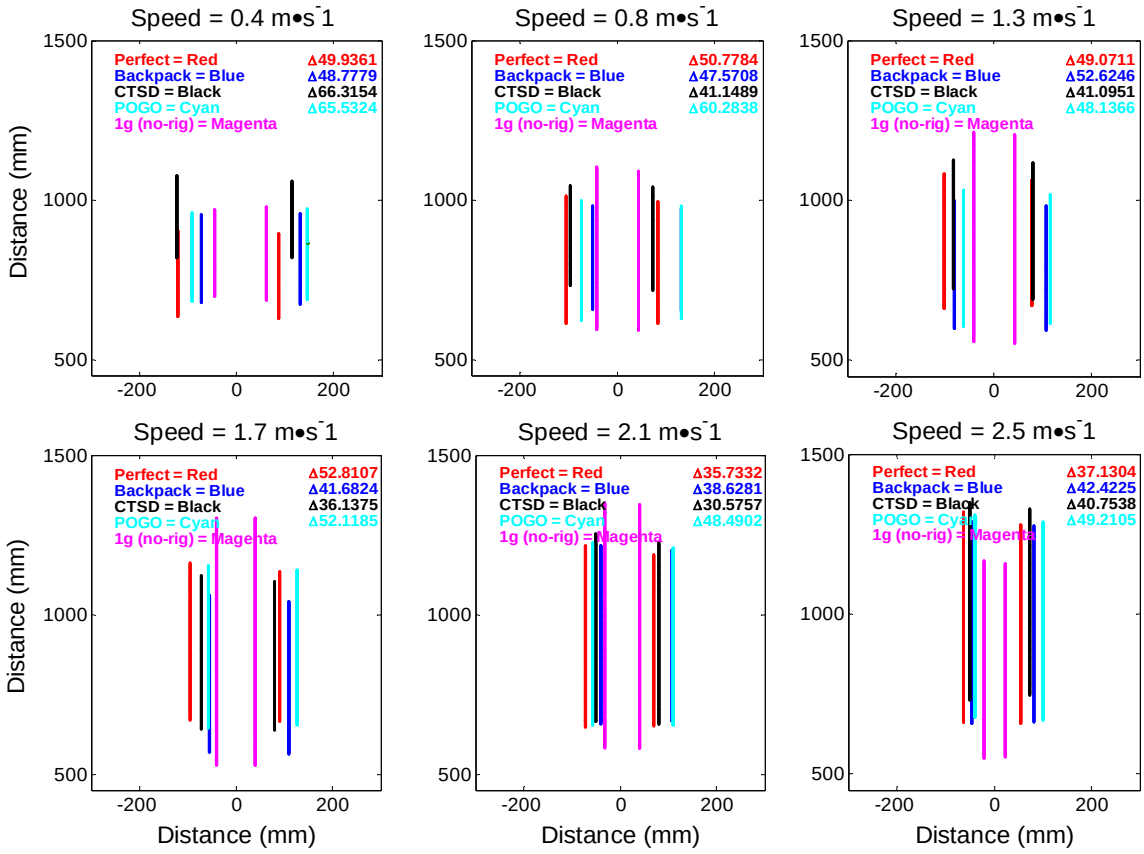

Figure 26. Change in step width among varying CG conditions and the 1-g, no-rig condition for tested ambulation speeds.

The inability of subjects to attain any consistent, cyclic motion in their gait pattern while ambulating at 0.4 m•s^{-1} led to greater variability in step width. In fact, the 1-g, no-rig condition appeared to have a wider step width at this speed than any other speed (Figure 26), suggesting difficulty in maintaining consistency of gait at this speed.

For all gait speeds other than the slowest (0.4 m•s^{-1}) and fastest (2.5 m•s^{-1}), the smallest difference from the 1-g, no-rig condition was observed for the "CTSD" condition. For both running speeds (2.1 and 2.5 m•s^{-1}), the "POGO" condition was associated with the greatest difference from the 1-g condition. This finding suggests that when subjects were ambulating at speeds requiring clear, single-leg support and a greater swing phase of gait (i.e. running), the "POGO" condition was detrimental to unsuited performance. One explanation for this may be that subjects needed greater effort to maintain an appropriate posture due to the additional inertia of the apparatus in that configuration. As such, they may have compensated via wider step width to maintain stability while ambulating at these higher speeds.

Kinematics

For the review of kinematic data, first it is important to define some of the terminology used to describe the joint kinematics in the following discussion. The term flexion describes a decrease in relative angles between segments, and extension is an increase in relative angles between segments (Appendix A). Flexion will always be referred to as a positive angle; extension will always be referred to as a negative angle. This is not to be confused with an isolated joint range of motion (ROM). For example, an isolated

hip flexion has a clearly defined starting and stopping point, namely the thigh segment moves from a neutral position of 0° and achieves some value of "X" before returning to the neutral position of 0° (Figure A-4). However, during gait the subject may never achieve a neutral position, given the dynamic nature of the movement. More specifically, gait is not a series of isolated movements; numerous concurrent actions are taking place during walking. Therefore, the accepted method of reporting joint angles is in terms of increases in relative angles between segments (extension) or decreases in relative angles between segments (flexion), or as total motion of the joint, expressed as a ROM. To be consistent with previous tests, the generic term *initial contact* will be used to describe the instant at which the foot just touches the floor; conversely, for end-of-the-floor contact, the generic term *end contact* will be used.

Joint angles typically tell a story of how the human body is adapting to internal and external conditions to make smooth ambulation possible. Deviations from normal gait are observed and analyzed as to their magnitudes, timing, and curve shape among others. During IST-3, joint angle ROM for the ankle, knee, hip, and torso in the sagittal plane of motion was recorded (Figure 27 and Figure 28). Notice in the figures that there was little consistency between 1-g gait and gait while in the CG rig.

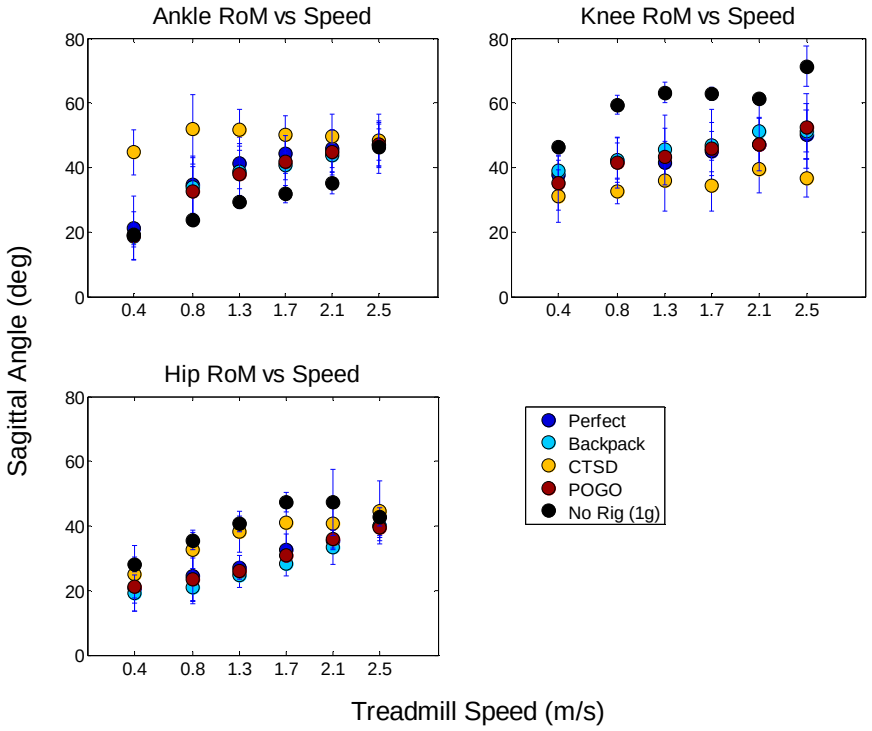

Figure 27. Joint angles averaged over subjects and gait cycles, categorized by CG condition, and plotted against speed. Error bars represent the standard deviation of the subject averages.

The one exception to this was at the highest speed for the ankle and hip ROM. It was also noted by analysis that the preferred method of ambulation while in the POGO was loping or hopping. This deviance changed for the ankle and hip angles at the fastest speed for all conditions as the subjects changed from a walk to a run in the 1-g condition. The knee and torso angles still retained their deviance. The difference in knee angles was due to the knee not having to flex as much to allow for toe clearance during the swing phase while hopping in the POGO. The torso angle difference was due to the restriction in movement by the POGO system, which prevents proper adaptation to changing conditions. Figure 29 shows changes in ROM with respect to 1-g ambulation. Most noteworthy in this graph is the fact that the difference in the torso angles remained high throughout all conditions and speeds as a result of the inability of subjects to lean during ambulation. Difference in knee angles also remained high as the lofting motion of the lope reduced the need for the knee to flex to create adequate toe clearance.

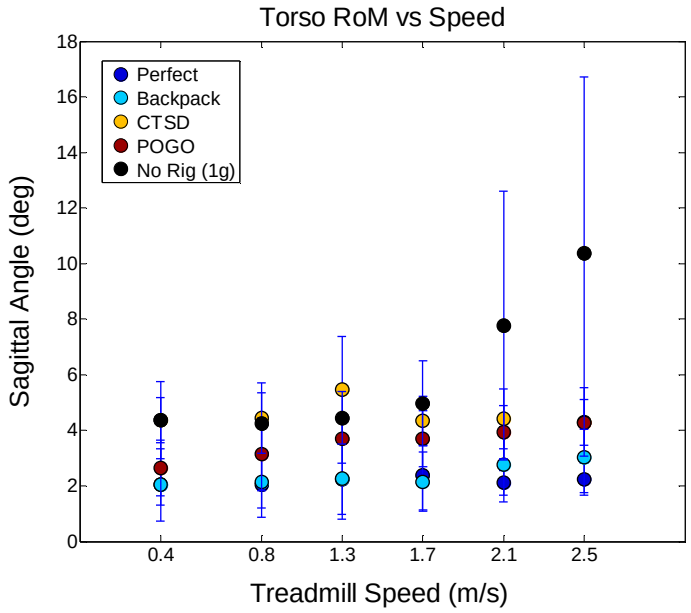

Figure 28. Torso joint angles averaged over subjects and gait cycles, categorized by CG condition, and plotted against speed. Error bars represent the standard deviation of the subject averages.

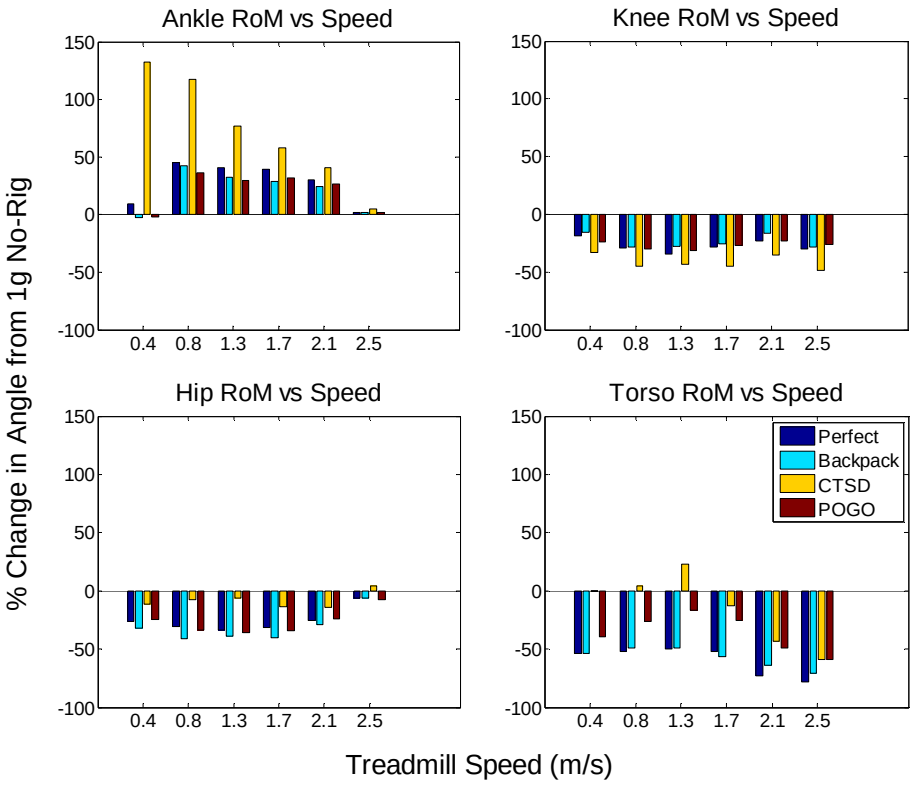

Figure 29. Percentage change in ROM of each CG condition from the unsuited 1-g baseline plotted against speed.

The next several graphs show the average angles for specific joints over the gait cycle separated by treadmill speed (Figure 30 to Figure 33) Most noticeably, in all the figures the distinct differences in patterns between unsuited Earth-gravity ambulation and ambulation on the POGO can be seen. These

patterns differ by shape, magnitudes, and timing of the maximum flexion and extension. Interestingly, little change was noted among the different CG conditions over the range of speeds, and only slight changes were noted among the conditions themselves. This presented a marked difference from the 1-g no rig condition, which had distinct changes in patterns and timing as the speeds progressed, especially at the highest speed (2.5 m•s^{-1}) when the subjects changed from a walk to a run.

For the ankle angle (Figure 30), the shape of the CG rig traces across all speeds were very similarly shaped to those of the 2.5-m•s^{-1} unsuited 1-g trace. This shape was primarily due to abrupt loading at the heel immediately followed by peak plantar flexing for end contact. Likewise, the timing patterns of the peak plantar flexion angle changed with speed in an unsuited, 1-g environment between a walk and a run. The timing of the unsuited 1-g trace at 2.5 m•s^{-1} was typical for running as the percentage of the gait cycle in contact with the floor decreases, allowing for a longer stride and greater speed.

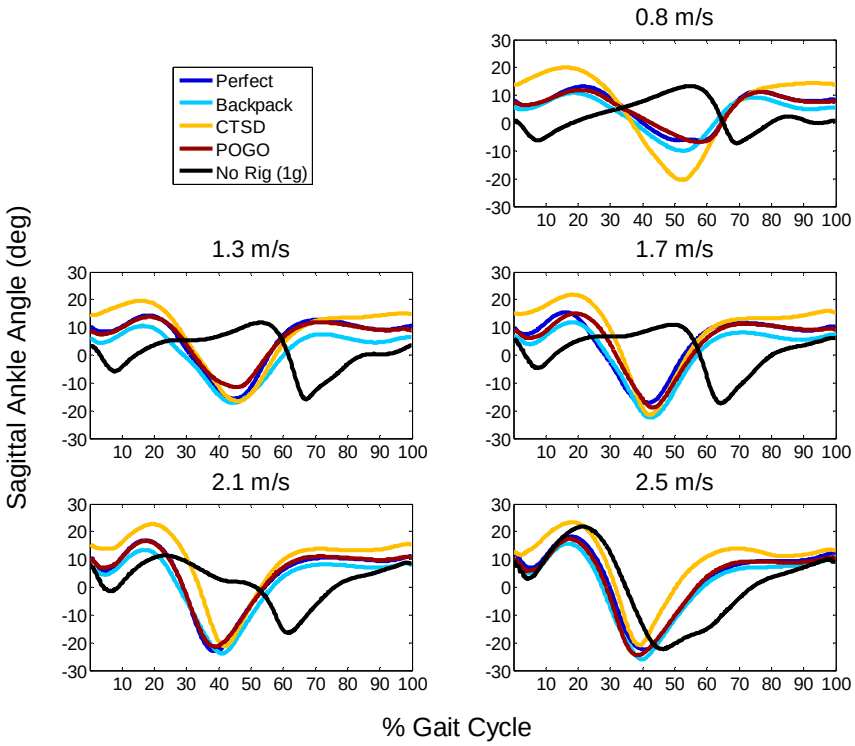

Figure 30. Ankle joint angle traces over one gait cycle for each CG condition. Each plot is at specific speed.

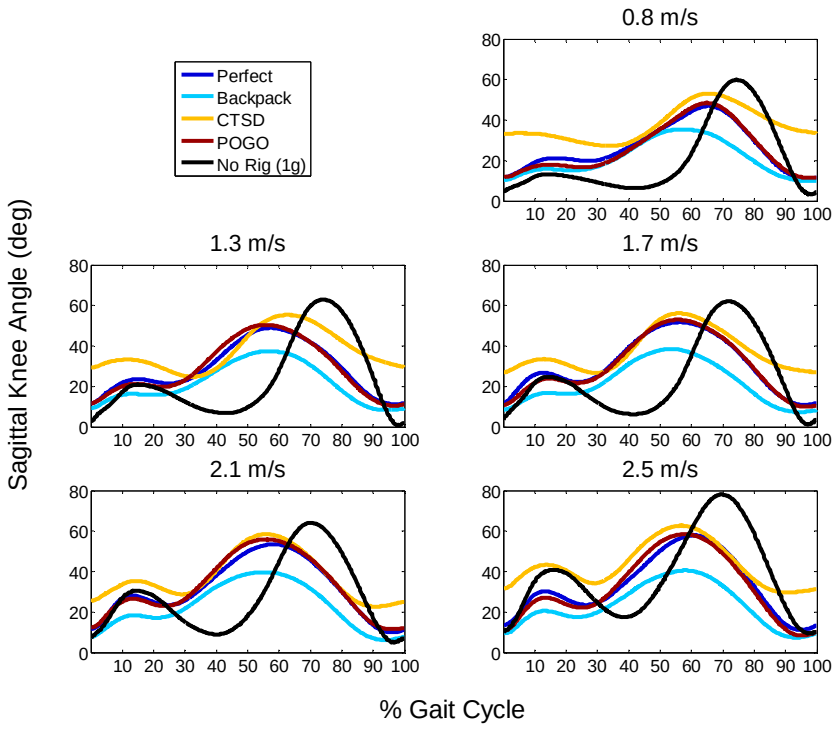

Figure 31. Knee joint angle traces over one gait cycle for each CG condition. Each plot is at specific speed.

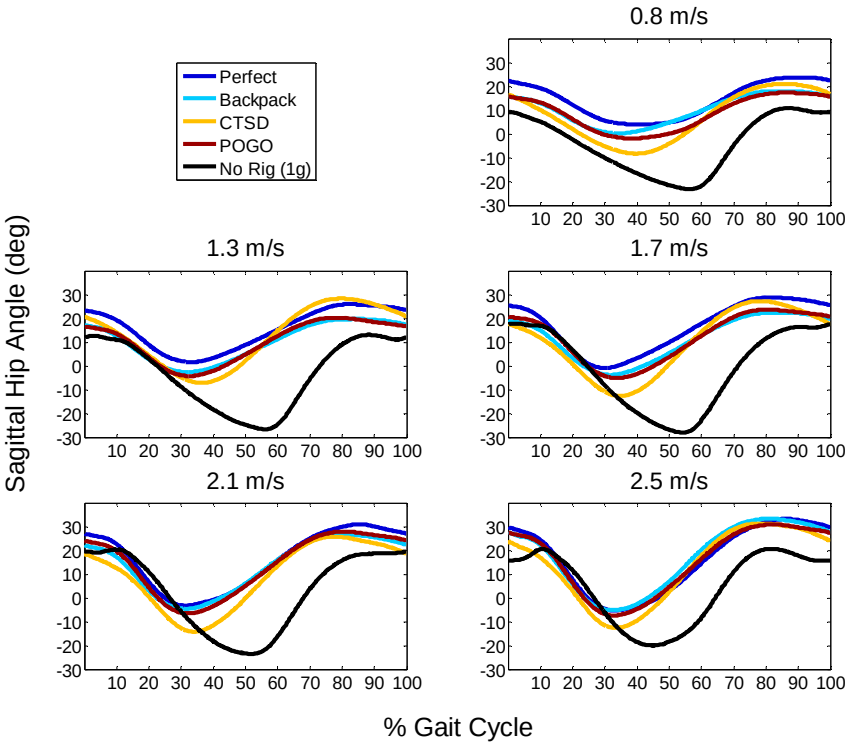

Figure 32. Hip joint angle traces over one gait cycle for each CG condition. Each plot is at specific speed.

For the torso angle (Figure 33), the shapes of the CG rig traces were fairly uniform in magnitude and amplitude as speed increased compared to the unsuited 1-g condition. For the unsuited 1-g condition, the angle decreased before it increased as the body used a strategy of transferring forward momentum from initial contact to end contact. As speed increased, this shifting became more pronounced. As the stance phase of gait cycle shortened with speed, tilting adjusted equally. The exception to this was again the CTSD condition, in which the subjects tilted back as the speed increased. In the other conditions, subjects remained at a constant forward tilt throughout the speed conditions.

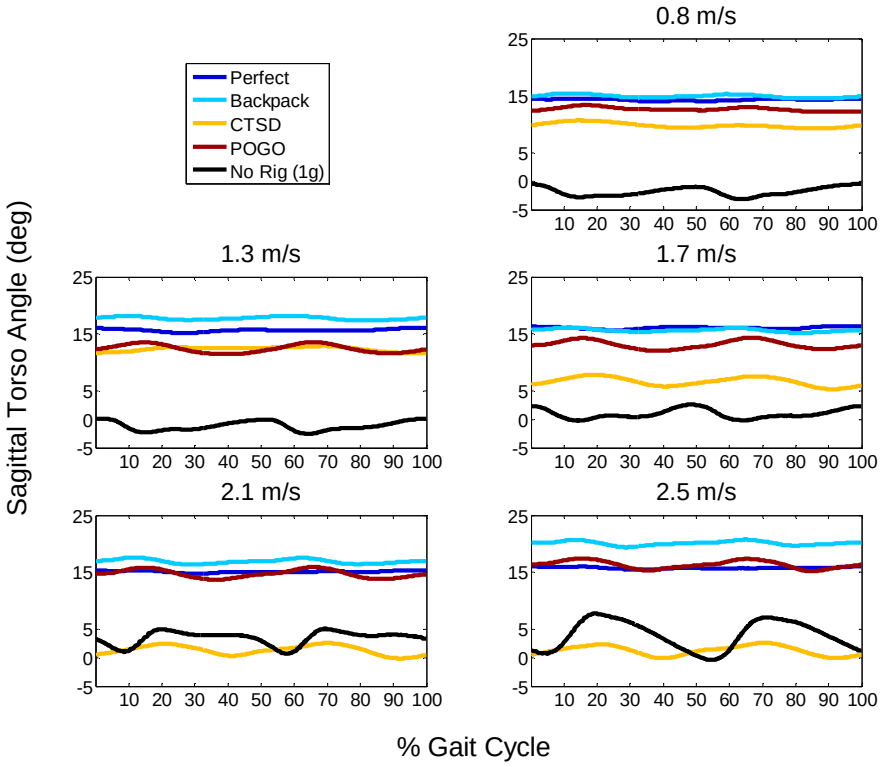

Figure 33. Torso angle traces over one gait cycle for each CG condition. Each plot is at specific speed.

Offloading mechanics

This section will take a more in-depth look at how the POGO and gimbal/CG rig systems are interacting with the human subject. This comparison will primarily be done in the sagittal plane.

Changes to traditional heel strike and toe-off patterns were not always observed during the CG rig trials. Figure 34 shows the difference in lower limb kinematics at end contact when unsuited (left) and in the CG rig (right). In the CG rig trial, stance phase of the gait cycle and the contact angle of the leg have been shortened so the leg can no longer produce as much propulsive force in the forward direction. Figure 35 shows the difference in lower limb kinematics at initial contact when unsuited (left) and in the CG rig (right). In the CG rig trial, stance phase of the gait cycle and contact angle of the leg have been shortened so the leg no longer absorbs energy produced by the body's forward momentum. The reduction of the stance phase of gait and of leg angles over that contact period would indicate that the body no longer imparts as much energy into the ground for propulsive means. If the body were still imparting force into the ground to move the body CG, the mechanics of the system dictate that the body was using primarily vertical propulsive forces.

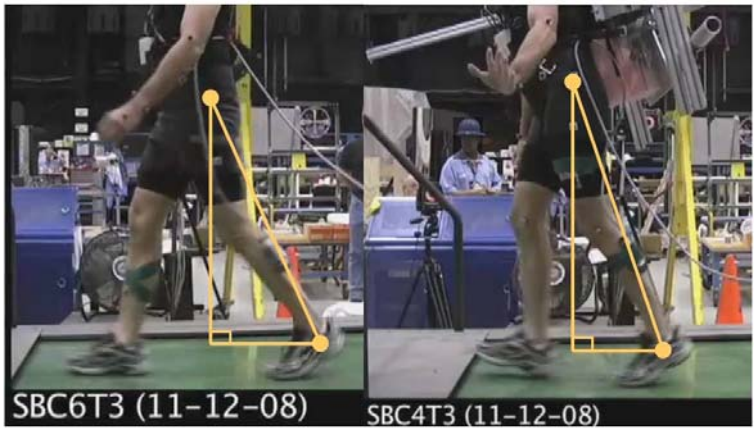

Figure 34. End contact shown unsuited (left) and on the POGO with a rig (right). Yellow lines indicate the angle of the leg with respect to vertical.

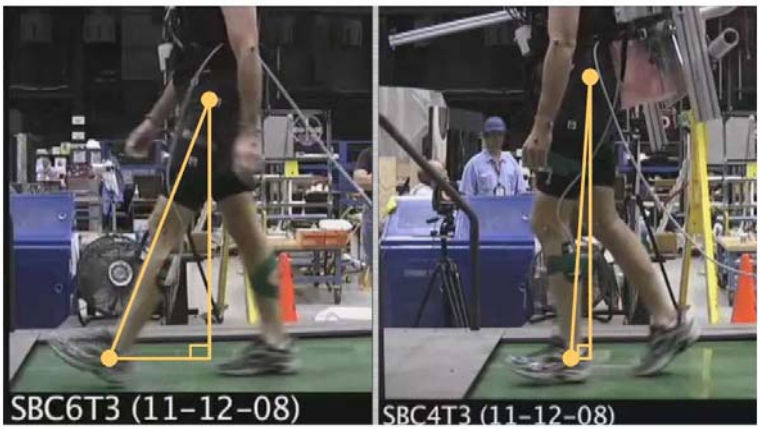

Figure 35. Initial contact shown unsuited (left) and on the POGO with a rig (right). Yellow lines indicate the angle of the leg with respect to vertical.

Figure 36 shows how the body had to compensate differently for the CTSD CG. In this case, the subject shown has compensated by lowering the pelvis and putting the hip, knee, and ankle in more flexion at initial contact and more hip extension at end contact. This type of compensation is seen when a human is pulling or pushing objects.

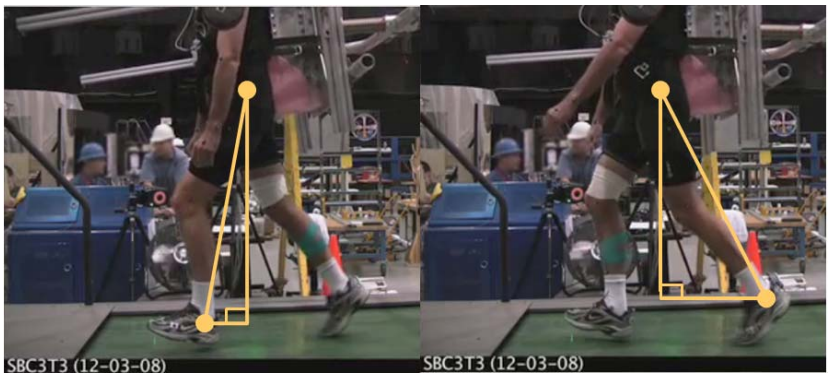

Figure 36. Initial contact and end contact on the POGO at the CTSD CG condition. Yellow lines indicate the angle of the leg with respect to vertical.

4.2.2.3 Electromyography

The subject's maximal voluntary contractions (MVCs) for the muscles were not recorded. Testing was done over a 2- to 3-day period. With the reapplication of electrodes days apart from the previous test day, the EMG signals were not comparable and; therefore, the MVC baselines would not be as useful. To compensate for this, a second method that applied a double-threshold detector to the raw EMG signal was used (18). However, an unforeseen complication was the heartbeat artifact in the rectus abdominis. High-pass filtering (19) was unsuccessful at removing this artifact due to the artifact having a frequency in the middle of the range of the EMG frequencies.

Due to complications during testing, only two subjects had a full data set to analyze. Because of the complexity of the post-data-collection analysis due to the aforementioned problems incurred during testing, only the erector spinae of one subject was analyzed for this report and presented as an example.

EMG results for the erector spinae at the level treadmill condition of 1.7 $m \bullet s^{-1}$ are presented in Figure 37. Shades of grey represent the instantaneous amplitude of the full-wave rectified signal. Three shades were chosen to show the level of activation based on the maximum of the rectified, smoothed signal. The darker shade signifies higher amplitude while a lighter shade signifies lower amplitude but still activation. The shade of gray is based on that trial only. Plots from all trials are included in Appendix E.

At this ambulation speed, toe-off occurred at approximately 35% of the gait cycle. The Perfect, Backpack, and POGO CG rig conditions were fairly similar, with the right side erector spinae firing during the middle of the swing phase, which was also the middle of the stance of the left foot. The CTSD CG rig condition showed a longer period of activation. This longer period of activation would indicate more work was being done by these muscles for this condition over that of the other muscles. A noticeable difference was noted between each of the CG rig conditions and the 1-g unsuited condition. The 1-g unsuited condition had a burst of activity during initial contact and during the swing phase, which was normally seen (20).

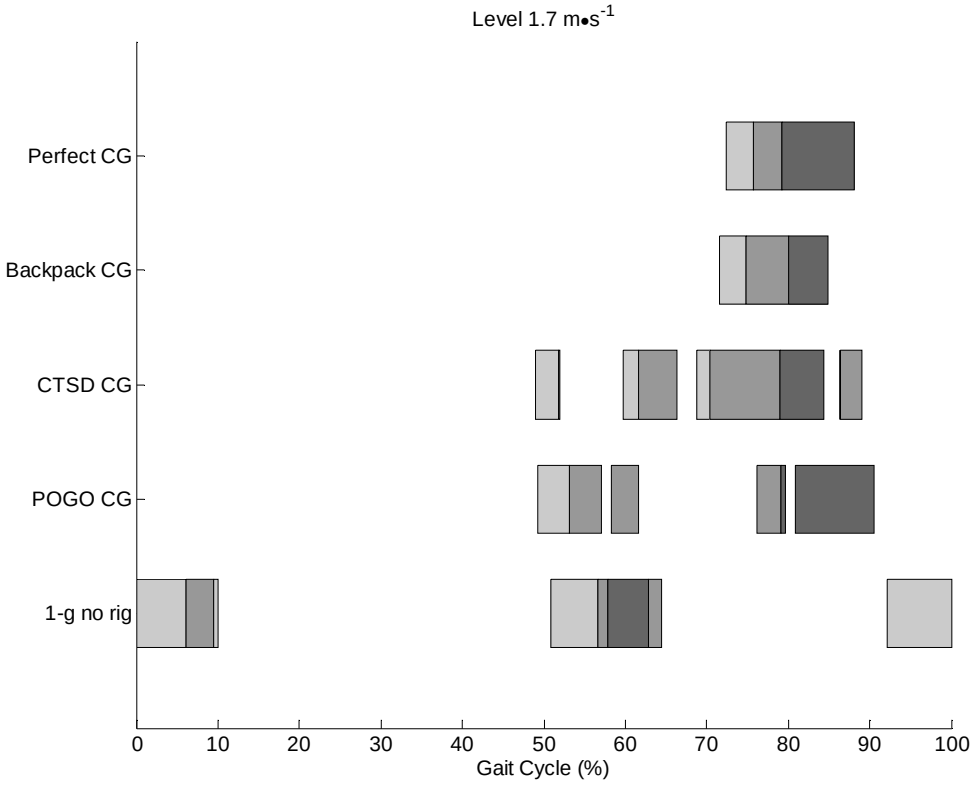

Figure 37. Erector spinae muscle activity during a gait cycle at 1.7 m•s^{-1}. The gray shading indicates the intensity of the contraction.

4.2.2.4 Subjective Results and Discussion

All references to subjective data refer to the end-of-stage subjective ratings taken at the 3-min mark unless otherwise stated.

4.2.2.5 Rating of Perceived Exertion

With the exception of 1-g data, RPE trends (Figure 38) were very similar to metabolic trends (Figure 14). Mean RPE for the CTSD condition was significantly greater than all other CG conditions across all speeds, although the standard deviation range did have some notable overlap with the other CG conditions that was not present in the metabolic data. The 1-g RPE ratings, seen at 2.1 and 2.5 m•s^{-1}, were very similar to the values of the non-CTSD CGs, which was not the case with the metabolic data. This indicates that subjects rated RPE differently under different conditions, such as freestanding in 1-g vs. offloaded while connected to the gimbal support structure with CG rig. This is a similar finding to what was seen in previous studies in which RPE was rated differently in the suited and unsuited conditions (5) (1) (2).

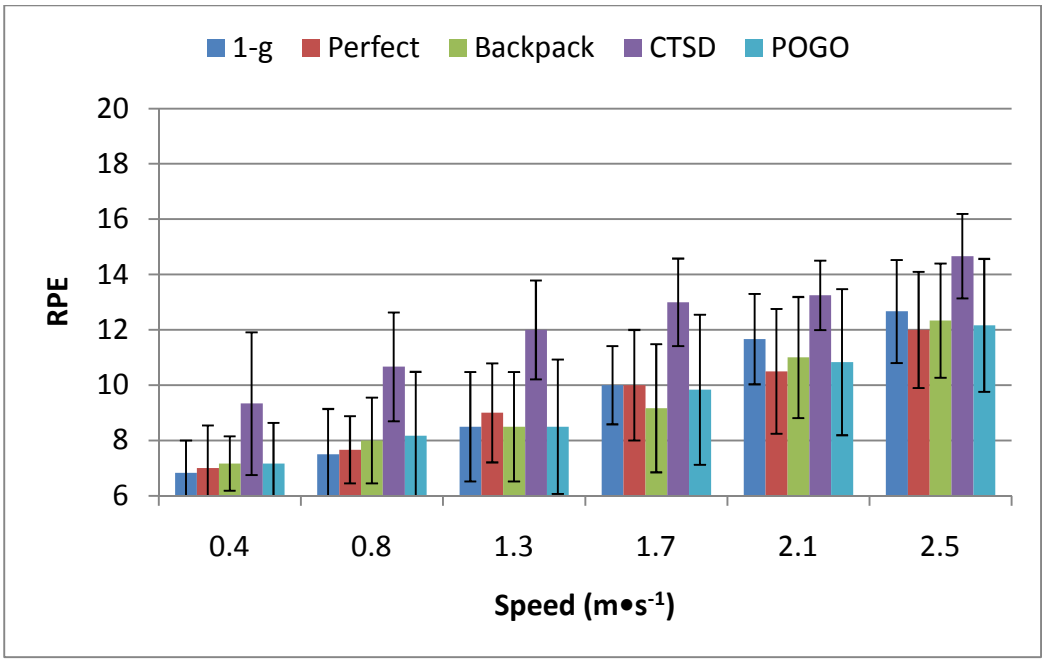

Figure 38. RPE at different CG conditions during shirt-sleeved ambulation on a level treadmill.

4.2.2.6 Gravity Compensation and Performance Scale

GCPS ratings, which are shown in Figure 39, were significantly greater with the CTSD CG than with any other CG. Mean ratings at the CTSD CG indicated that modifications were warranted or required to attain desired performance. Ratings at all other CGs were similar and trended towards either desired performance or some modifications warranted to achieve desired performance. In addition, there was a subtle trend for GCPS to increase with speed, with the greatest increase coming at speeds $\geq$ 2.1 m•s^{-1}.

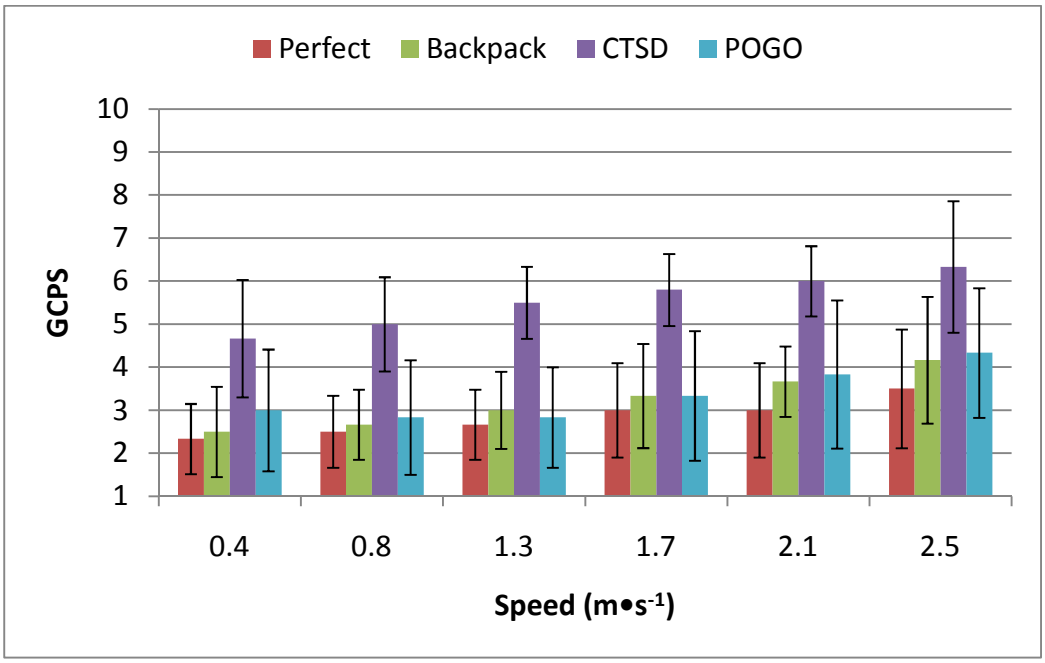

Figure 39. GCPS at different CG conditions during shirt-sleeved ambulation on a level treadmill.

4.2.2.7 Subjective Rating Changes from 30 to 150 Seconds

In previous ground-based studies, RPE has been measured only near the end of steady-state tasks. Aside from a few exceptions, RPE was taken after 2+ min of steady-state activity, including level and graded ambulation, shoveling, rock transfer, and busy board tasks (5) (1) (2). GCPS has been used on both short and long tasks, and was taken at the same time RPE was obtained or taken immediately on completion of shorter tasks. In this study, RPE and GCPS were measured at both the 30-s and 150-s mark of the 180-s trials. Figure 40 shows the change in RPE and GCPS from the 30-s mark to the 150-s mark of the 180-s trials during level ambulation. In over 90% of the trials, the ratings either stayed the same (71% RPE, 82% GCPS) or increased by one (23% RPE, 12% GCPS).

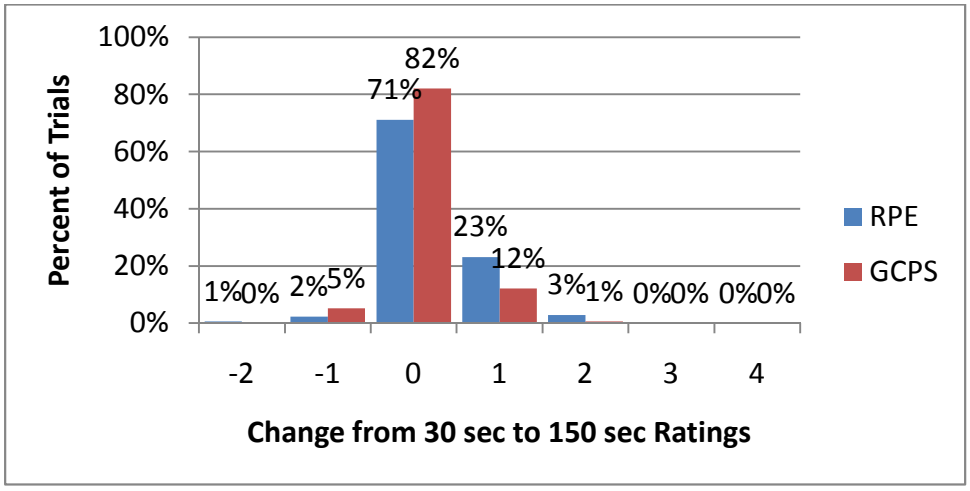

Figure 40. Change in subjective ratings from the 30-s mark to the 150-s mark in a 180-s level-ambulation trial (*n* = 173).

4.3 Graded Ambulation

Out of 120 trials, 114 were completed. All of the missing trials come from the CTSD CG condition. Half of the missing trials were not completed because the subject exceeded the maximum HR, as described in Appendix F, during the prior trial. The other half were not completed because of subject discomfort and positioning difficulty. An additional 30 trials from the level-ambulation data set are included in the graded ambulation dataset because they provide 0% incline data at 0.8 $m \cdot s^{-1}$.

4.3.1 Metabolic results and discussion

Metabolic rate was very similar for all varied CGs, except for CTSD, which had significantly higher mean metabolic rates at all grades (Figure 41). With the exception of the aforementioned CTSD results, the baseline 1-g results were similar to the varied CG conditions at -10% and 0% grade. Baseline 1-g results were slightly greater than all but the CTSD at 10%, and were significantly (>3.5 $mL \cdot min^{-1} \cdot kg^{-1}$) greater during 20% and 30% trials than all other CG conditions.

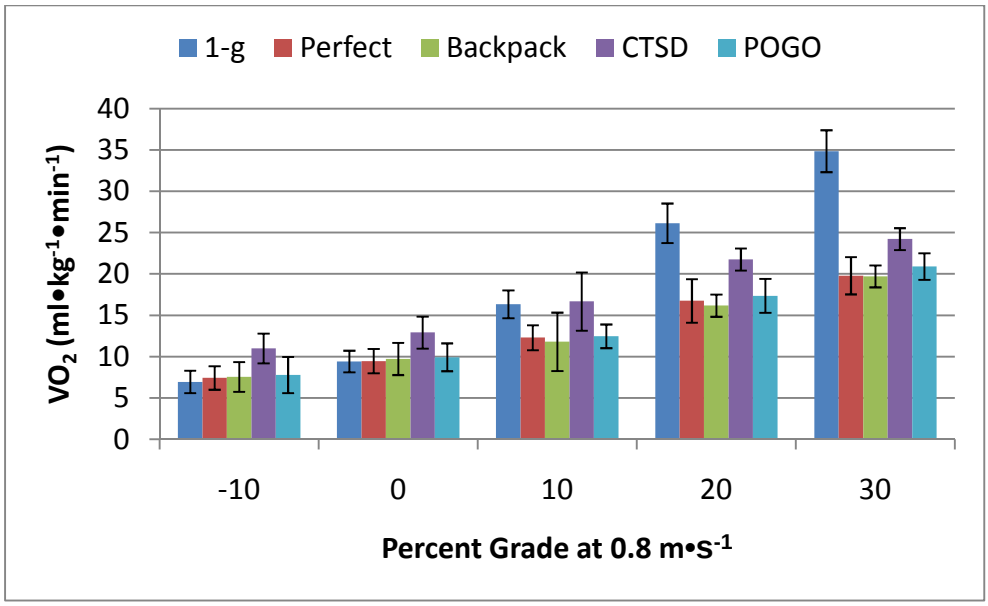

Figure 41. Metabolic rate for different CG conditions during shirt-sleeved ambulation on an inclined treadmill.

Figure 42 shows the nearly complete overlap of the Perfect, Backpack, and POGO CG conditions. CTSD trended significantly higher on average than all other CGs. Results were similar to the level treadmill data. Again, higher metabolic rates in the CTSD condition were assumed to be explained by system CG misalignment with the gimbal axes of rotation. All but the baseline 1-g data showed linear trends relating metabolic rate to grade at a constant speed of 0.8 $m \bullet s^{-1}$ at simulated lunar gravity.

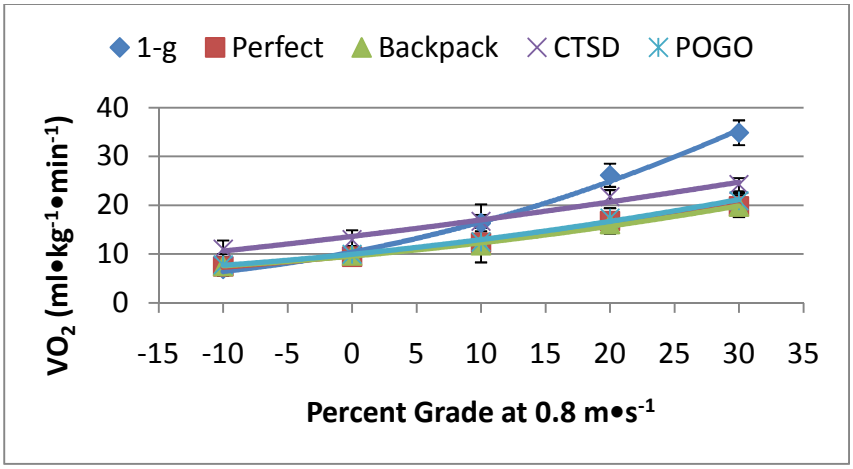

Figure 42. Metabolic rate for different CG conditions during shirt-sleeved ambulation on an inclined treadmill.

Figure 43 shows similar metabolic responses for all subjects during 1-g graded treadmill ambulation at 0.8 $m \bullet s^{-1}$. For the varied CG conditions, individual differences were not clearly evident for any CG other than the CTSD. Subjects were able to complete all trials at each condition other than the CTSD CG. The overall trends for individual subjects show a homogenous response to each CG condition with similar results and trends.

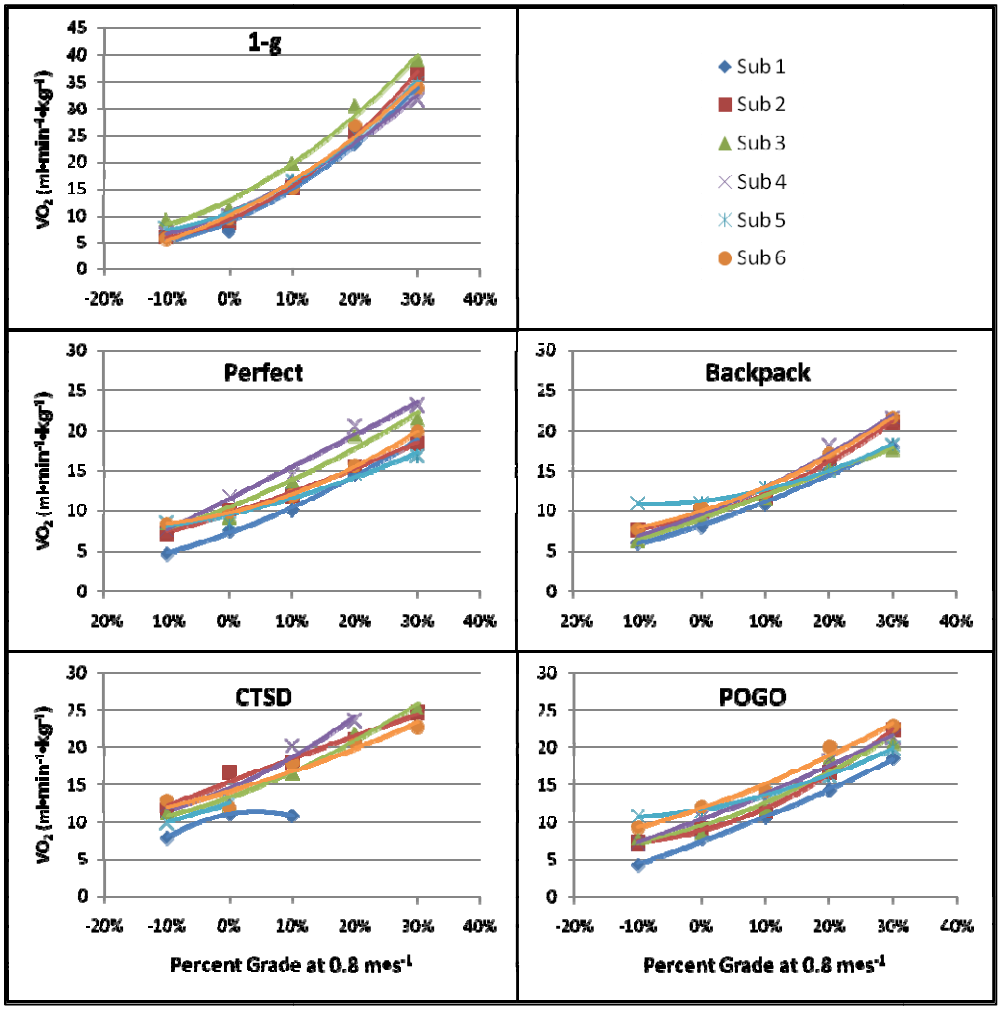

Figure 43. Individual metabolic rate responses to increasing grade on treadmill at 0.8 m•s^{-1} in 1-g and at different CG configurations at simulated lunar gravity.

4.3.2 Biomechanics results and discussion

4.3.2.1 Kinetics

Ground reaction force

Peak normalized GRF data were analyzed for subject ambulation at varying treadmill surface grades, including -10%, 10%, 20%, and 30% incline (Figure 44). All of these trials were performed at an absolute ambulation speed of 0.8 m•s^{-1} (1.9 mph). In addition to the comparison between varying surface grades, results were compared to level ambulation (ie, 0% incline) at the same absolute speed on the treadmill.

Results from the 1-g, no-rig condition reveal a small variation in mean peak normalized vertical GRF across subjects between varying surface inclines and level ambulation (Figure 44). Although not markedly smaller than for other conditions, mean GRF values were lowest for level (0%) grade ambulation. This may be attributable to subjects' familiarity with level treadmill walking compared to walking at declined or inclined surface grades. The 10% decline condition yielded the largest peak normalized vertical GRF (mean approximately 1.4 times BW), although this was not a significant increase compared to level and incline ambulation. Additionally, the largest variation was observed during subject ambulation at the 10% decline, which may be attributed to the unfamiliar task of decline ambulation on a treadmill.

The variability of mean peak vertical GRF data across subjects for offloaded, varied CG conditions was notably greater than for the 1-g condition for all ambulation speeds (Figure 44). For the CTSD condition,

mean peak vertical GRF tended to decrease with an increase in treadmill incline (approximately 0.7 BW at level (0%) walking to 0.5 BW at 30% incline), but a minimal change was observed in mean values between level and decline walking. Mean values for the CTSD CG condition exhibited a small, but consistent, decreasing trend in GRF with an increase in surface incline; but mean values for the other CG rig conditions did not reveal consistent trends across surface incline conditions.

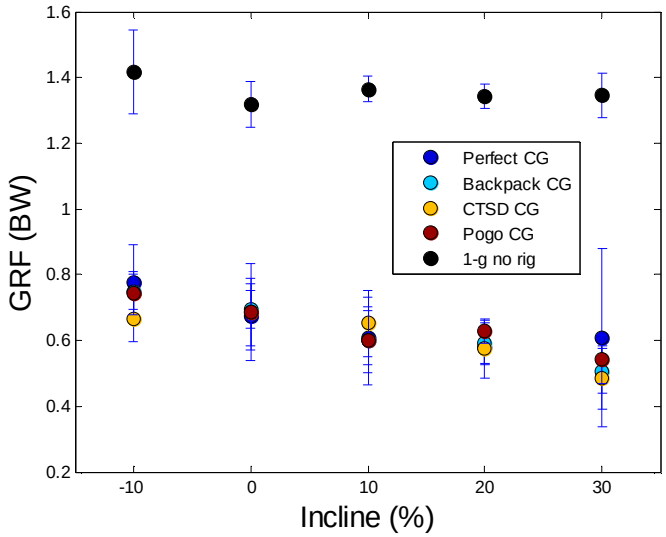

Figure 44. Mean peak vertical GRF, normalized to subjects' 1-g body weight for shirt-sleeved ambulation on a level treadmill (0%) and at surface grades of -10%, 10%, 20%, and 30%. An ambulation speed of 0.8 m•s^{-1} was used across all varying surface grade conditions. All varied CG conditions were performed at simulated lunar gravity.

4.3.2.2 Temporal-spatial Characteristics

Stance time

Figure 45 illustrates mean stance time for ambulating at 0.8 m•s^{-1} at varying surface grades. The 1-g condition shows an increase in mean stance time across subjects with increased treadmill grade from the 10% decline to the 20% incline. Mean stance time results for the various CG rig conditions do not appear to follow the same trends observed for the 1-g, no-rig condition. For all CG rig conditions except "Perfect CG," an increase in stance time was seen from level treadmill to ambulation at the 10% surface decline. No clear trends were observed across CG rig conditions regarding mean stance time for ambulating at varying surface inclines. The POGO CG and Backpack CG conditions yielded an increase in mean stance time between level walking and 10% incline, but exhibited a decrease in mean stance time as incline increased. The Perfect CG condition followed a similar pattern at these steeper inclines. The CTSD CG condition, however, showed a decreased stance time from level to 20% incline, with a slight increase in stance time between 20% and 30% incline (Figure 45). It should be noted that, except for the POGO CG condition at the -10% decline, mean stance times for all CG rig conditions were less than those for the 1-g, no-rig condition across the tested surface grades.

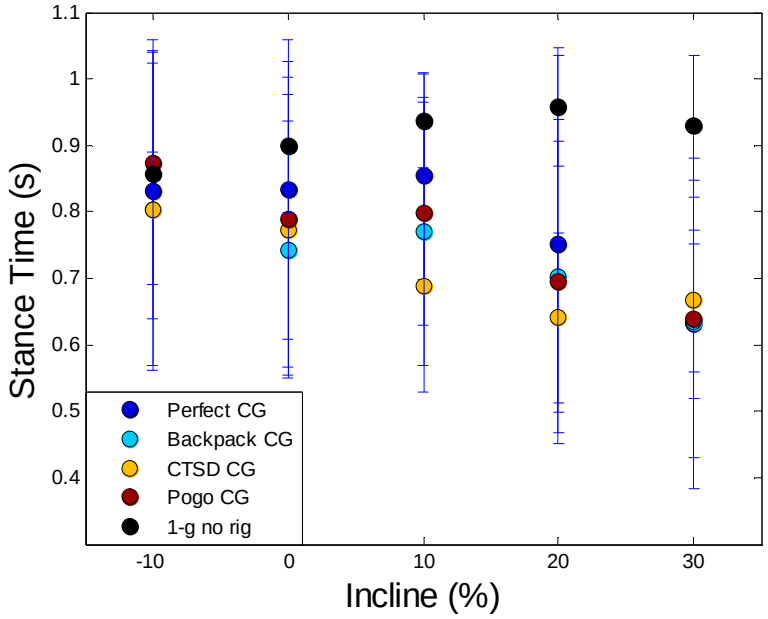

Figure 45. Mean stance time for all subjects and conditions tested across surface grades of -10 decline, 0% (level), and 10%, 20%, and 30% treadmill incline.

As shown in Figure 46, mean stance time for all conditions, except the POGO CG at the -10% decline, is less than mean stance time for the 1-g, no-rig condition. At the steepest incline (30%), stance time for all CG rig conditions was less than stance time for 1-g ambulation at the same incline by greater than 25%.

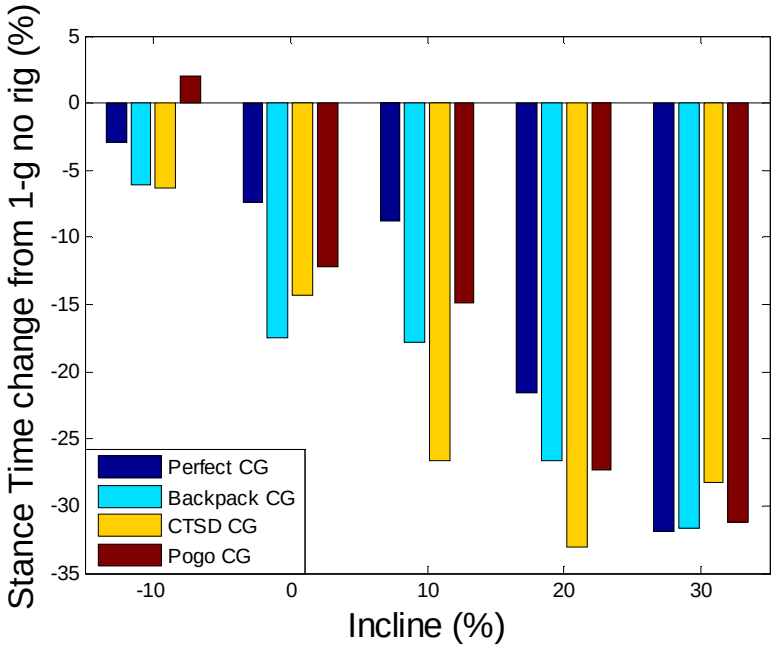

Figure 46. Percentage difference for stance time between varying offloaded conditions and the 1-g, no-rig condition across surface grades of -10% decline, 0% (level), and 10%, 20%, and 30% treadmill incline.

Step width

Figure 47 shows minimal differences in mean-step width across varying surface grades for 1-g, no-rig ambulation. All mean values for this condition corresponded to a step width of approximately 0.1 to 0.15 m. Mean-step width values for all varying CGs were larger than values for the 1-g, no-rig condition. The largest deviation from the 1-g condition was observed at the -10% treadmill grade (~120% greater than 1-g conditions), while the smallest deviation (~5% greater than 1-g) was seen at the 20% treadmill grade for the POGO, Perfect, and Backpack (Figure 48). The percentage difference between the CTSD and the 1-g conditions increased between level walking and 20% grade conditions. No remarkable difference was observed in percentage difference from 1-g between 20% and 30% grades.

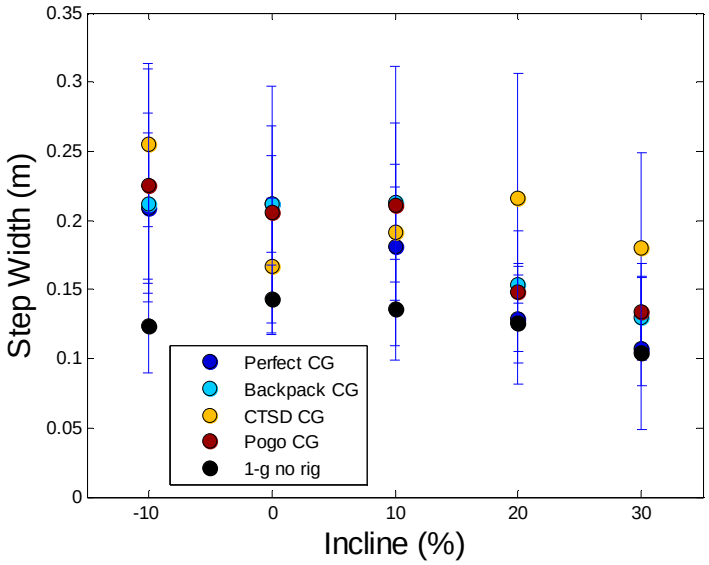

Figure 47. Mean step width (m) for all subjects and conditions tested across surface grades of -10% decline, 0% (level), and 10%, 20%, and 30% treadmill incline.

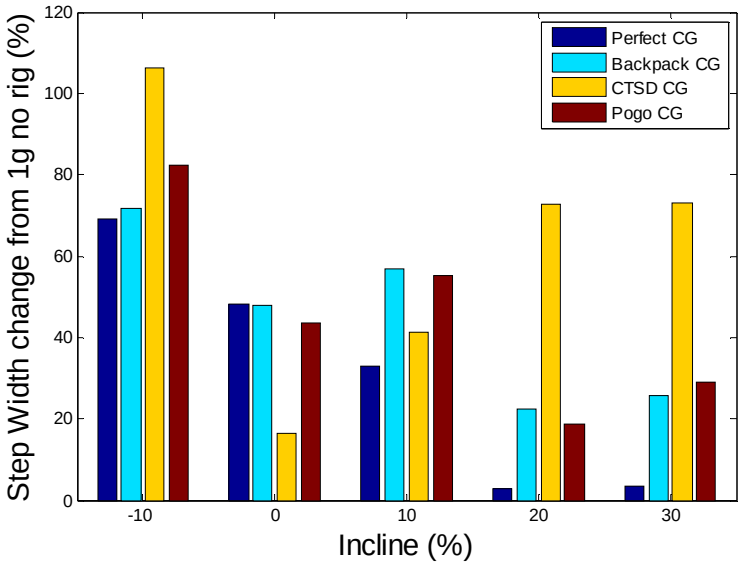

Figure 48. Percentage difference for step width between varying offloaded conditions and the 1-g, no-rig condition across surface grades of -10% decline, 0% (level), and 10%, 20%, and 30% treadmill incline.

4.3.2.3 Kinematics

Walking on an incline as compared to walking on the horizontal can be distinguished by the following factors: the requirements to raise or lower the body's COM, the vertical displacement during each stride, foot clearance, and joint ROM. The following paragraphs address these factors.

Numerous studies have demonstrated that the angle of incline is a factor influencing the hip, knee, and ankle angles (21). These studies concluded the governing factor regarding the effect of incline on lower-extremity joint angle may be the orientation of the COM of the upper body during these tasks. For this stage of IST-3, the joint angles were recorded for the ankle, knee, hip, and torso in the sagittal plane of motion while the treadmill was inclined or declined at different percentage grades. In Figure 49 and Figure 50, joint ROMs are displayed with respect to the incline and the condition. As shown in these figures, the angles between unsuited gait and CG rig gait joint angle ROM are not very close, but the general change in ROM follows the same pattern. The decrease in knee and hip ROM and the increase in ankle ROM indicate the subject was not using the same kinematics to adapt to the changes in the environment. Figure 51also shows a relatively consistent percentage difference between the unsuited 1-g condition and the CG rig conditions.

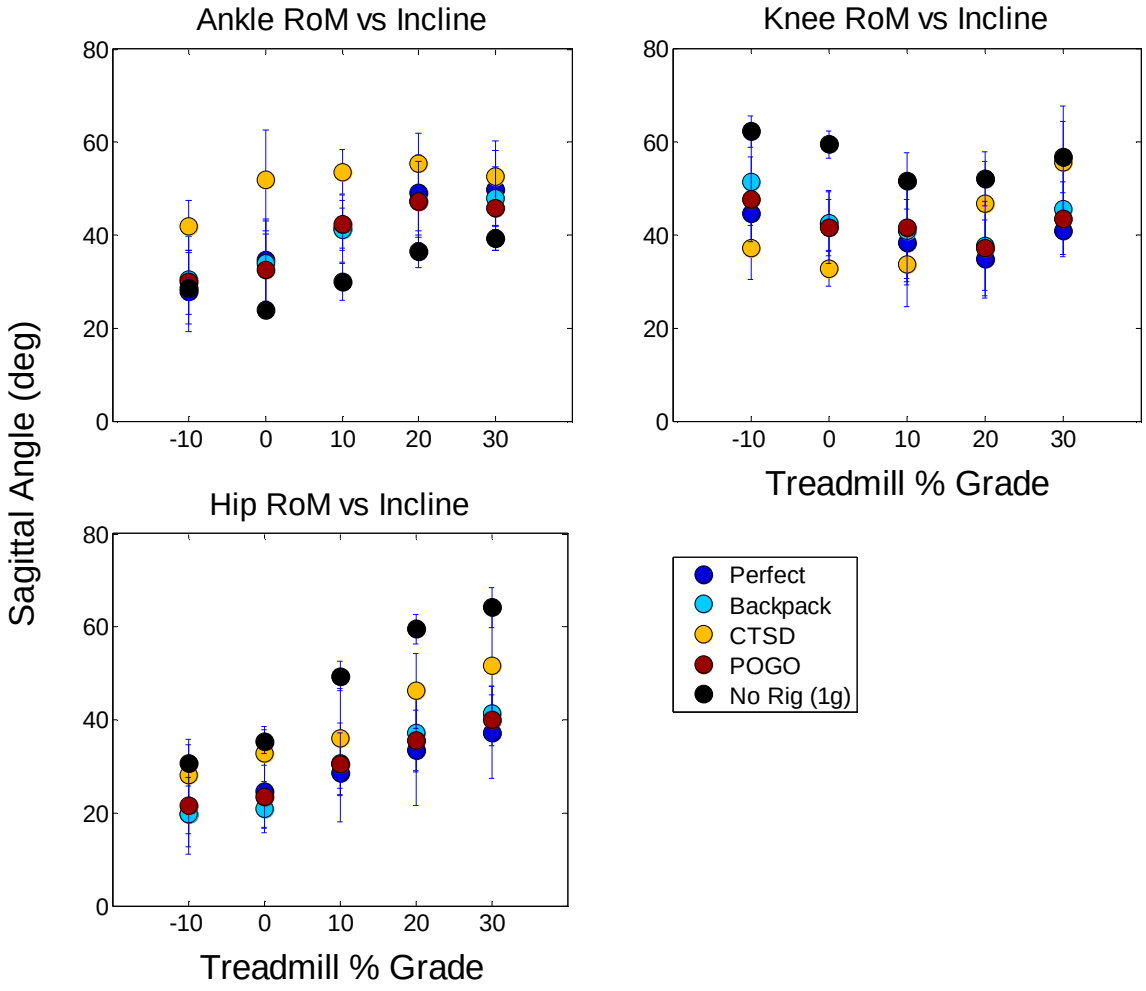

Figure 49. Joint angles averaged over subjects and gait cycles, categorized by CG condition, and plotted against incline. Error bars represent the standard deviation of the subject averages.

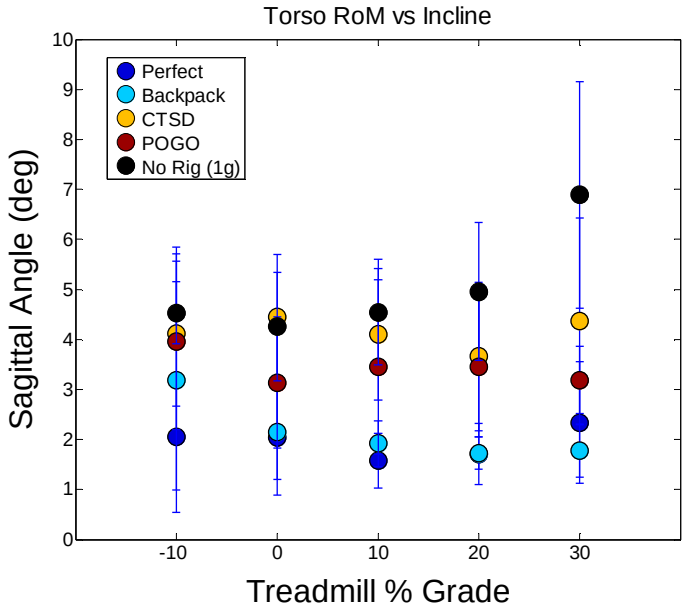

Figure 50. Joint angles averaged over subjects and gait cycles, categorized by CG condition, and plotted against incline. Error bars represent the standard deviation of the subject averages.

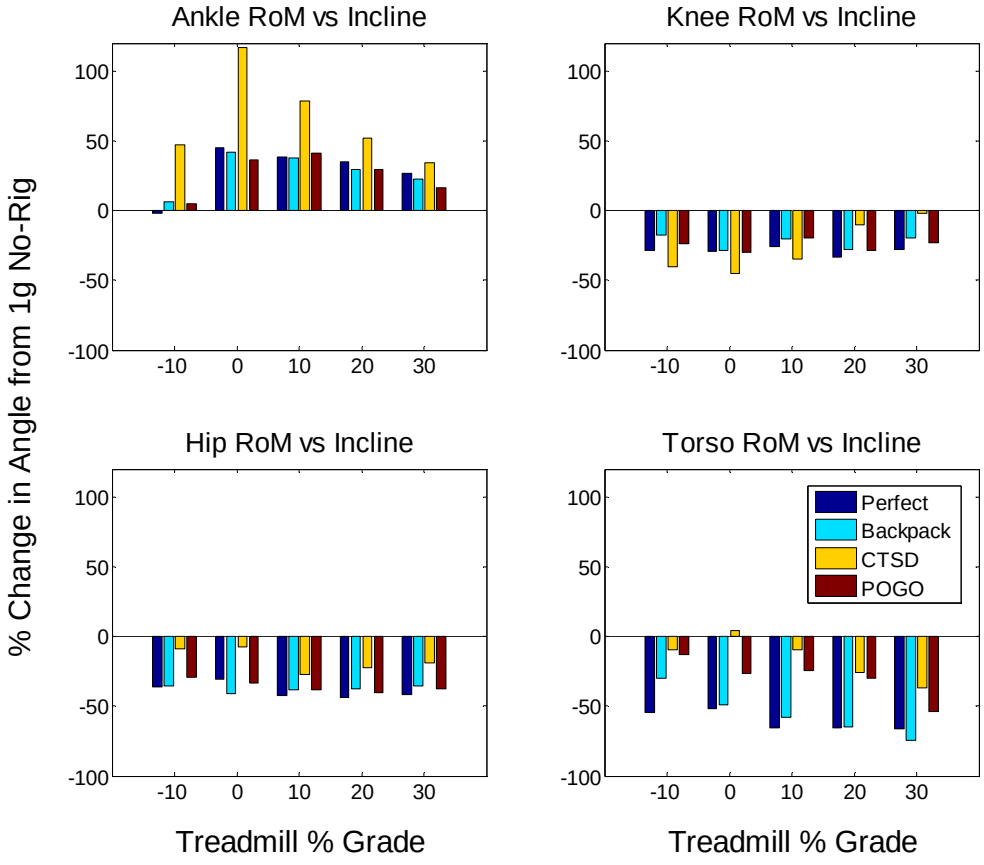

Figure 51. Percentage change in ROM of each CG condition from the unsuited 1-g baseline plotted against incline.

The next several graphs show the average angles for specific joints over the gait cycle, separated by treadmill incline (Figure 52 to Figure 55) Distinct differences in patterns are noticeable between unsuited Earth-gravity ambulation and POGO ambulation. These patterns differ by shape, magnitudes, and timing of the maximum flexion and extension. Again, there is little change between the different CG conditions over the range of inclines and only slight changes between the conditions themselves, the exception being the CTSD condition that displays a little more variability. The patterns noticeably differ from the unsuited condition, which has distinct changes in patterns, magnitudes, and timing as the inclines progress.

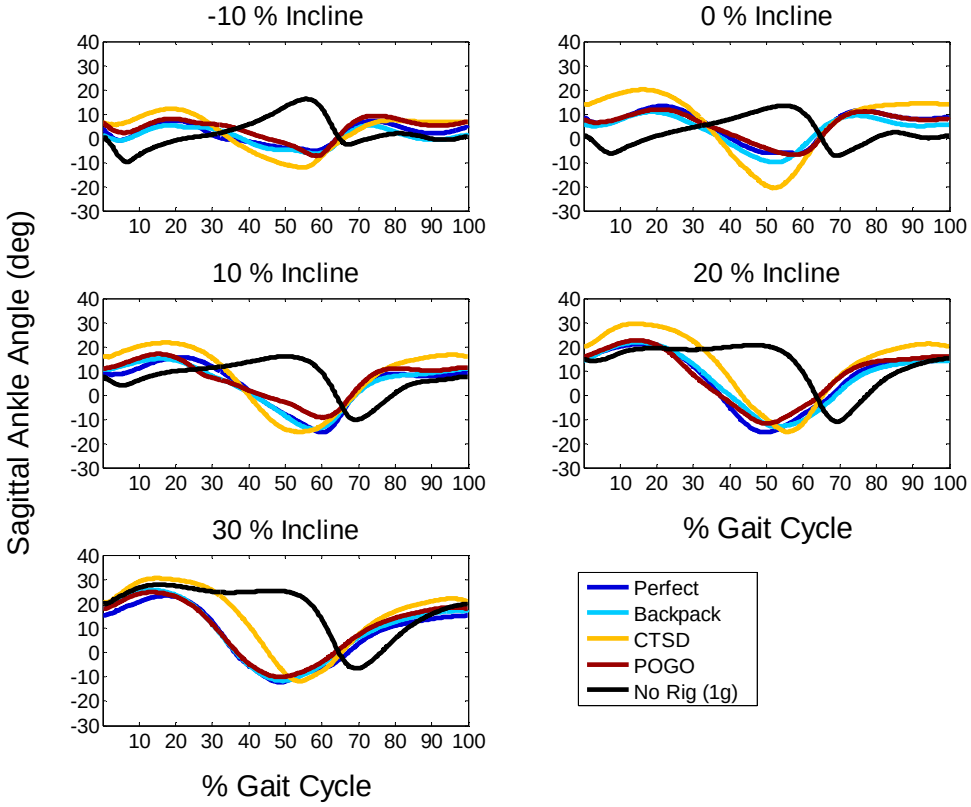

Figure 52. Ankle joint angle traces over one gait cycle for each CG condition. Each plot is at specific incline.

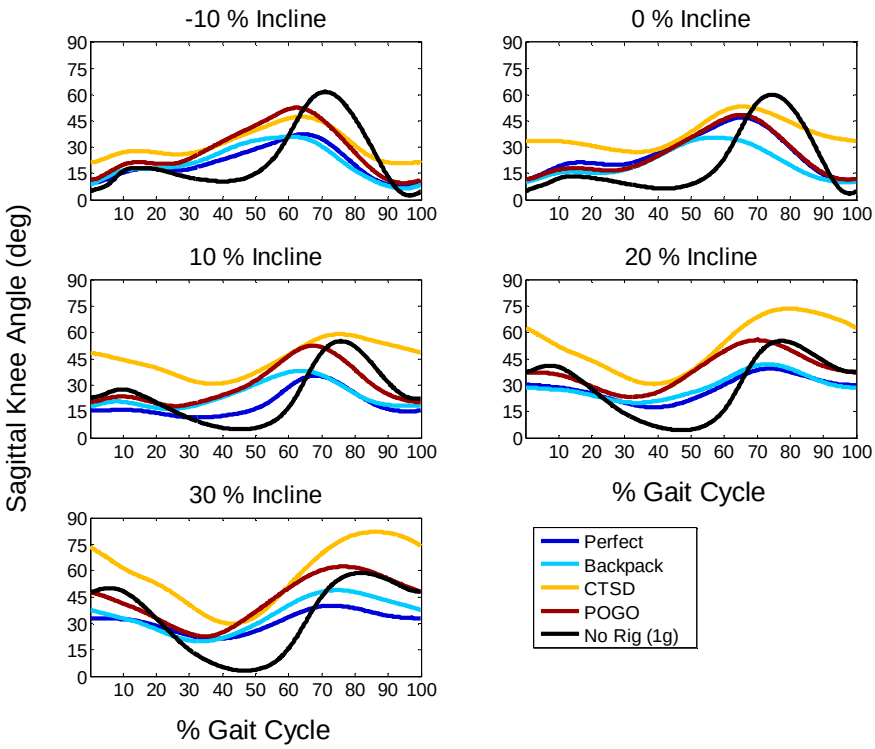

Figure 53. Knee joint angle traces over one gait cycle for each CG condition. Each plot is at specific incline.

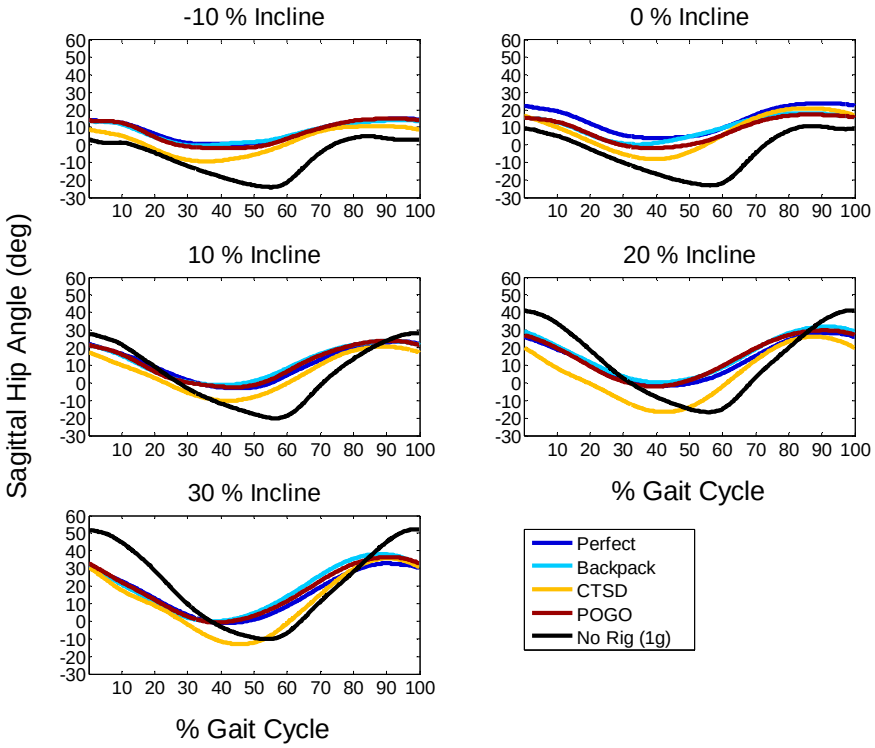

Figure 54. Hip joint angle traces over one gait cycle for each CG condition. Each plot is at specific incline.

Differences between the CTSD CG and all other CGs are seen in the comparison of sagittal torso tilt among the conditions (Figure 55). As the incline changes from a negative to a positive grade, the unsuited torso adjusts its tilt accordingly from a backwards to a forward lean to keep the body CG in a balanced position. The CTSD condition does not increase past 10°. The rest of the CG conditions slowly increase the amount of torso tilt as the incline increases. One noticeable difference between the CG rig conditions and the 1-g condition is that the overall range of tilt between the incline conditions is significantly reduced in the CG rig, especially in the CTSD condition.

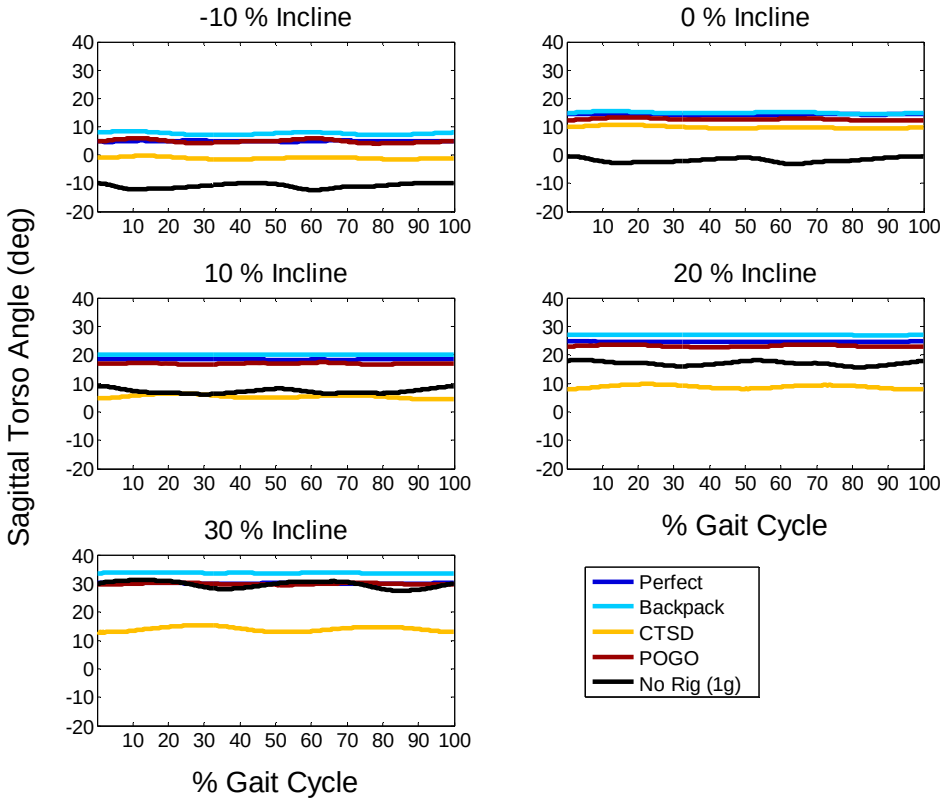

Figure 55. Torso angle traces over one gait cycle for each CG condition. Each plot is at specific incline.

4.3.2.4 Electromyography

As described previously, only two subjects had a full data set to analyze. For several reasons, including problems during testing and lengthy data-reduction processes, only the erector spinae of one subject was analyzed for this report and presented as an example.

For the decline condition, all configurations had muscle activity after the left foot strike (Appendix E). All the CG rig configurations had the activity during the swing phase, but it ended before initial contact. Compared to level-ground walking, the amount of high-intensity muscle contraction was high. As the incline increased from level, the duration of contraction increased and the duration of higher magnitude of contraction also increased. The EMG results for the erector spinae at the 10% incline are presented in Figure 56. This incline condition was presented because the 20% and 30% grades were not performed for the CTSD CG rig condition. Once again, the 1-g condition showed activation during swing and at initial contact, while the CG rig conditions were primarily activated during swing. Of note was the burst during stance for the Perfect CG rig condition. Interestingly, at the highest incline, the CG rig configurations showed higher-intensity contractions.

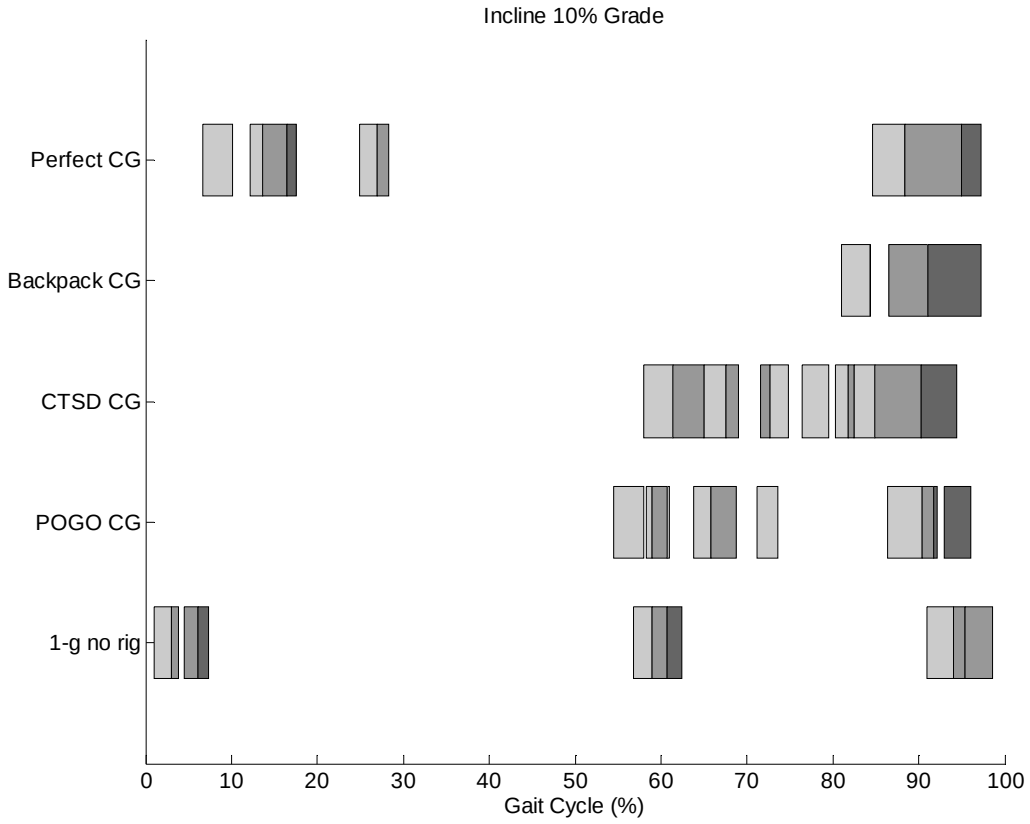

Figure 56. Erector spinae muscle activity during a gait cycle. Gray shading indicates the intensity of the contraction.

4.3.2.5 Subjective Results and Discussion

Rating of perceived exertion

With the exception of 1-g data, RPE trends (Figure 57) were similar to metabolic trends (Figure 14). Mean RPE for the CTSD condition was significantly greater than all other varied CGs for grades of -10%, 0%, and 10%, although the standard deviation range did notably overlap the other CG conditions, which was not present in the metabolic data. At 20% and 30% grade, considerable overlap was noted among CG conditions, and no significant differences were noted. This could possibly be related to a few subjects that could not complete the higher grades in the CTSD condition. These subjects did not complete the 20% and 30% incline trial because they would have exceeded exertional limits set as test termination criteria. If they were allowed to complete these stages, the mean RPE ratings likely would have been much higher. The 1-g RPE ratings seen at 10%, 20%, and 30% grade were very similar to the values of other CGs; this was not the case with the metabolic data. This indicates that subjects rated RPE differently under different conditions, such as freestanding in 1-g vs. offloaded while connected to the gimbal support structure with CG rig. This finding is similar to that of previous studies in which RPE was rated differently in the suited and unsuited conditions (5) (1) (2).

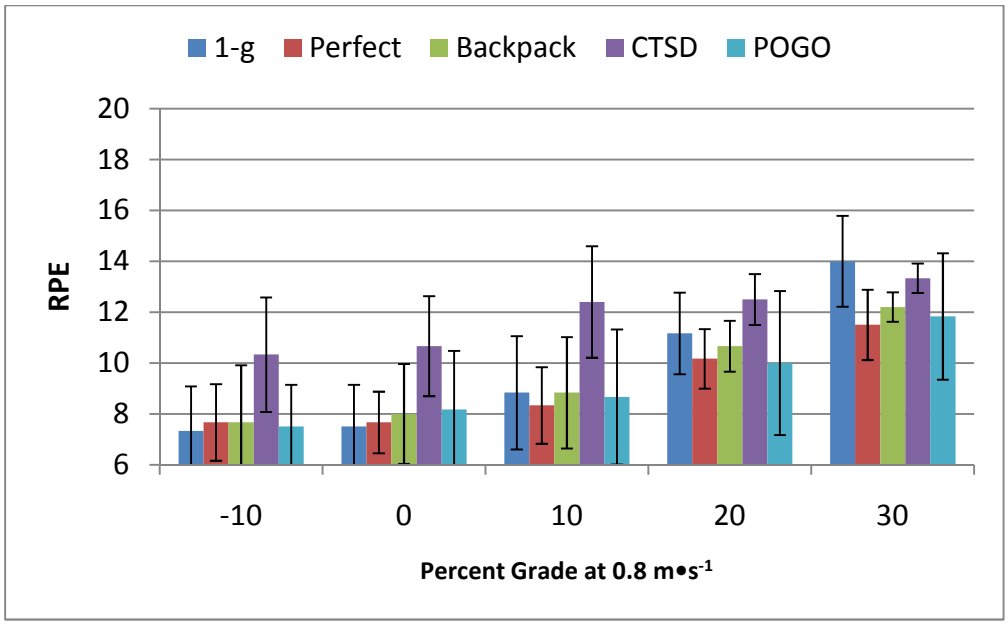

Figure 57. RPE at different CG conditions during graded ambulation on a treadmill at 0.8 m•s^{-1}.

Gravity compensation and performance scale

GCPS ratings were significantly greater with the CTSD CG (Figure 58) compared to other CG configurations. This was most notable at grades ≤ 10%. At 20% and 30%, there was just enough change in the mean that the CTSD condition would still be considered significantly greater than the other CG configurations, but there was considerably more overlap in the range of ratings. Mean ratings at the CTSD CG indicated that modifications were warranted or required to attain desired performance. Ratings at all other CGs were similar and trended towards either desired performance or adequate performance. In addition, there was a subtle trend for GCPS to increase with grade.

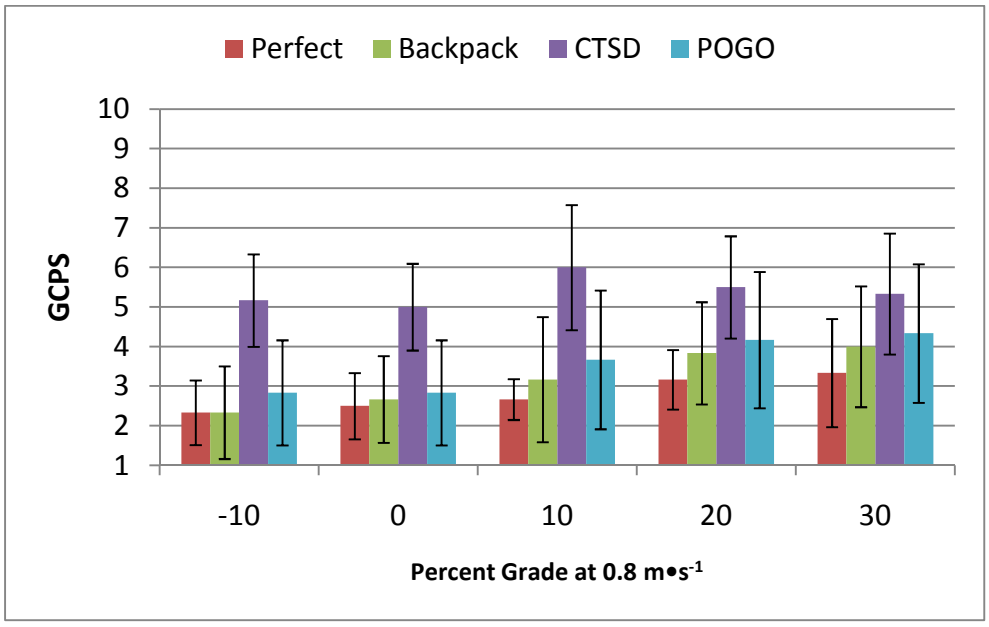

Figure 58. GCPS at different CG conditions during graded ambulation on a treadmill at 0.8 m•s^{-1}.

4.3.2.6 Subjective Rating Changes from 30 Seconds to 3 Minutes

In this study, RPE and GCPS were measured at both the 30 and 150-s mark of the 180-s trials. Figure 59 shows the change in RPE and GCPS from the 30-s mark to the 150-s mark of the 180-s trials during graded ambulation. In over 90% of the trials, the ratings either stayed the same (62% RPE, 82% GCPS) or increased by one (32% RPE, 11% GCPS). Unlike the level-ambulation trials, the graded ambulation trials required a break to be taken between each different incline to reset some of the data-collection equipment. This may account for the increased frequency of the RPE increasing by one rather than staying the same. GCPS seems to be less affected by duration, as would be expected.

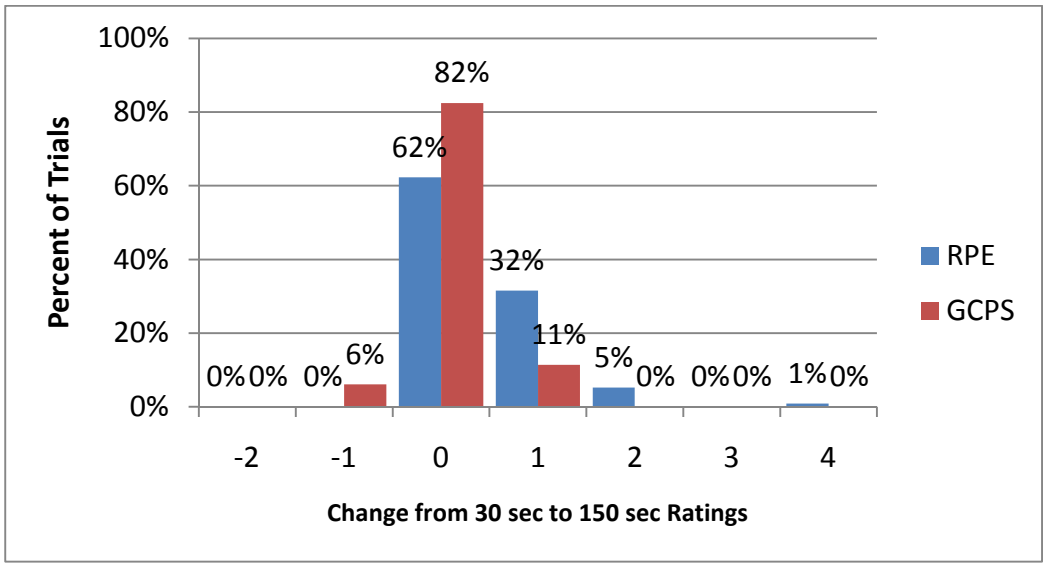

Figure 59. Change in subjective ratings from the 30-s mark to the 150-s mark in a 180-s graded ambulation trial (*n* = 114).

4.4 Exploration Tasks

As discussed previously, one subject from the ambulation trials could not complete the final exploration task and postural stability session due to scheduling conflicts. A subject with previous experience from IST-1 and -2 was included as the replacement. From the 108 total exploration test points from all test subjects, seven test points were either not attempted or led to a GCPS rating of 10, indicating the subject could not complete the task at that condition.

4.4.1 Biomechanics results and discussion

4.4.1.1 Strategy

In the current study, subjects performed a series of exploration tasks, including rock pickup, shoveling, and kneel-and-recover. The varying movement strategies adopted by subjects to complete these exploration tasks do not lend themselves well to traditional biomechanical analyses. Therefore, alternative analyses were considered to characterize the performance of these tasks.

Certain methodological limitations prevented customary biomechanical analyses from being provided. For example, all offloaded conditions were performed while donning a 111-kg (245-lb) CG rig with long arms and a significant amount of mass attached to each arm. The CG rig itself therefore may be considered a confounding factor for unsuited subjects, as increased inertial properties associated with it may have caused the subjects to alter their movement strategies.

As each subject adopted a different strategy to complete various exploration tasks, analysis of movement during trial performance began with examination of qualitative measures (ie, observation). This approach was selected to provide meaningful interpretation of exploration task data, given the difficulty inherent in generalizing kinematic analyses of variable adopted movement strategies to a popu-

lation. Additionally, it was worthwhile to determine whether, through a qualitative analysis of subjects' adopted strategy, the system itself and its associated inertial properties had a confounding effect on task performance (eg, CG rig inertia forced subjects to adopt a strategy other than that selected in 1-g).

It should be noted that, in addition to the other CG rig configurations, the 1-g (Perfect) CG rig condition was tested for exploration tasks only.

Rock pickup task

When performing the rock pickup task, subjects approached and then stood on dual force platforms (Advanced Mechanical Technology, Inc. [AMTI], Watertown, Mass.) with one foot on each force platform, attempting to maintain contact with the force platforms throughout the duration of the task. Subjects performed three trials for each of the various CG/gravity conditions.

Five of the subjects included in the current study report being right-hand dominant, while one subject is considered ambidextrous. Based on previous testing in the Mark III technology demonstrator suit and the effect that the offloading system appeared to have on subjects' chosen method of performing the rock pickup task, it was deemed worthwhile to examine how the current CG rig and gimbal structures affected the adopted strategy of the subjects. For example, it was of interest to examine how subjects chose to pick up and set down the rock when performing this task to help determine whether the CG rig and gimbal components affected how the subjects approached and completed the task.

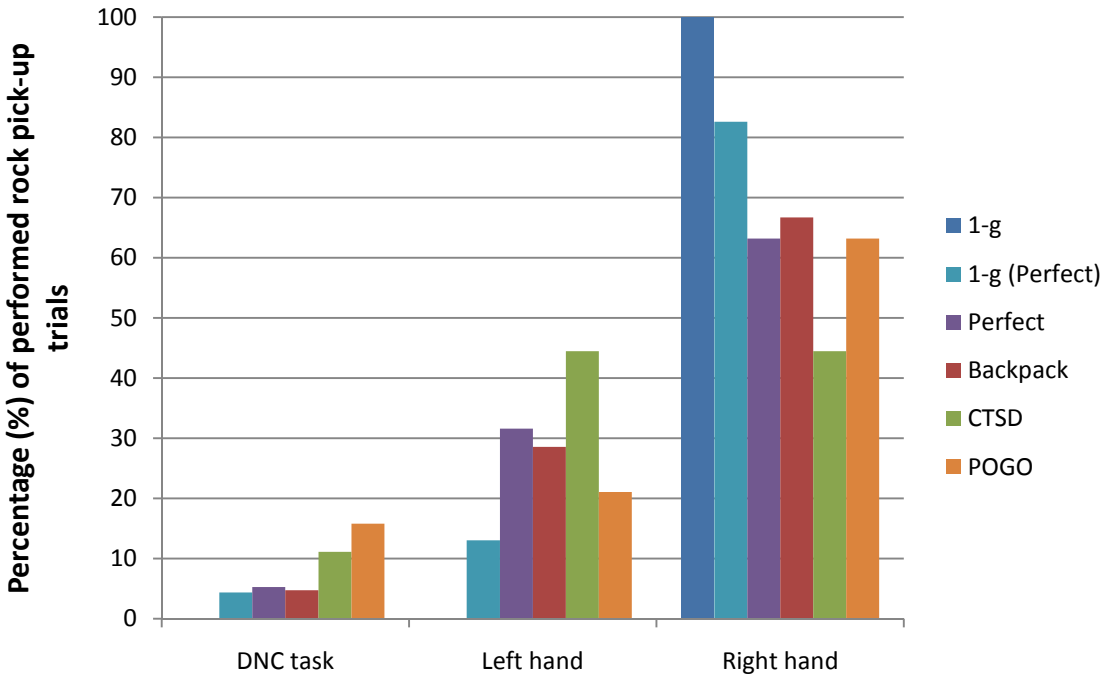

Figure 60. Hand involvement by subjects to perform the rock pickup task for all tested conditions. DNC = did not complete.

All subjects picked up the rock with the right hand when performing the task under 1-g, no-rig conditions, thus providing a baseline from which to compare other conditions. As seen in Figure 60, not all trials performed under offloaded conditions involved the use of the right hand. For example, approximately 45% of the trials performed at the CTSD CG rig condition involved use of the left hand to pick up the rock. This suggests that while unconstrained (eg, under 1-g conditions), the subjects freely selected the most efficient movement pattern to complete the task; but when performing the task under varying offload conditions in the CG rig, the movement pattern selected was based more on restrictions placed on the subject by the components of the system offloading them.

This observation is further confirmed by qualitative examination of movement coordination between the upper and the lower body to perform the rock pickup task. Again, consistency is observed in the interaction of movements between the upper and the lower body when performing the rock pickup task unencumbered in 1-g, no-rig conditions, in that every trial performed by every subject involved squatting evenly straight down and picking up the rock with the right hand. Table 5 presents the frequency of each combination of upper and lower body interaction when performing the rock pickup task.

Table 5. Upper- and Lower-extremity Coordination – Rock Pickup Task

CG condition	Pick up with left hand			Pick up with right hand		
	Bend down to left	Bend down to right	Squat straight down	Bend down to left	Bend down to right	Squat straight down
1-g	N/A	N/A	N/A	0	0	18
1-g (Perfect)	0	0	3	6	0	13
Perfect	0	2	4	6	0	6
Backpack	0	0	3	7	0	7
CTSD	0	2	6	3	0	7
POGO	0	0	4	6	0	6

When picking up the rock with the left hand, subjects never bent down to their left. Similarly, when picking up the rock with the right hand, subjects never bent down to their right. One possible explanation for this finding pertains to the need for subjects to maintain balance to complete the task. It may have been easier for the subjects to counteract their reach for the rock with appropriate lower-extremity movement (eg, squat down or bend down in the opposite direction). Based on the 1-g baseline findings for this task, we could reasonably assume that the CG rig used in the offloaded conditions introduced extra, artificial inertial factors that had to be accounted for by subjects when performing the task, thus resulting in the movement patterns observed for these conditions.

Foot placement was observed for each trial to determine whether subjects were capable of maintaining consistent contact with the force platforms throughout the duration of the trial performed. This examination was performed in an attempt to provide a qualitative estimation of subject stability while performing this task. Stable foot placement was defined, for purposes of the current test, as minimal to no foot movement from the time the task was initiated until the time the task was completed. All trials in the current test, performed under 1-g no rig conditions, corresponded to stable foot placement by the subjects. Conversely, 50% of the trials performed in the CTSD CG condition and nearly 60% of the trials performed in the 1-g (Perfect) CG condition yielded unstable foot placement. Aside from the 1-g, no-rig condition, the Perfect and POGO CG conditions included the most trials in which subjects exhibited stable foot placement on the force plates while performing the rock pickup task (Figure 61).

Kneel-and-recover task

Subjects performed a kneel-and-recover task that involved bending down until the right knee came in contact with the ground, then returning to an erect standing posture. Two major techniques were observed (Figure 62) when examining performance of the kneel-and-recover task: a controlled, deliberate movement when rising from a kneeling position (ie, “standing up”), and a jumping technique in which subjects performed the rise phase via a movement primarily characterized by a disconnect between the feet and the ground on rising (ie, “jump up”). Kneel-and-recover under 1-g conditions typically does not involve rapid, explosive jumping back up to the standing position, mainly due to the considerable amount of muscular effort that would be required to perform such a maneuver.

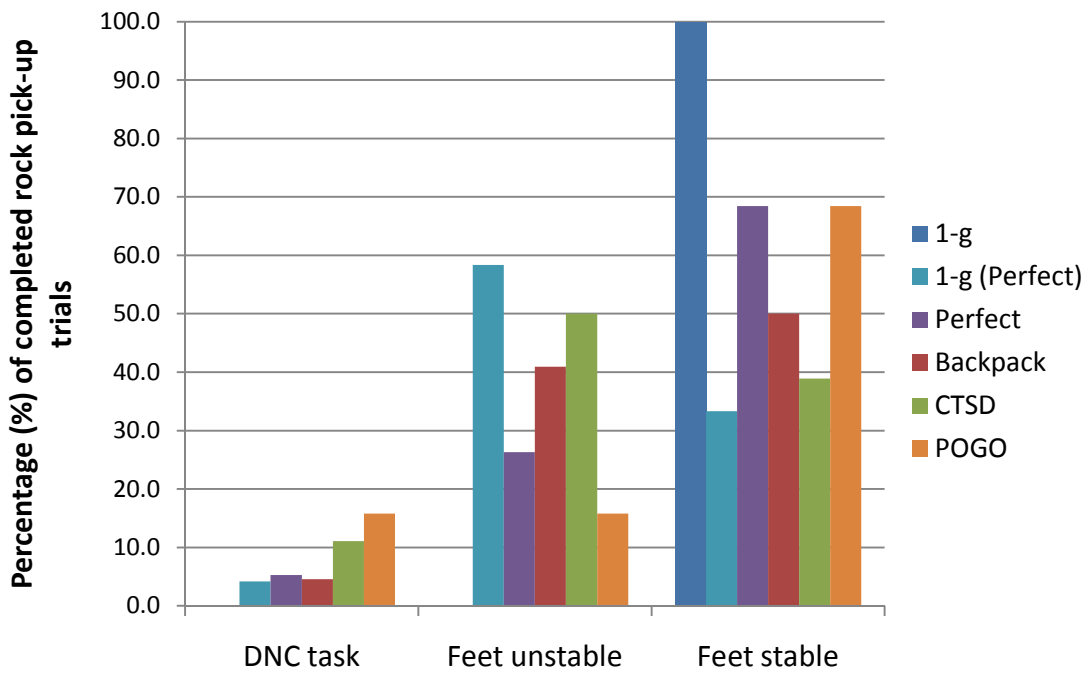

Figure 61. Percentage of performed rock pickup trials in which subjects demonstrated either stable or unstable foot placement on the force platforms, or did not complete the task. DNC = did not complete.

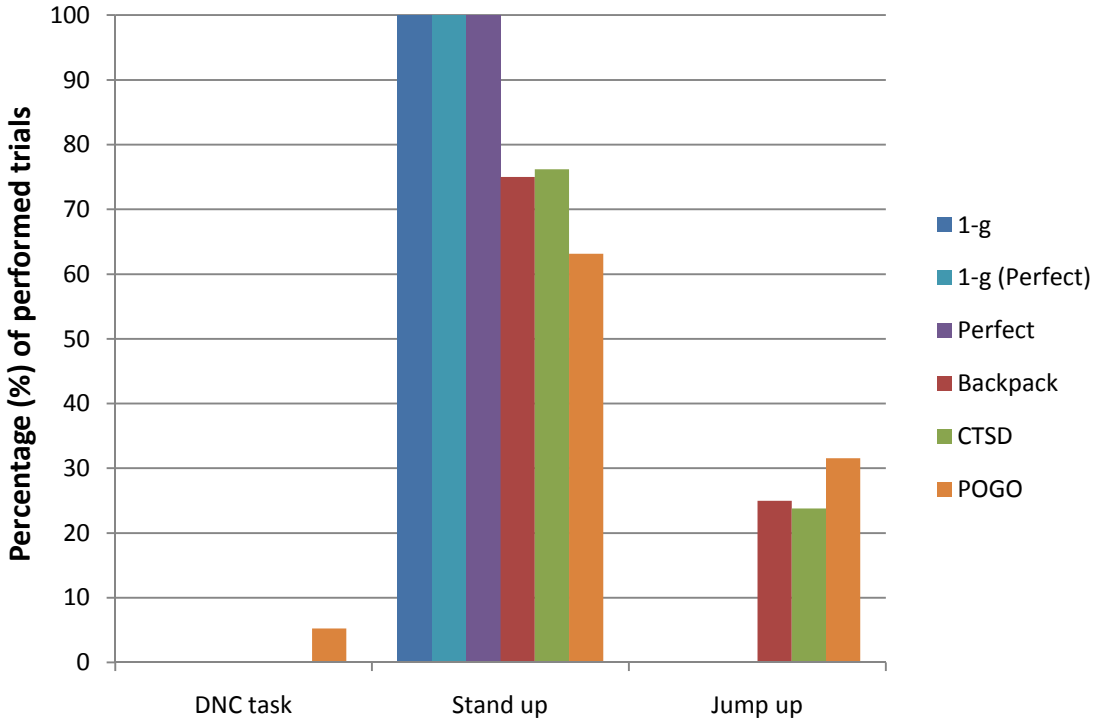

Figure 62. Percentage of kneel-and-recover trials performed in which subjects either did not complete the task, stood up from the kneeling position, or jumped up from the kneeling position. DNC = did not complete.

The preferred strategy under all conditions when performing the kneel-and-recover task was standing up rather than jumping up. As expected, no subjects jumped up from a kneeling position when under 1-g conditions (1-g no rig and 1-g [Perfect]). However, approximately 25% of the trials performed with the Backpack and CTSD settings and over 30% of the trials performed with the POGO CG setting resulted in subjects electing to jump up from the kneeling position. This may be a result of assistance afforded to the subjects by the offloading system, as well as the fact that these CGs often pulled the subjects backward (Figure 63). It would conceivably be easier for the subjects to take advantage of the system and jump up if the CG configuration did not allow a shift of their COM forward enough to stand up in a controlled fashion with their weight more over the lead leg.

Figure 63. Effect of the CG rig ("CTSD" CG configuration, on right) on subject posture at the kneeling portion of the kneel-and-recover task when compared to 1-g, no-rig controls (on left). Backward lean of the trunk caused by the CG rig, combined with the offload of the subject by the POGO system, allowed subjects to more easily jump up than stand up in certain conditions.

Shoveling task

Subjects also performed a shoveling task that, like the rock pickup, involved the subject standing on a dual-force platform setup (one foot on each platform). Subjects used an Apollo-era-type shovel to move a bean bag from an elevated platform (~50 cm higher than the top of the force plates) to the floor. This approach was used in an attempt to maintain consistency with previous tests in this series. The complexity of the shoveling task resulted in varying interactions between upper and lower extremity segments across subjects, and whole-body coordination was required to perform the task effectively and efficiently. Coupling movement complexity with other test factors (eg, offloading the subject via the POGO gimbal, varying CG rig conditions, and limited force platform dimensions on which to stand) may provide some explanation for trends observed in the movement strategies selected for this task. As with the rock pickup task, examination of foot placement on the force platforms throughout each trial helped provide a qualitative assessment of stability during task performance (Figure 64).

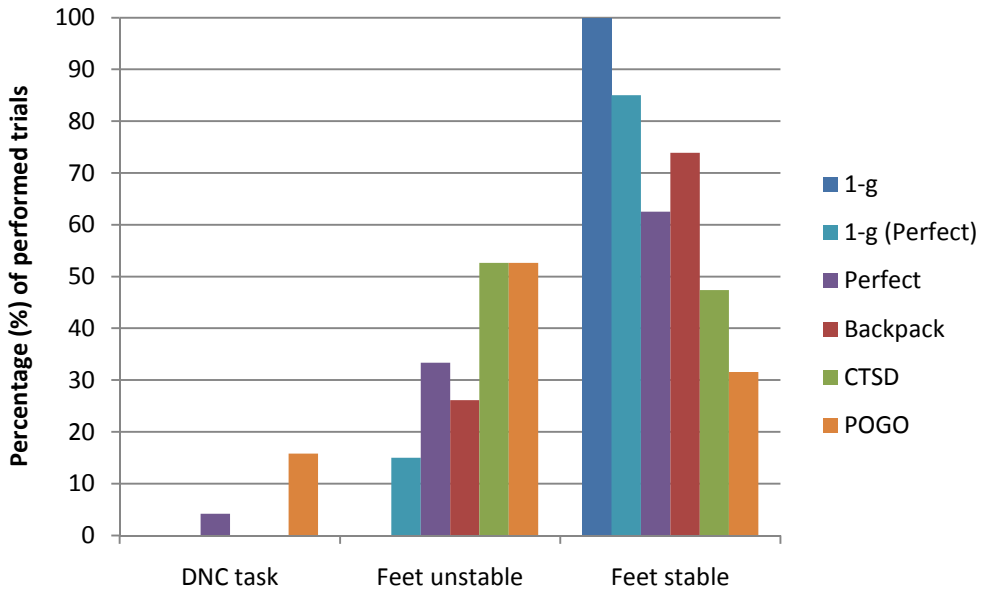

Figure 64. Percentage of performed shoveling trials in which subjects demonstrated either stable or unstable foot placement on the force platforms, or did not complete the task. DNC = did not complete.

Stable foot placement on the force plates was observed for all 1-g, no-rig trials (Figure 64). The 1-g (Perfect) condition also had a high percentage of completed trials in which subjects had observed stable foot placement throughout the duration of the trials. Of the lunar-offloaded trials, subjects maintained stable foot placement the most consistently with the Backpack and Perfect CG conditions (Figure 64). Conversely, over 50% of performed trials for both the CTSD and POGO CG rig conditions had observable, unstable foot placement by subjects when shoveling.

Several movement strategies were employed by subjects to complete the shoveling task; the exercise of these varying strategies may have also been the reason for observations of unstable foot placement in certain trials. For instance, subjects varied the position and orientation of their hands on the shovel handle, effectively altering their approach to the task. This may have been a result of the difficulty experienced from trying to shovel bean bags from an elevated platform, as well as the long length of the shovel handle itself, and the subjects possibly attempting to keep the end of the shovel handle from interacting with the CG rig when performing the task. This often led to subjects pushing the bean bag off the elevated platform rather than actually scooping the bean bag and moving it.

These factors may also have led to subjects trying to scoop up the bean bag from various angles, thus frequently causing the entire elevated platform to move. If subjects were applying any weight through the shovel to the platform and were inherently less stable due to POGO offloading, sudden movement of the platform would have caused an instability that required measures to be taken by the subject to remain under control (ie, alter/readjust foot placement) to complete the task.

One other factor to discuss as possibly affecting strategy and, therefore, stability during shoveling task performance was the interaction between the CG rig and the POGO gimbal. Specifically, a horizontal bar located at the bottom of the CG rig would move about the roll axis with movement by the subject, causing one side of the bar to come in contact with (and often become stuck against) the POGO gimbal structure (Figure 65). Such collisions were only noticed during the Perfect CG condition.

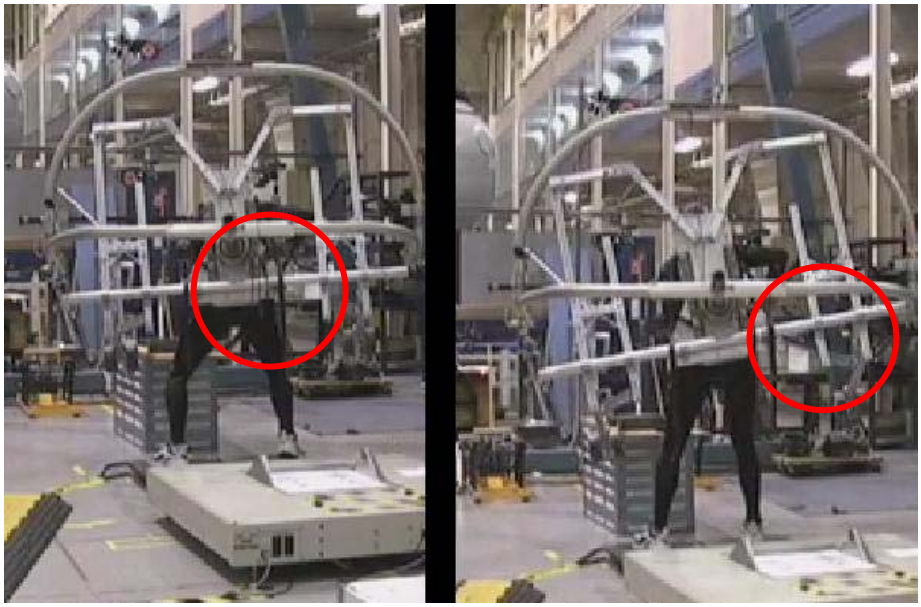

Figure 65. Visual comparison of interaction (circled) between CG rig and POGO gimbal. On the left, the horizontal bar of the CG rig is free from contact with POGO gimbal.

Once the CG rig came into contact with the gimbal, subjects would either have to forcefully lean to free the rig from the gimbal or continue to perform the task without this degree of freedom, thus leading to an alteration of strategy to complete the task. Either method was associated with some compensatory action that may have, in turn, affected subjects' stability on the force platforms.

4.4.1.2 Stability

Another method of analyzing the exploration data involved the examination of the COP in relation to the placement of the feet, the base of support (BOS). For the rock pickup and shoveling tasks, subjects were asked to step onto the force plates, stabilize themselves (eg, allow the mechanical system of the subject, rig, and POGO come to rest), perform the task, stabilize themselves, and step off the force plates. For each frame of data, the BOS was calculated using the x, y, and z coordinates of the feet from the motion capture data, and the COP was calculated using the moments and forces collected from the AMTI force plates.

Four metrics were computed and analyzed to determine the effects of varying CG on COP: (a) the percentage of time the COP was outside the BOS, (b) the number of times the COP fell out of the BOS, (c) the average area of the BOS, and (d) the total distance the COP traveled during the task. Each metric is an indicator of the subject's stability when completing the specific task. More specifically, both the percentage of time the COP was outside the BOS and the number of times the COP fell out of the BOS represents the amount of time and frequency during the trial a subject was unstable. The BOS was determined from three-dimensional motion capture data for each frame. Thus, solely examining the percentage of time the COP was outside the BOS and the number of times the COP fell out of the BOS may be misleading. Placement of the feet could change for different configurations, thereby effectively reducing or increasing the area on which the subject had to support himself. Hence, examining the average area of the BOS for each frame of data is more representative of stability when examined with the percentage of time the COP was outside the BOS and the number of times the COP fell out of the BOS. The total distance traveled by the COP is also a measure of stability in that the less the COP travels, the greater the stability.

Figure 66 is a graphical depiction of the how the metrics for this analysis were computed. The red and blue lines represent the calculated COP for the right foot and left foot, respectively. The combined

COP total is shown as the green line. The black lines are the maximum area the subject used to complete the task.

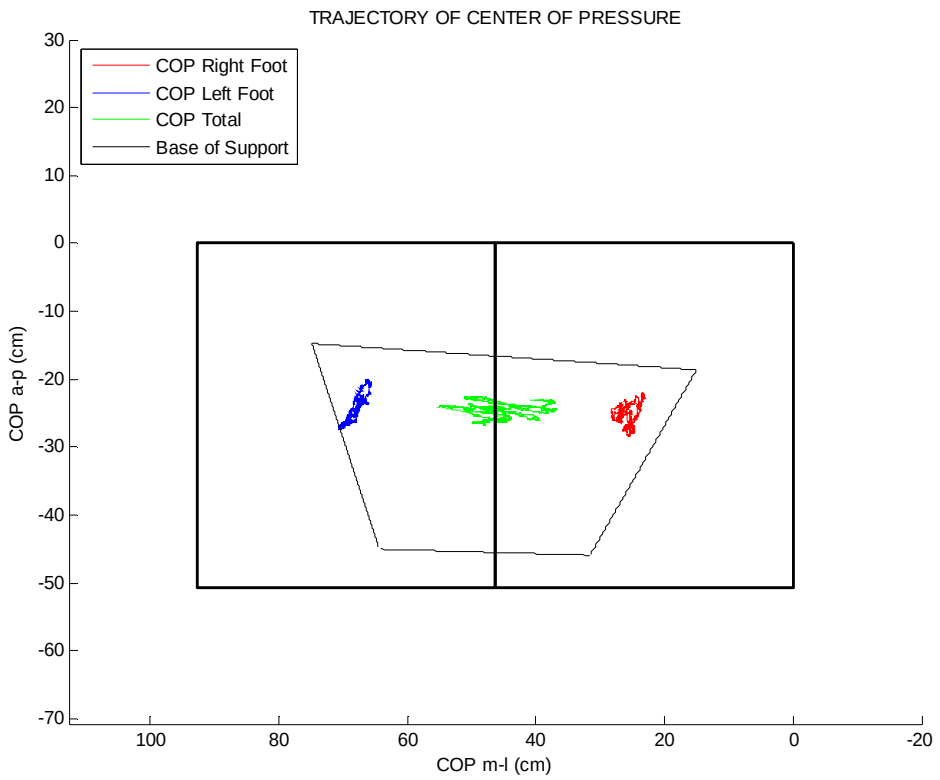

Figure 66. Example plot of rock pickup COP trajectory.

The order of testing is important to note as it may have negatively impacted the results. All neurological platform testing was completed first, followed by three kneel-and-recovers, three rock pickups, and three shoveling tasks. Further, the first three conditions were always performed in the same order: 1-g with no rig, Perfect CG with only the weight of the rig offloaded, and Perfect CG at lunar weight. The remaining three configurations were randomized. The lack of randomization among conditions may have influenced the results of the stability analysis in that any trends observed may be the result of the order tested and not the parameter in question. Note that one subject was not included in this analysis because no motion capture data were collected for CTSD and POGO CG configurations.

Rock pickup task

The protocol for rock pickup included subjects stepping onto the force plates, stabilizing themselves, bending down, picking up the rock, bending down, setting the rock back down, and stepping off the force plates. However, not all subjects adhered to this protocol. Subject 3 bent down to pick the rock up but dropped it onto the platform without bending back down, thus only completing half of the trial. Therefore data for Subject 3 were carefully scrutinized when comparing his data with the data of the other subjects. Further, for the majority of the trials, the subjects performed the tasks on their toes rather than with their feet planted firmly on the force plates.

The percentage of time that each subject's COP was outside the BOS is shown in Figure 67. The CTSD CG recorded the most percentage of time outside the BOS for all subjects. On average, almost half of the trial was spent outside the BOS, which may be due to CG configuration but was more likely due to the CG misalignment with the gimbal axes of rotation. For all other CG configurations, the time spent outside the BOS was minimal.

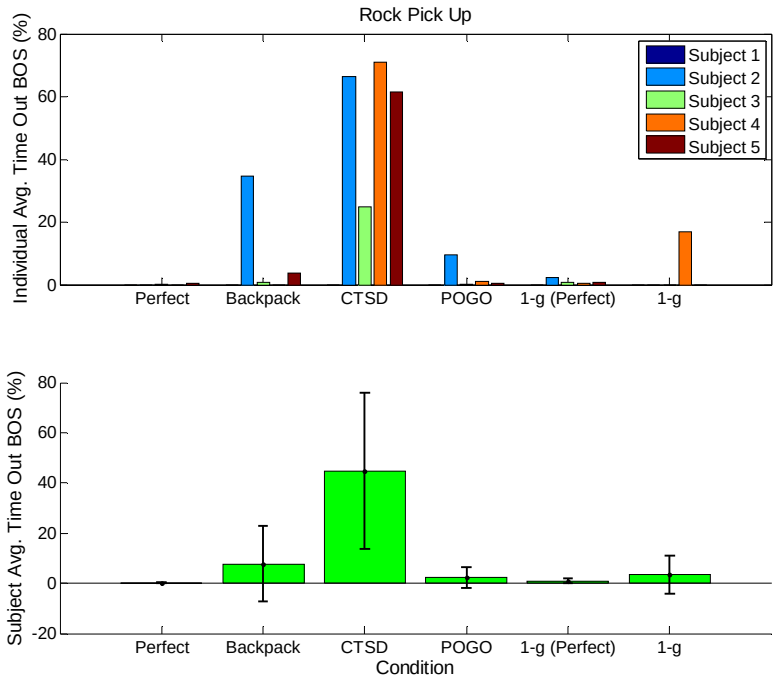

Figure 67. Average percentage of time the COP was outside of the BOS during the rock pickup task.

Results demonstrated that only Subject 1 had little difficulty in maintaining stability. Subject 4 had a high percentage outside the BOS in the 1-g condition; a possible reason for this may be that the subject did not stabilize before beginning his task. As the subject stepped on the force plate, he was already bending down to pick up the rock. Only for his first trial did this subject have a high percentage outside the BOS, with the other two trials around 1%. This also may be due to posterior swaying, as the subject stood up from placing the rock down. Subject 3 did not follow the testing protocol by properly replacing the rock as instructed. Therefore, results showed that Subject 3 recorded significantly less percentage outside the BOS compared to the other subjects at the CTSD CG configuration. The Backpack CG configuration for Subject 2 resulted in a higher percentage outside the BOS compared to that of the other subjects. This may be due to several factors; eg, configuration being the last tested for the test day and the technique that the subject chose (eg, lunged down instead of bent down) proved to be more difficult. Further, the subject's core strength may have been an issue because, across almost all conditions, this subject recorded on average a higher percentage outside the BOS compared to other subjects.

Figure 68 represents the number of times the COP fell outside the BOS. CTSD CG had the greatest frequency of recorded times outside the BOS. Subject 2 scored a higher number due to the alternative method of the subject hopping into a lunge to pick up the rock. Subject 5 was also noted to use a jumping-into-position technique for the Backpack CG configuration. These higher frequencies outside the BOS for these subjects may be attributed to the sudden movements for which the outcome would be a quick shift in COP, resulting in the COP falling out of the BOS.

It is understood that a subject widens his stance when he is unstable. This gives the COP more room to move inside the BOS without resulting in instability. From the data, the CTSD CG had the smallest average area of support and the POGO CG had the largest average area of support compared to the different CG configurations (Figure 69). From these results it could be concluded that the CTSD CG configuration caused the subjects to have less of a BOS whereas the POGO CG resulted in the subjects creating the largest BOS. Results from the area analysis are useful in validating the other stability

metrics. For example, Subject 1 recorded the least amount of time outside of the BOS (Figure 67), which may be due to the increased area of the BOS (Figure 69).

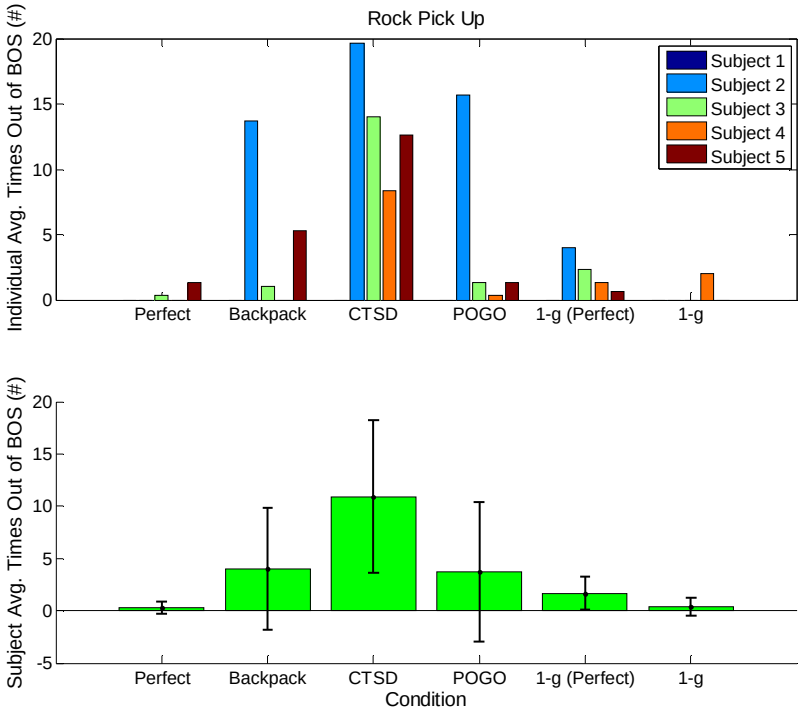

Figure 68. Number of times the COP crossed to the outside of the BOS for the rock pickup task.

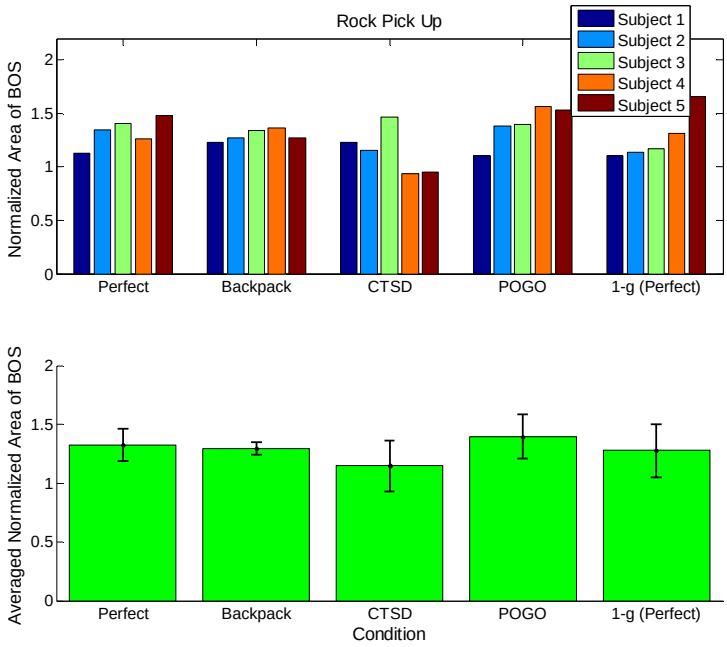

Figure 69. Average area normalized to 1-g for the rock pickup task.

When comparing CG configurations, there were no observable trends for how far the COP travels (Figure 70). Looking at the individual subject results in combination with the average area results revealed individual stability. For example, Subject 4 had one of the largest areas of support but, as seen in Figure 70, the COP traveled the least compared to that of the other subjects. Normalizing the total COP travel to the 1-g condition did not improve the results and revealed no observable trends.

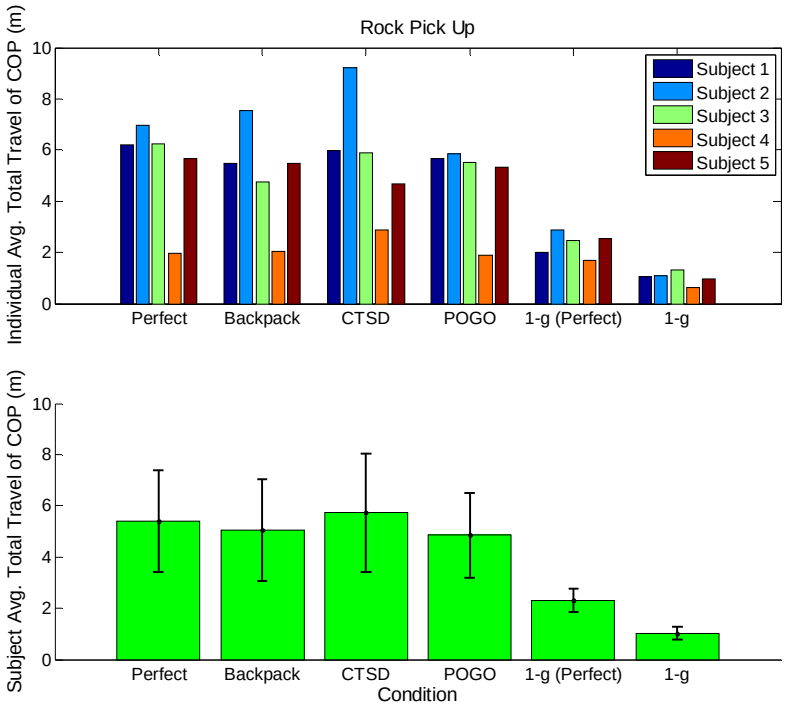

Figure 70. Average total distance the COP traveled during the rock pickup task.

Shoveling task

The shoveling task protocol was similar to the rock pickup task except that the subject only performed one shovel per trial. Further, this was the last task tested for each condition, so subjects were able to familiarize themselves with the configurations before this task.

The average percentage of time outside the BOS for each subject is seen in Figure 71. The results from this analysis revealed no observable trends except that three of the five subjects had some difficulty maintaining the COP inside the BOS for the CTSD CG configuration. The CTSD CG condition may have recorded more time outside the BOS because three subjects had a similar method of leaning or falling forward when scooping up the lead bag. For example, video evidence demonstrated that Subject 3 for this condition used the momentum from stepping onto the force plates to fall forward, and that this subject anticipated the inertia of the system to help accomplish the task. Subject 4 recorded the most amount of time outside the BOS. This may be because the CTSD CG configuration was the last one tested for this subject, resulting in fatigue that may have made the task more difficult.

Subject 3 had a high percentage time outside the BOS for the Perfect CG configuration compared to that of the other subjects. A possible reason for this may be due to the settings of the spider and gimbal of this configuration. The weighted arms of the rig were lower, and the right-hand corner of the horizontal bar of the CG rig was caught on the gimbal for all shoveling trials for this condition. Another contributing factor could be that this was the first configuration offloaded to lunar weight.

Results from the 1-g condition were unexpected. Four out of five subjects recorded time, albeit minimal, outside the BOS. This may have been a result of the subjects keeping their feet in the center of

each force plate. The force plates were lined up horizontally to the task setup. Performing the task unsuited gave the subjects greater visibility of the force plates compared to being suited. Thus, the subjects could easily ensure that they were on the force plates and not near the edges. For terrestrial shoveling, the feet are usually staggered with the foot opposite of the shovel in front. As the setup forced the subjects to perform the task using a novel method, the subjects had more instability. This most likely would not be a method used on the moon.

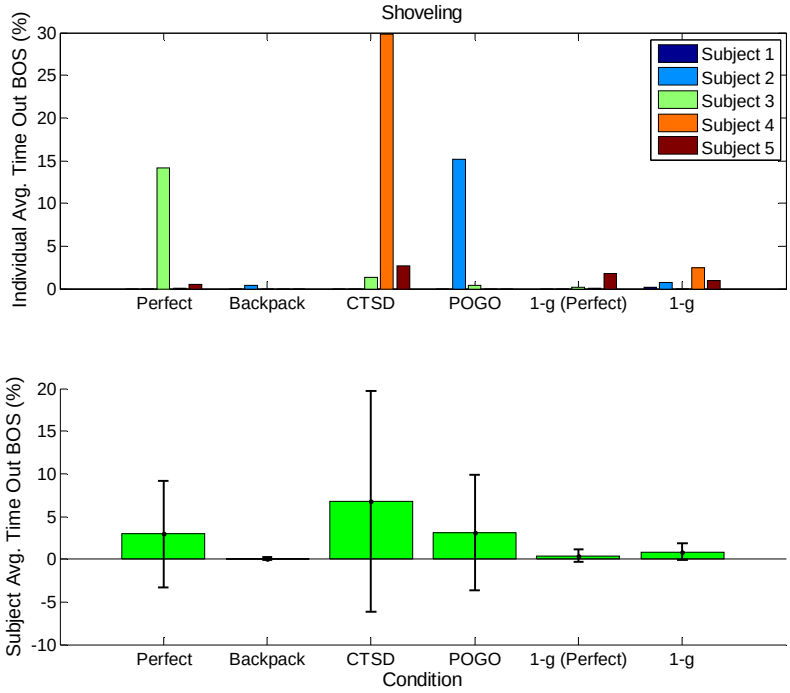

Figure 71. Average percentage of time the COP was outside of the BOS during the shoveling task.

Figure 72 demonstrates how each configuration affected subjects differently. The average data does not correctly represent the results, ie, that some subjects were greatly affected by the different CG conditions compared to others. Thus, one must look at individual subjects. The subjects who had a difficult time with the percentage of time the COP was outside the BOS also were seen to have problems with the number of times the COP fell out of the BOS. Just as the percentage of time outside the BOS data demonstrated, the number of times outside the BOS for the 1-g condition revealed that all subjects except one had on average one to two occurrences of the COP falling outside the BOS. The possible explanations coincide with those given previously for the percentage of time outside of the BOS.

There were no observable trends for the average area of the BOS, as seen in Figure 73. By just adding the CG rig, the areas were approximately 1.5 times greater than 1-g. Individual subjects either maintained a similar size BOS or adjusted it, depending on the configuration. For Subject 5, the configuration with the largest amount of time outside the BOS was CTSD CG. For that subject, the area of support for CTSD CG was smaller compared to Backpack and POGO CGs, which had no falling out of the BOS. Other subjects (eg, Subjects 2 and 4) kept the area consistent over all configurations, although the COP fell out of the BOS. These findings demonstrate that subjects employed different strategies. Some subjects chose a consistent stance across all conditions, while another subject seemed to adjust his stance according to the condition tested.

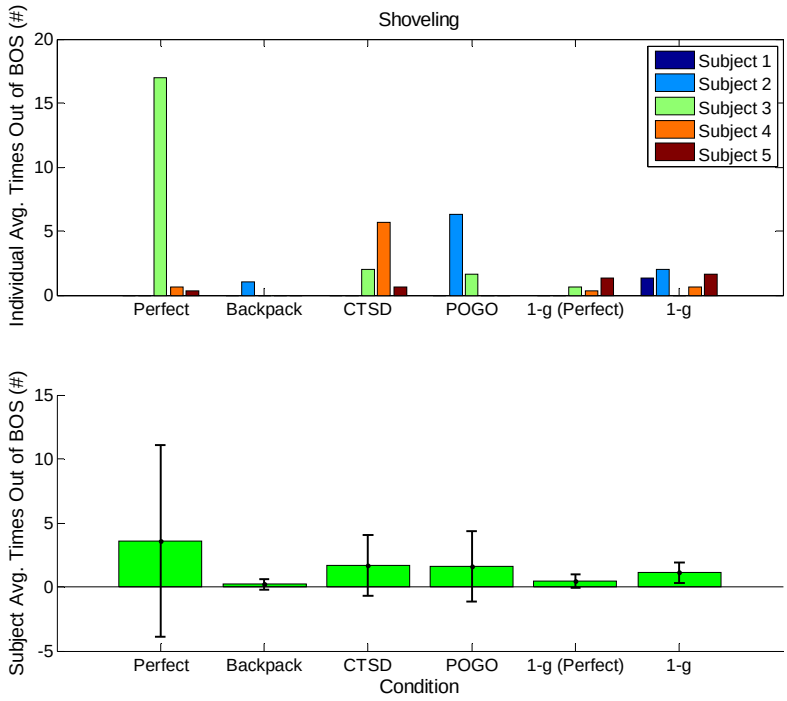

Figure 72. Number of times the COP crossed to the outside of the BOS for the shoveling task.

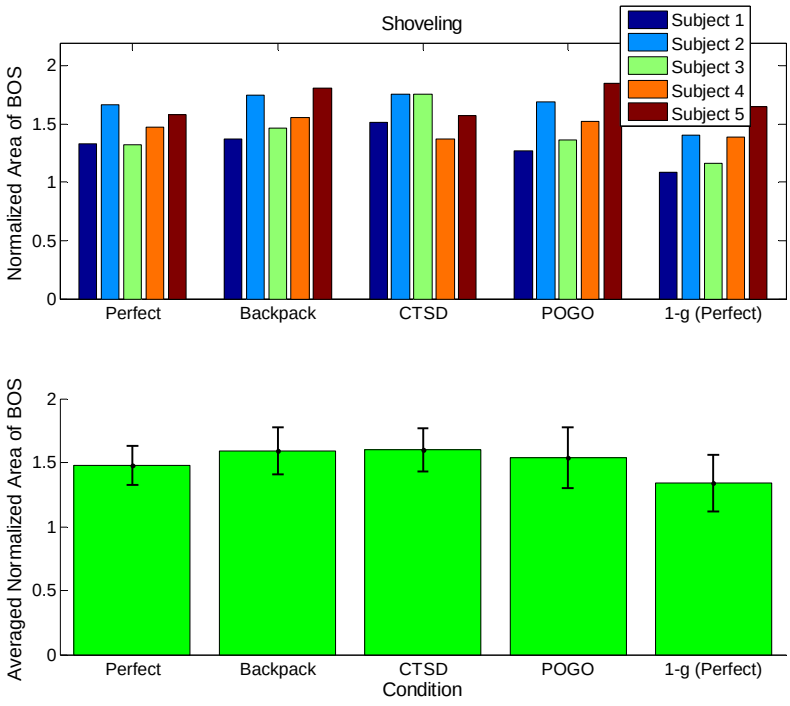

Figure 73. Average area normalized to 1-g for the shoveling task.

The total distance traveled by the COP shows that the COP traveled slightly more for the CTSD CG than the other CGs (Figure 74). Subject 4 had the least-traveled COP but also had one of the smaller areas of support and spent a larger amount of time outside the BOS. Subject 3, in the Perfect CG configuration, had the largest amount of total travel of the COP, but also, as seen in Figure 72, the smallest area of support. Variability among subjects once again suggests there could be interactions between the test environment and the subjects' strength capabilities. All configurations at lunar offload had, on average, approximately three times greater COP travel than 1-g.

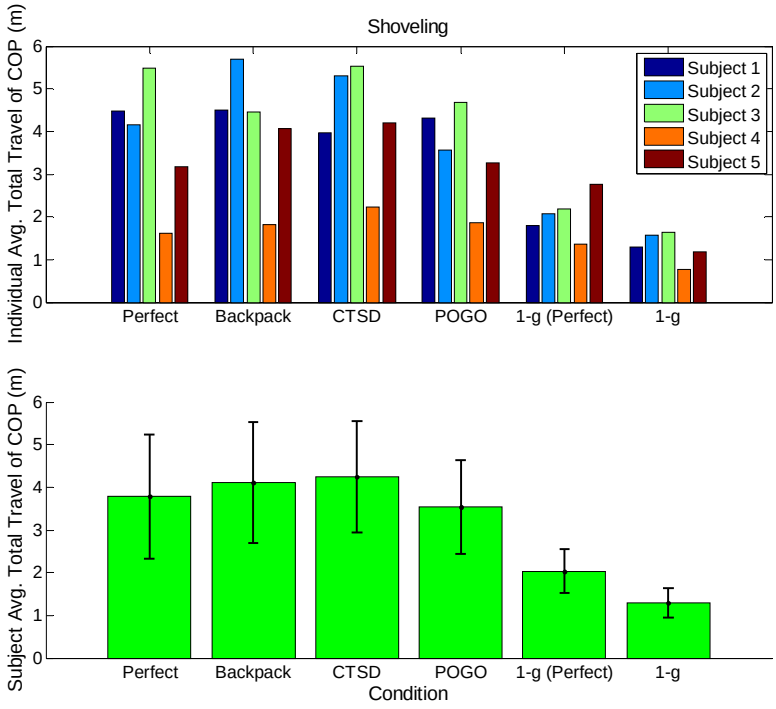

Figure 74. Average total distance COP traveled during the shoveling task.

4.4.1.3 Subjective Results and Discussion

Rating of perceived exertion

RPE results for the exploration tasks are shown in Figure 75. Comparing the 1-g, no-rig condition to the 1-g with rig offloaded indicated that the addition of the rig increased mean RPE by 2.2, 2.0, and 1.5 units for the kneel/recover, rock pickup, and shoveling tasks, respectively. This further indicated that notably more effort was required because of the increased inertia of the CG rig. For the varied CG conditions, the CTSD condition had the greatest mean RPE and the greatest variability. There were no notable differences among the Perfect, Backpack, and POGO CG conditions.

Gravity compensation and performance scale

GCPS results for the exploration tasks are shown in Figure 76. Comparing the 1-g, no-rig condition to the 1-g with rig offloaded indicated that the addition of the rig increased mean GCPS by 1.2, 2.0, and 1.5 units for the kneel/recover, rock pickup, and shoveling tasks, respectively. These changes further indicated that inertial components of the CG rig significantly affected results. For the varied CG conditions, the CTSD condition had the greatest mean GCPS, but the POGO condition had the greatest variability. Although significantly less than the CTSD condition, the POGO CG condition had the second greatest mean GCPS for all tasks. There were no notable differences between the Perfect and Backpack CG conditions.

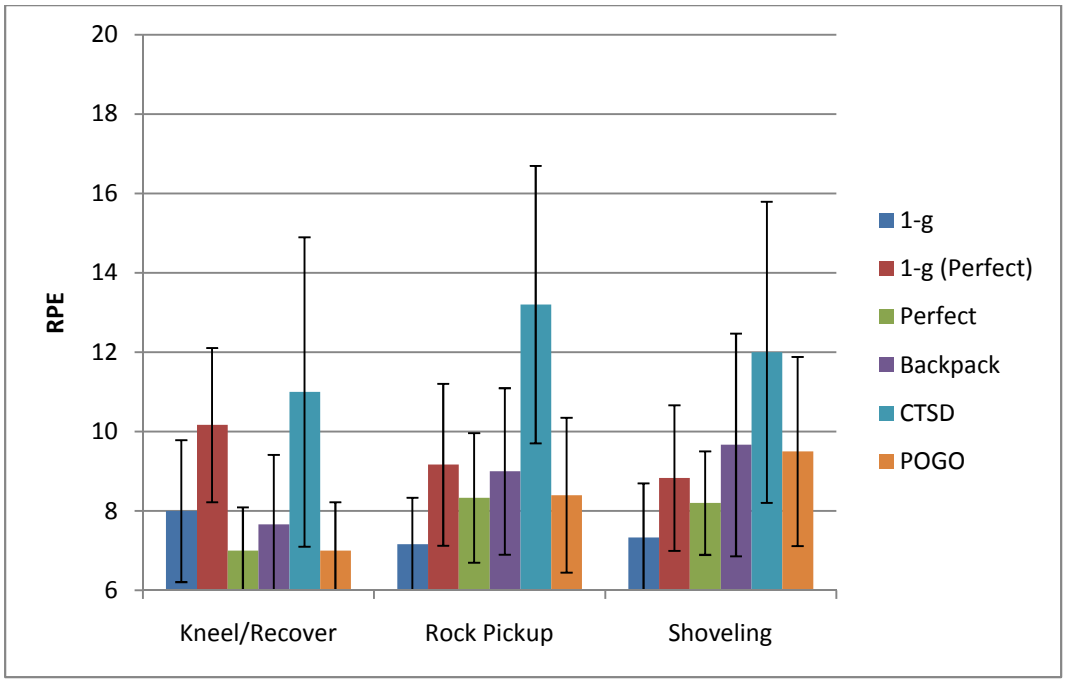

Figure 75. RPE for short-term exploration tasks at different gravity/CG conditions.

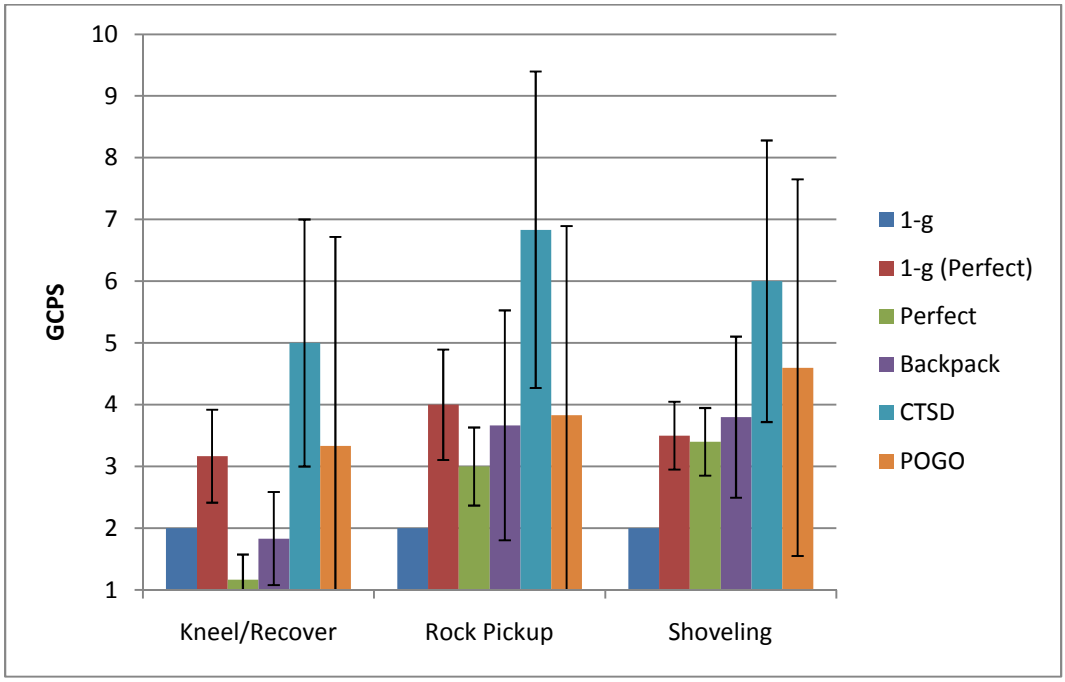

Figure 76. GCPS for short-term exploration tasks at different gravity/CG conditions.

4.5 Postural Stability Results and Discussion

4.5.1 Subject weight

The effects of the POGO system and varied CG configuration on subject weight are illustrated in Figure 77. Subject weights ranged from approximately 142 to 185 lb before donning the POGO gimbal support structure (Figure 77, 1-g). TGAW was largely unchanged by donning the gimbal support

structure configured to the Perfect CG and adjusting the POGO offload to maintain equivalent TGAW to what was seen during the 1-g, no-rig trials. Decreasing the subject-gimbal combination to lunar weight using the POGO system reduced the weight of all subjects to approximately 60 to 70 lb; reconfiguring the CG locations did not affect the weight in any substantive way.

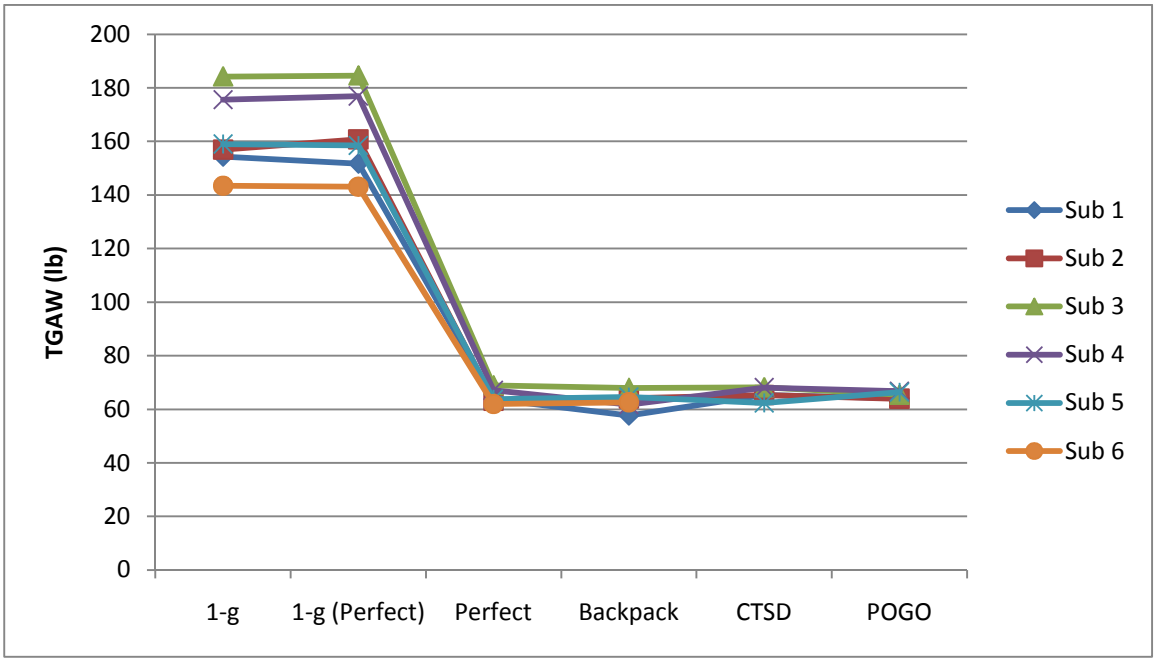

Figure 77. Subject weights measured during SOT 1 trials for each CG/offload configuration.

4.5.2 Quiet stance performance

The effects of each CG/offload configuration on postural stability control during the quiet stance tests were initially assessed using the standard clinical measure, EQ score (Figure 78). The shaded regions represent the normal 1-g-performance range (5^{th} to 95^{th} percentile) for a large group of test subjects studied under that condition. Scores below the 5^{th} percentile are considered abnormal.

For SOT 1, the standard clinical eyes-open Romberg test, it is clear that all the 1/6-g conditions disrupted postural stability when compared to the Baseline condition and to the normative population performance (Figure 78, top). The CTSD CG configuration had the greatest negative effect, with two of six subjects losing balance during the first 20 s of the 100-s trial, and one of six subjects feeling too unstable to attempt the trial. The POGO system alone appeared to have a stabilizing influence, as evidenced by the small apparent performance improvement observed in transitioning from the 1-g, no-rig condition to the 1-g (Perfect) condition in which the weight of the gimbal and CG rig were offloaded. Whether this putative improvement was caused by a posture-stabilizing mechanical or the haptic benefit of the POGO support system or by increased task vigilance caused by the stability-threatening load of the POGO gimbal system could not be discerned from the data. However, as neither of these factors should have been changed between the 1-g and 1/6-g offloads at the Perfect CG, it seems likely the performance decrement associated with this transition was caused by factors related to the offload transition, which could include an unappreciated decrease in the gain requirement for the control-system generating motor responses to counter postural balance errors detected by the visual, vestibular, and somatosensory systems or a reduction in the sensitivity of the somatosensory detectors.

EQ scores during the SOT 4 trials were generally lower than those during the SOT 1 trials, demonstrating the influence of distorting somatosensory inputs on postural stability control (Figure 78, bottom) As with SOT 1, CTSD had a substantial negative effect on postural stability, with only two of six subjects

performing within the normal range of performances for the 1-g version of this test condition, and three of six subjects losing balance or being unable to attempt the trial. The stabilizing influence of the POGO system was also apparent in SOT 4 as a performance improvement associated with transitioning from the 1-g condition to the 1-g (Perfect) condition. However, no new information allowed discrimination between a potential mechanical benefit and increased task vigilance as the cause. Unlike the SOT 1 trials, no obvious decrement in performance was associated with the transition from 1-g to 1/6-g. This strongly suggests that the decrement observed in SOT 1 was caused by a reduction in the sensitivity of the somatosensory detectors at the reduced loading level rather than by an unappreciated decrease in the gain requirement for the control-system.

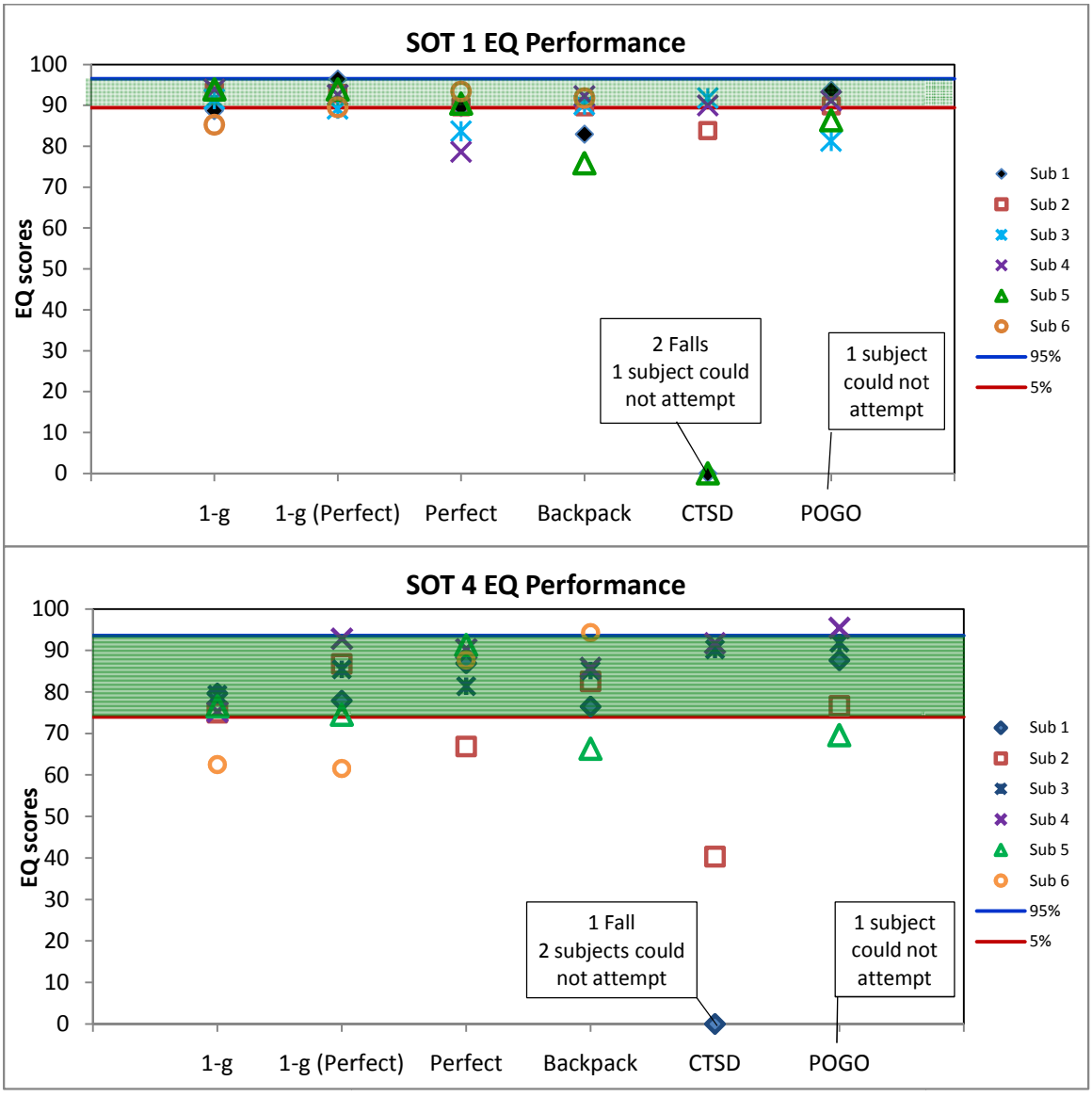

Figure 78. Effects of the six CG/offload configurations on each subject's postural stability control performance during SOT 1 (top) and SOT 4 (bottom) trials, as assessed by EQ score. The shaded region represents the normal performance range (5th to 95th percentile) for a large group of test subjects.

EQ score is a useful index to perform a clinical assessment but may be insufficient to fully assess postural stability control because it is based on only the worst-case body sway (position) excursions over

a 20-s period. We, therefore, computed TTC, which combines both position and velocity information, over the entire 100-s SOT trials. Two stability performance indices were derived from the TTC time series: the minimum TTC (TTC_{min}), which is analogous to EQ score in that it estimates the worst-case performance, and the integrated TTC (iTTC), which provides a broader estimate of performance over the whole trial. The effects of each CG/offload configuration on TTC_{min} and iTTC are shown in Figure 79 and Figure 80, respectively.

For SOT 1, transitioning from 1-g to 1-g (Perfect) did not change TTC_{min} or iTTC, but caused increased variability in each (Figure 79 and Figure 80, top). As with the EQ score, transitioning from 1-g to 1/6-g reduced postural stability for both TTC indices: TTC_{min} was decreased (Figure 79, top) and iTTC was increased (Figure 80, top). At lunar gravity loading levels, Perfect, Backpack, and POGO CG conditions resulted in similar performances, but CTSD caused substantially worse performance as assessed by both TTC indices.

For SOT 4, transitioning from 1-g to 1-g (Perfect) caused little change to TTC_{min}, except in one subject who exhibited much more stable performance (Figure 79, bottom). However, as with the EQ score, iTTC appeared to be improved by the POGO system (Figure 80, bottom). As with the EQ Score, at 1/6-g, Perfect, Backpack, and POGO had similar effects on postural stability performance, but CTSD caused substantially reduced performance as assessed by both TTC indices.

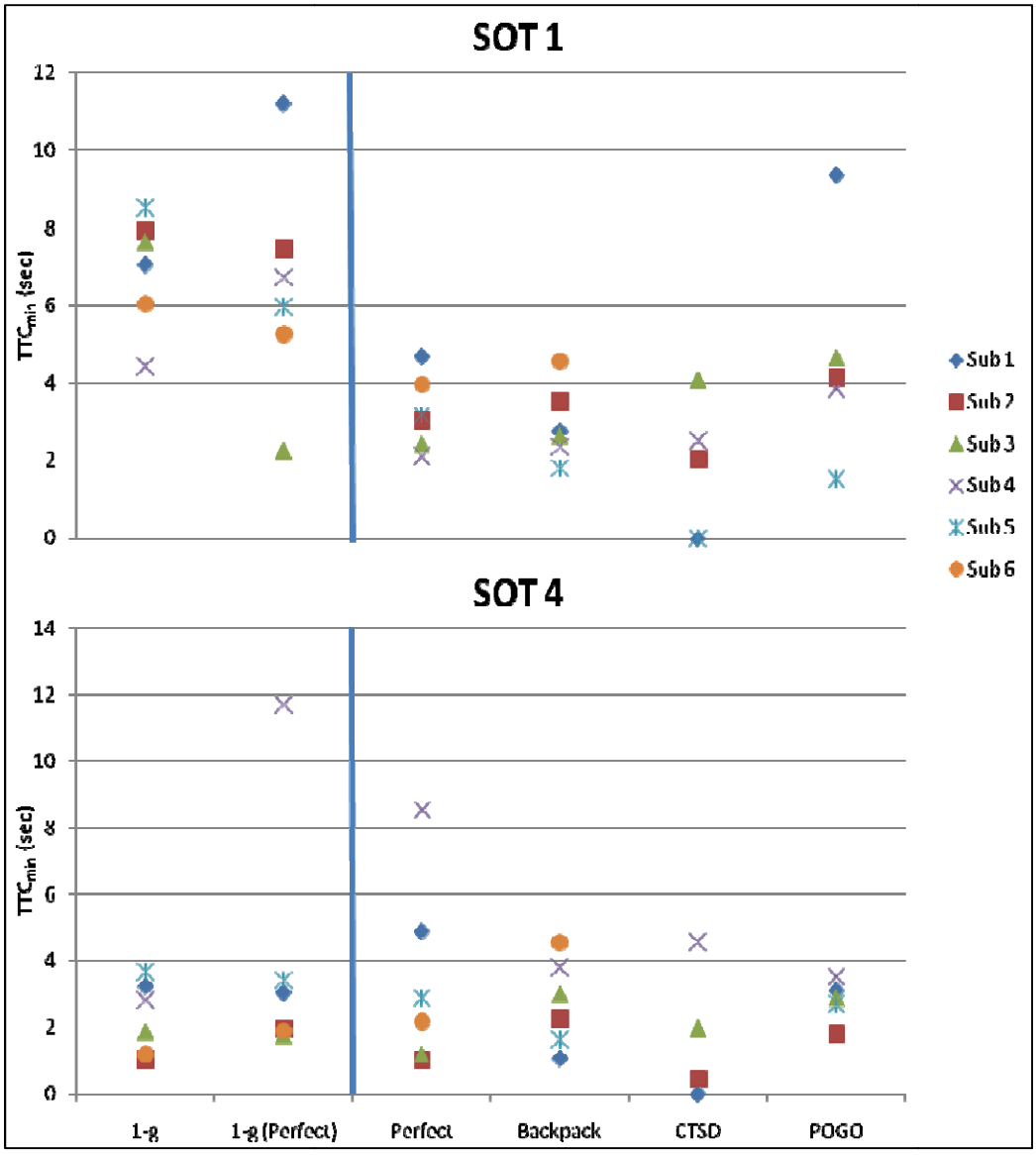

Figure 79. Effects of the six CG/offload configurations on each subject's postural stability control performance during SOT 1 (top) and SOT 4 (bottom) trials, as assessed by TTC_{min}. Note that one subject refused to attempt the CTSD and POGO conditions owing to a perceived instability.

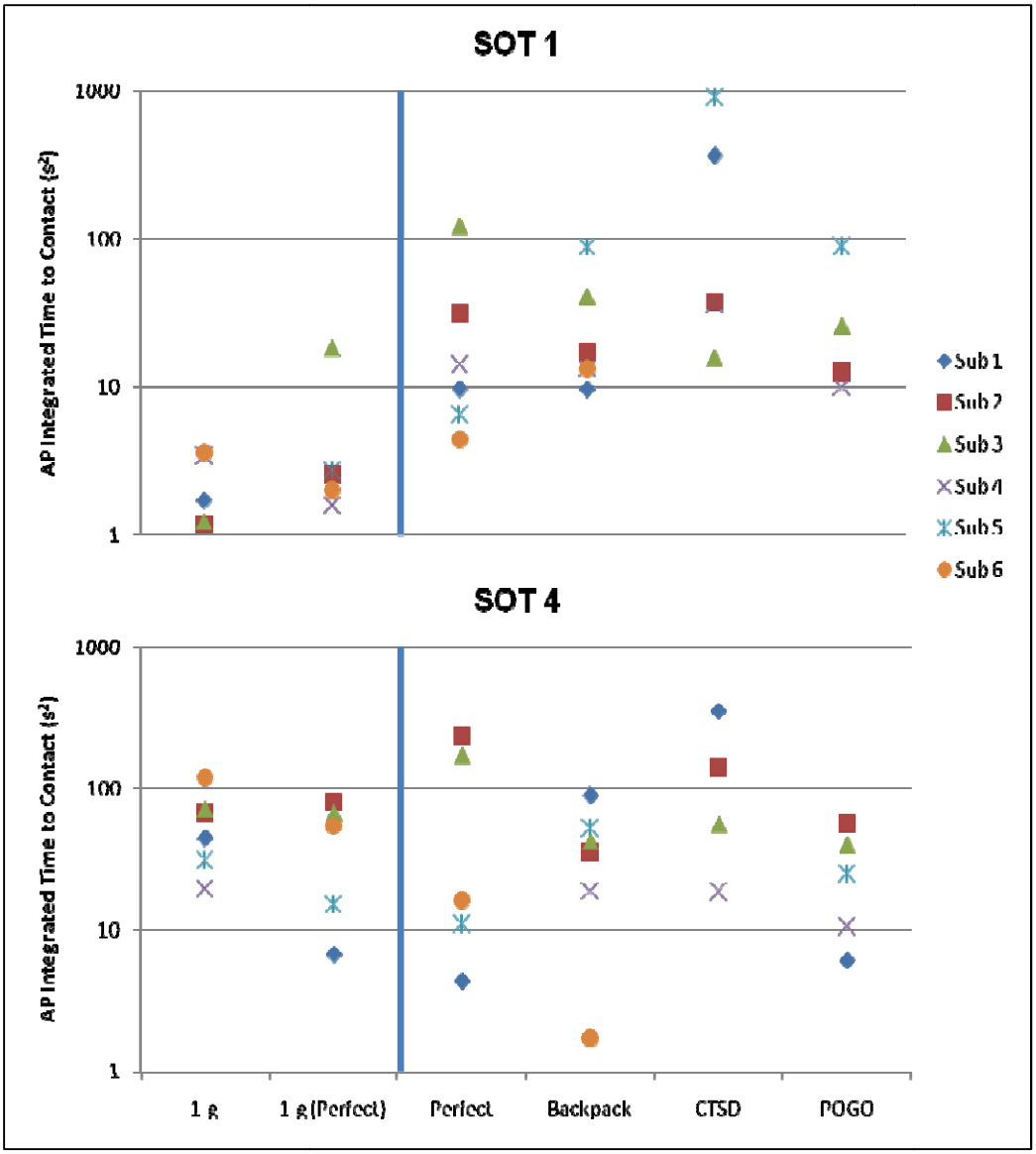

Figure 80. Effects of the six CG/offload configurations on each subject's postural stability control performance during SOT 1 (top) and SOT 4 (bottom) trials, as assessed by iTTC. Note that one subject refused to attempt the CTSD and POGO conditions owing to a perceived instability.

4.5.3 Response to postural perturbations

The effects of each CG/offload configuration on postural stability control during sudden postural perturbations were assessed using the TTC indices described above, although the assessment period included only the 9-s recovery period following the perturbation. The effects of each CG/offload configuration on TTC_{min} and iTTC are shown in Figure 81 and Figure 82, respectively.

The effects of the POGO system and lunar gravity on postural stability during perturbation trials were similar to those observed during the SOT 1 quiet stance trials: stability was improved somewhat by the POGO system and degraded somewhat by increasing the offload. As with the quiet stance trials, the CTSD CG also substantially degraded postural stability control during TU and TD perturbations as assessed by either TTC_{min} or iTTC, with five of six subjects losing balance or being unable to attempt the TU trials and three of six subjects losing balance or being unable to attempt the TD trials . For the other lunar CG configurations, there was an obvious difference between TU and TD perturbations, with the TU perturba-

tion being more stability threatening. This was particularly evident with the Backpack CG, which caused substantial performance deficits during TU rotations but not during TD rotations (compare, for example, the upper and lower panels of Figure 81 for the Backpack configuration).

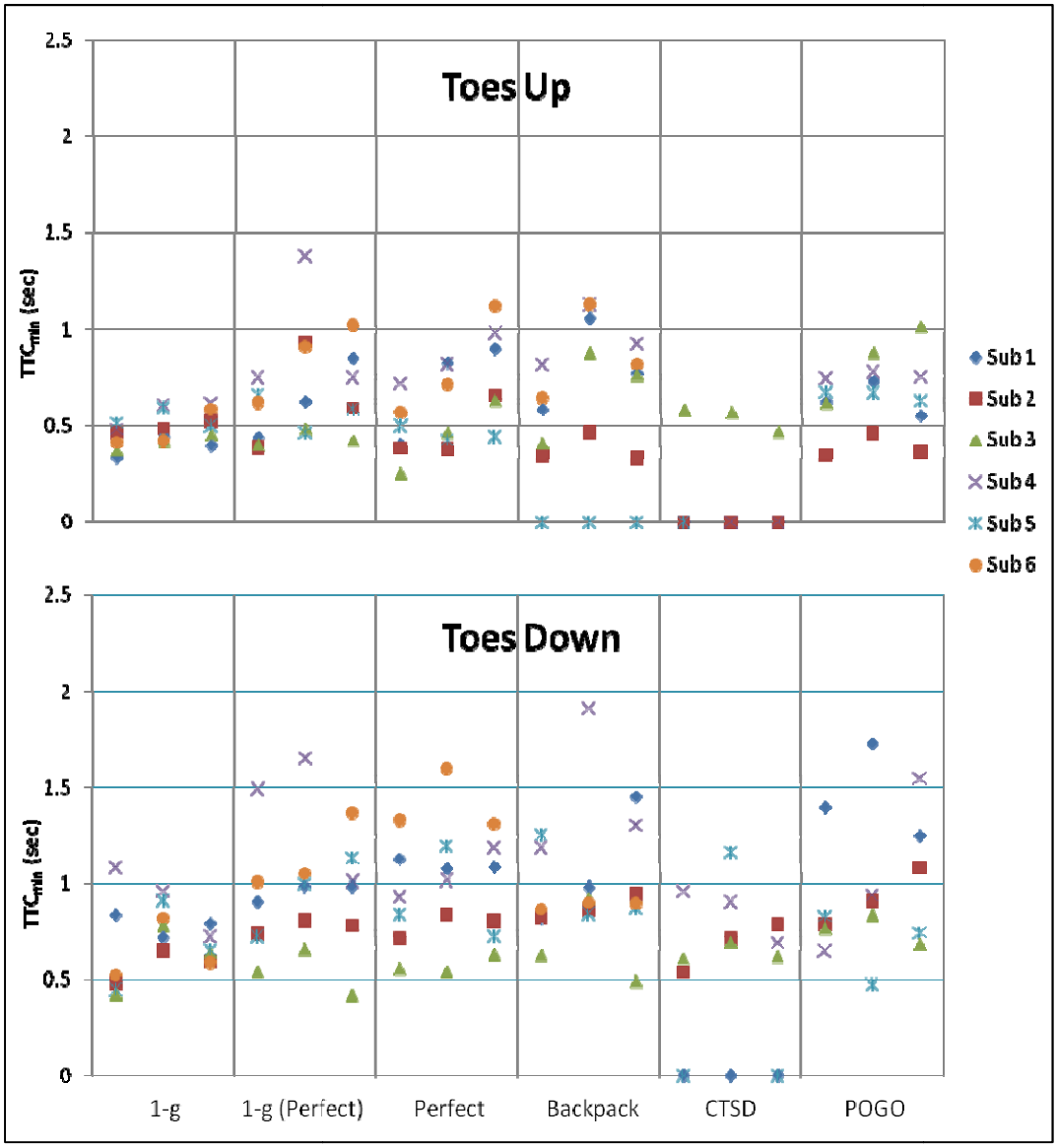

Figure 81. Effects of the six CG/offload configurations on each subject's postural stability control performance during sudden TU (top) and TD (bottom) trials, as assessed by TTC_{min}. Six randomized perturbation trials (three TUs, three TDs) were performed at each CG-weight configuration. All trials are displayed in the figure.

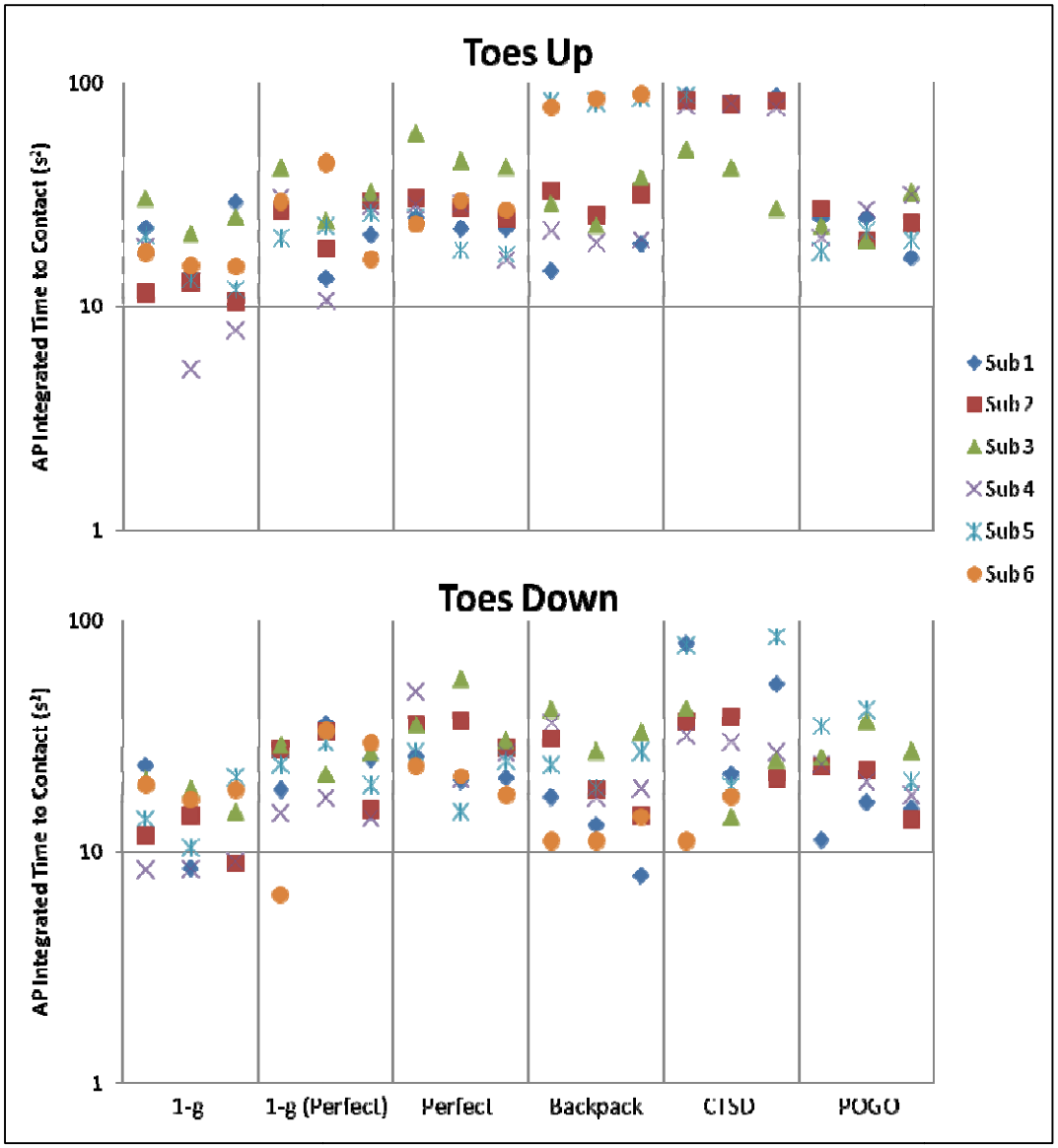

Figure 82. Effects of the six CG/offload configurations on each subject's postural stability control performance during sudden TU (top) and TD (bottom) trials, as assessed by iTTC. Six randomized perturbation trials (three TUs, three TDs) were performed at each CG/offload configuration. All trials are displayed in the figure.

4.5.4 Subjective ratings

For all postural stability trials, the 1-g, 1-g (Perfect), and Perfect CG conditions had similar results for both RPE and GCPS, and were also the lowest compared to the other three CG/offload conditions (Figure 83 and Figure 84). Both RPE and GCPS were highest at the CTSD CG for all postural tasks. Ratings at the Backpack CG were low for the SOT 1, SOT 4, and TD tasks, but increased significantly with the TU tasks. This could possibly be related to having more mass farther out on the CG rig arms and the subjects thus having to deal with a larger moment of inertia with the perturbation. Results for the POGO CG were generally the next greatest, except for the TD RPE and the TU GCPS (Backpack > POGO in both cases).

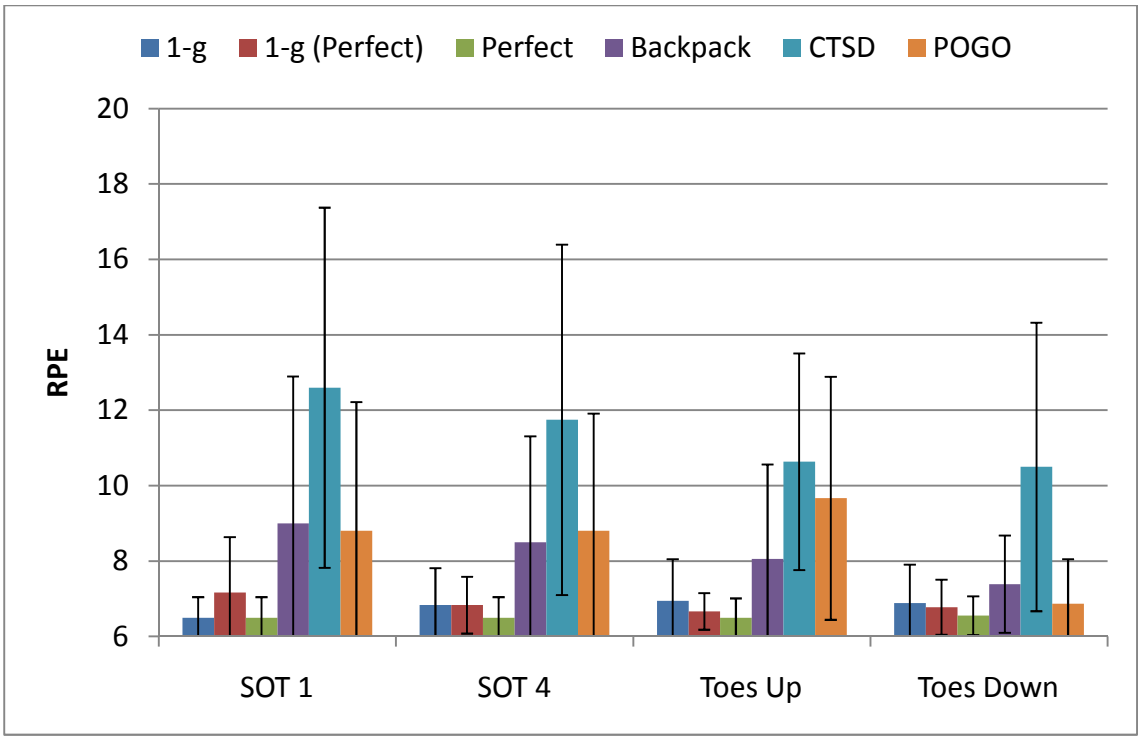

Figure 83. RPE for postural stability tasks at different CG/offload profiles.

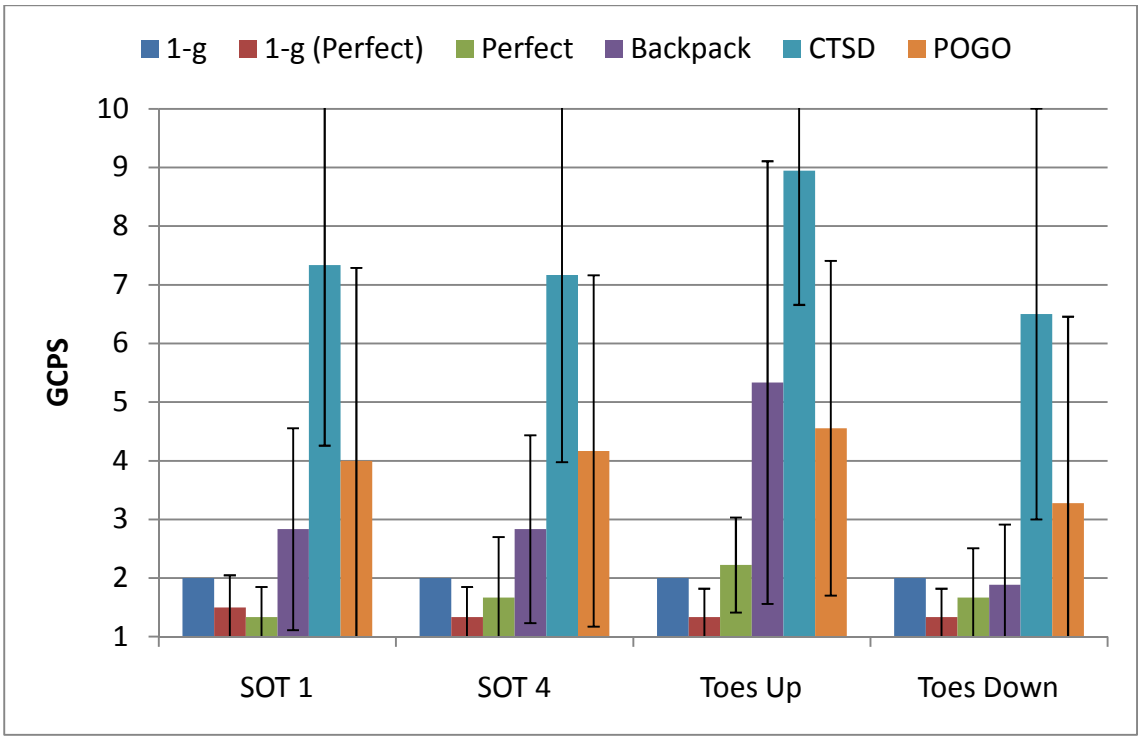

Figure 84. GCPS postural stability tasks at different CG/offload profiles.

5 Discussion and General Conclusions

5.1 Level and Graded Ambulation

For purposes of general conclusions, level and graded ambulation will be discussed together.

5.2.1 Metabolic rate

The primary trend to note with metabolic rate is that the metabolic rate was significantly higher with the CTSD CG condition for all ambulation cases. This could be attributable to two reasons. The first option, that the system CG location in relation to the subject's CG was placed in such a way that performance was compromised, is unlikely. The second option, that the system CG location in relation to the gimbal axes of rotation was placed in such a way that performance was comprised, is the likely cause. Post-test analysis, involving recalculation of the system CG alignment in relation to the gimbal axes of rotation, clearly shows how the CTSD CG was aligned in a manner that would negatively affect performance (Figure 85).

Investigators did not expect the lack of difference among the other CG conditions. Preliminary results from NEEMO/NBL studies indicated that a high/aft CG would negatively affect ambulation performance (3). While this was artificially the case with the CTSD CG, the POGO CG, which was even more high and aft, had very similar metabolic results to the Perfect and Backpack CGs. Testing varied CG conditions using overhead suspension systems, such as the POGO, increases the complexity because there are two areas of support: the feet and the vertical lift column. As there are two places in which subjects can stabilize themselves, an artificial stabilization may be induced that would not be seen in non-overhead suspension environments (ie, 1-g, underwater, or parabolic flight).

Comparing the varied CG data to the 1-g baseline shows a clear linear trend for the varied CGs at 1/6-g, whereas a second-order polynomial relationship was a better fit for the 1-g data. The second-order relationship is needed at 1-g due to the variation in energetics between a walk and a run. The linear relationship for the varied CG conditions indicates that there was no change in the energetics required to ambulate at speeds ranging from 0.4 to 2.5 $m \bullet s^{-1}$.

5.2.2 Kinetics

A notable increase was seen in normalized mean peak GRF values for 1-g trials with an increase in ambulation speed, especially at 2.1 and 2.5 $m \bullet s^{-1}$ (ie, running trials). Conversely, normalized peak vertical GRF for all CG rig conditions tended to plateau after subjects reached a 1.7-$m \bullet s^{-1}$ ambulation speed. For the incline trials, greater peak vertical GRF may have been present in the 10% decline as a result of the body having farther to fall with each step, attempting to control this descent, and maintaining stability while walking downhill. For this study, no definitive conclusions can be drawn regarding the effect of the individual CG rig settings on GRF during ambulation at varying speeds.

The variability of normalized mean peak GRF data across subjects for CG rig conditions was notably greater than for the 1-g condition for all ambulation speeds and inclines. CG rig data differ greatly from 1-g running and walking data (13). Whereas a 1-g GRF does not plateau until sprint speeds, the CG rig GRF plateaus at a moderate walk. This may be because ambulating at these varying speeds and grades while offloaded with a large attached mass altered the gait patterns adopted by subjects. There was a decrease in GRF with an increase in incline. This is in large part because the force platform in the treadmill only records forces normal to the treadmill surface. As the incline is increased, a larger part of the GRF will be incorporated into the anterior/posterior shear force, which is not registered by the platform.

A major issue at work in this testing environment is the fact that the weight of the CG rig system and the subject are offloaded to lunar gravity, but the mass and inertia of the subject and CG rig remain unchanged. This plays into effect when looking at CG excursion in the test environment and how the subject is compensating for the large inertial load. Recent studies have found that reducing CG excursion in normal 1-g walking does not decrease energetic cost, but actually increases it (16) (17). However, with an increased mass, the subject is forced to either expend more energy to get the same performance or reduce performance to save energy requirements. Kinetic energy in this case is derived from inertia, mass, linear

velocity, and angular velocity terms (Eq. [1]). As kinetic energy terms and mechanical work terms are interchangeable, we can consider an increase in system energy a direct result of work done by the subject or POGO (see Appendix D for variable explanations). Equations (2) and (3) show the interchangeability of work and energy in a dynamic system.

$$KE = \frac{1}{2}mv^2 + \frac{1}{2}I\omega^2 \tag{1}$$

where,

$$\frac{1}{2}I\omega^2 = I\alpha\theta \tag{2}$$

and

$$\frac{1}{2}mv^2 = mad \tag{3}$$

U.S. Army backpack studies have shown that subjects try to optimize energy expenditure with increased mass by reducing angular movements with the torso, but not necessarily by reducing vertical CG excursion. One study showed that joint rotation and vertical excursion of the CG during initial contact increased as a function of speed but not of load (22). These results would suggest that, normally, a human will maintain the same CG vertical excursion across the speeds tested regardless of unsuited 1-g or CG condition. This constant level of CG excursion is most likely a result of increased metabolic cost due to a deviation in normal gait mechanics. However, this was not observed to be the case in the current test environment. This lack of relationship between CG vertical excursion and speed indicates the current mechanical system (CG rig, gimbal, POGO) is restricting normal adaptation in gait mechanics.

It must be pointed out, however, that the mass increase in this study was actually much greater than could be studied under normal 1-g conditions. This adaptation may have resulted from the subjects being incapable of accelerating the system mass (CG) faster as the treadmill speed increased, and; therefore, plateaued at a "maximum" point.

The CG rig vs. subject CG data show that the CG rig and subject are acting somewhat independently of one another (**Error! Reference source not found.**). If we simplified the system and modeled it (Eq. [4]) as two separate masses connected by simple linear springs (ignoring the friction and damping), we will begin to see the independent and dependent nature of the test system.

$$k_1 x_1 + m_1 \ddot{x}_1 + k_2 (x_1 - x_2) + m_2 \ddot{x}_2 = 0 \tag{4}$$

Figure 85 shows a diagram of the simplified system with subject (m_1) and the CG rig (m_2). In this simplified model, the subject is the driving force of the system and the POGO is a passive, constant force.

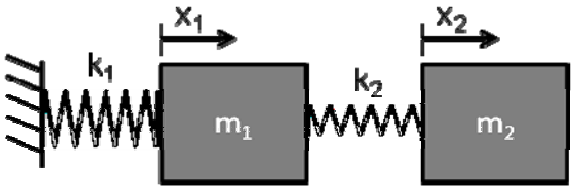

Figure 85. Illustration of a simplified diagram of the CG rig and subject mass-spring system.

Figure 86 shows the resultant simulation data from the simplified system. From the simulation data we can see that, because the two masses are non-rigidly attached to each other, they do act independently to some extent.

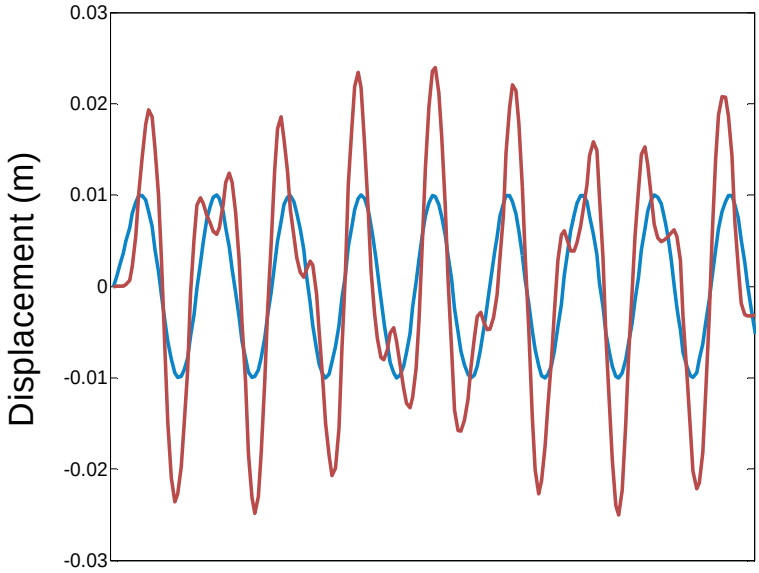

Figure 86.Simulation data of the previously mentioned mass-spring system. The blue line is the displacement of a sine wave that is driving the m_1 element (subject); the red line is the resulting displacement in the m_2 element (CG rig).

In a system such as this, complex interactions make it difficult to predict the state of the second mass. In the actual CG rig system, it is equally difficult to predict interactions between the subject and the CG rig, making accurate calculations of system outputs impossible without a detailed model. The second issue with such systems is that the second mass element (m_2) has more energy than the driving mass element (m_1). This is similarly seen in the actual system (Figure 20), and it may also be a factor in the reduced CG excursion observed as subjects attempt to reduce the amount of energy in the CG rig and diminish impacts with it as speed increases.

IST-3 data showed similar trends of CG excursion reduction with the CG rig conditions as compared to the unsuited 1-g condition. The reductions at the faster speeds were most likely due to the subject compensating for the very large inertia of the CG rig and attempting to reduce energy expended during ambulation. IST-3 test results for lower-extremity joint rotations, which increased with speed and allowed the body to increase speed while keeping the CG excursion minimized, were also similar to the reported studies (22). However, at slower speeds, an increase in CG excursion was seen, most likely as a result of an ability to build up a large momentum with the increased mass of the mechanical system at a reduced cost because of the constant weight offload. Once this mass is put in motion, the subject can then take advantage of the large inertia of the POGO system and effectively reduce energy expenditure as the combined system's CG completes its trajectory.

The first major limitation to this study is the amount of compensation required by subjects due to the inertial characteristics of the gimbal and CG rig, which were much larger than an actual suit and PLSS. Therefore, the data can only be looked at as a trend.

A second major limitation is shown in the CG excursion traces as a difference between the CG rig and the human body. These traces show both a greater level of kinetic energy in the mechanical system than in the subject's body and a phase difference. This out-of-phase behavior demonstrates that the POGO system with the CG rig is not able to follow human motion closely enough, resulting in small collisions of the two masses. These collisions will be consciously minimized by the subject in an attempt to reduce the

energy input from the body into the mechanical system. This minimization is accomplished by compensation in the gait mechanics.

A third limitation could be that of the slow system oscillations represented by the slower waveform of the average CG over the trial period (Figure 21). This vertical translation also will influence gait biomechanics by increasing or decreasing joint rotations to stretch or contract the total leg length to accommodate the change in distance from the pelvis to the floor as the average distance of the subject CG to the floor changes. This hypothesis is unproven, however, and could be influenced by small, dynamic changes in treadmill pitch. Unfortunately, no reference data were taken for the treadmill during the trials.

5.2.3 Temporal-spatial characteristics

A consistent decrease in mean stance time was observed with increased ambulation speed for all tested conditions. Additionally, the variability (ie, standard deviation from mean values) across tested conditions notably decreased with increased ambulation speed. With the exception of the "POGO CG" condition at 10% decline ambulation, mean stance times for all CG rig conditions were less than those for the 1-g, no-rig condition across the tested surface grades.

A modest decrease in mean-step width was observed with increased ambulation speed across all tested conditions. Mean-step width for the 1-g condition was consistently lower than mean-step width for the varying CG rig conditions at varying ambulation speeds, suggesting greater stability during ambulation under 1-g conditions. Increases in step width in the CG conditions in comparison to the 1-g condition may be due in part to the effects of the donned harness associated with the CG rig used in the current study. This harness used support straps around the upper thighs that may have altered subjects' preferred gait patterns by forcing their legs into a wider stance. Minimal differences in mean-step width across varying surface grades were observed for the 1-g, no-rig condition. All mean values for this condition corresponded to a step width of approximately 0.1 to 0.15 m. Mean-step width values for all varying CG conditions were larger than values for the 1-g condition (Figure 23 and Figure 47). The greatest increases occurred at the -10% decline ambulation condition. This may be the product of several factors, including the aforementioned effects of the harness on subjects' adopted gait and the difficulty inherent in ambulating down a -10% grade while offloaded to lunar gravity in a CG rig that involved considerable effort by the subject to maintain a stable gait pattern.

5.2.4 Kinematics

Differences seen in gait mechanics when walking over ground compared to walking on a treadmill (23) are small and generally constant (although changes are different for males and females), allowing for substitution of one test environment for another when studying gait mechanics.

5.2.4.1 Speed vs. Center-of-gravity Condition and Offloading Mechanics

The gait kinematics of the subjects studied are considered to be normal (ie, without significant pathology). Kinematics of the lower body of the IST-3 subjects at the 1.3-m•s^{-1} speed were closely aligned to published normative data taken at an average of 1.3 m•s^{-1} (2.9 mph) (14) (24). Changing the gait speed affects the gait kinematics by requiring greater power output from the body as speed increases.

Little change was observed among CG conditions across the varied speeds for the lower body kinematics. One study showed there was a reduction of joint rotation for subjects while wearing a backpack from the no-pack condition across walking speeds (25). However, this study also showed an increase of joint rotation across both rig and no-rig conditions with this increase in speed. The lack of difference among CG rig conditions would indicate there was no change to compensation strategy.

Lower-body gait kinematics are expected to change in simulated, reduced-gravity environments as body weight support is increased. These changes stem from the reduced dependence on loading to produce forward and vertical motion. Previous studies showed the kinematic changes in the lower-body joints as body-weight support was increased from 10% to 70% (26) (27). Changes observed in the IST-3 test between the unsuited 1-g and the CG rig conditions followed similar trends to those reported, but the

changes in the IST-3 were much greater than the changes in these two studies in both angle magnitude and time of occurrence (26) (27). At the 1.3-m•s^{-1} speed, there was a shortening of the time to end contact in the gait cycle, a shortening of the hip and knee angles, but an increase in ankle angles. These changes no longer allow the body to produce large propulsive forces in the forward direction because of the small horizontal component of the vector from the ground-contact point to the COM (Figure 34 and Figure 35). This would indicate a reduced dependence on forward propulsion but a continued dependence on vertical propulsion. CG conditions at all speeds were similar to the 1-g no-rig running-speed ankle kinematics. This similarity illustrates the mechanics being used in the POGO. While running, the body contracts the anterior and posterior shank muscles to increase the stiffness of the ankle, thus allowing for more efficient energy storage and transfer. The fact that while on the POGO the same strategy is implemented for the CG rig conditions means the subject was no longer constrained by normal walking biomechanics and could use the more efficient energy storage and transfer system of a stiffened ankle joint.

Given this information, we are left with a conundrum: Have the subjects taken advantage of the treadmill velocity (ie, a moving reference frame), or are they still producing actual propulsion forces in a reduced amount commensurate with the decrease in gravity? Would a person restrict his/her power output on the moon and conserve all possible energy or use the available power to advantage and increase his/her traveling speed? How do we test the change? Currently, we cannot measure shear forces and verify our proposition. However, logic suggests that if the subjects took advantage of the true lunar environment, they would still produce their normal propulsive forces, as they still have the full amount of muscular power generation possible. They could do two things: (a) increase both vertical and horizontal-force generation proportionally, as they would in a 1-g environment, or (b) increase the horizontal-force generation but not the vertical, as they no longer need the large vertical reaction force in a reduced-gravity environment to elicit the same horizontal movement outcomes.

Unfortunately, the subjects' data did not fit to our logical estimations of change in gait for the changing environment, nor did they continue to follow normal 1-g gait mechanics. C. R. Taylor found that when humans adopt a jumping mode of ambulation, their jump frequency does not change from jumping in place to increased velocities on a treadmill (28). This paper also showed little change in peak GRF values among speeds; however, the loading duty cycle decreased with speed. Given these facts, it is apparent that the IST-3 subjects were able to take advantage of the treadmill belt velocity by continuing to jump vertically with little extra effort to travel horizontally (Appendix C). In an over-ground situation, the subject would have to increase both horizontal and vertical forces to increase his/her speed and/or linear distance traveled. One of the major factors that allows subjects to possibly take advantage of the relative treadmill belt velocity is the inertia of the overhead POGO cylinder. This cylinder stabilizes subjects, allowing them to jump vertically without having the necessary forward propulsive force that would normally be required to remain on the treadmill at a given velocity.

Torso tilt of normal gait follows a pattern of flexion and extension as muscles of the legs and torso pull and push the hip when the body initially contacts the floor before it progresses into mid-stance (24). As speed increases for the 1-g no-rig condition, the magnitude and timing of the tilting ROM increases accordingly as more energy is put into the system and the gait patterns change (29) (30). Tilting in the CG conditions for this study was very minor in comparison, and was out of phase by close to 90°. For the CG conditions, the torso remained in a permanently forward-tilted state. The CTSD condition was the exception in which, at faster speeds, the tilt offset was reduced to a near-neutral point. The POGO and gimbal system causes the subject's torso to take on a static-tilt angle as the lifting forces and CG align. The system may also impede the subject from dynamically tilting at the hip joint by increasing the difficulty in performing that motion. One theory is most of the reduction in tilt will be due to the gimbal's sagittal pivot point being out of alignment with any of the body's joints, thereby increasing the force needed to tilt the torso dramatically. Another theory links most of the reduction in tilt to the overhead mass of the POGO pneumatic cylinder. To bend forward, the subject must pull the POGO pneumatic cylinder forward and down, thus increasing the force needed to tilt the torso. The constant tilt offset is created by the subject and the CG rig and gimbal pitching forward to reduce any internal moments and acquire a static equilibrium position. Both of these events restrict the body from using its normal strategies and dynamics when

ambulating (Figure 34 and Figure 57). The exception to this was the CTSD CG, which seemed to compel an upright posture during all test conditions, most likely because the system CG was located high and aft of the gimbal axes of rotation.

5.2.4.2 Incline vs. Center-of-gravity Condition

Walking on an incline or a decline changes the basic mechanics of ambulation as your joints are required to bend more to raise your foot for the next step on an incline or less when letting it fall farther in a decline. The unsuited 1-g conditions follow closely those of reported normative data for walkway and stair ascent and descent (Figure 49 through Figure 55) (21) (31).

At the -10% grade, the ankle flexion ROM data for the CG conditions were closely aligned to the 1-g no-rig condition. Beyond this specific incline and joint, large differences were seen in magnitude between the CG conditions and the 1-g no-rig condition. Again, the CTSD condition showed a high level of change over the range of inclines whereas the other CG conditions remained relatively static. All CG conditions showed the same general trends in changes of ROM with change in incline, except for the torso-tilt angle, which did not show any agreement in trends as the incline was changed.

However, the actual angle traces show stark differences between the 1-g no-rig condition and the CG conditions. The ankle angle traces had the worst comparison, showing little in common in both shape and timing. This was primarily due to the subjects never reaching full foot contact with the floor in the CG conditions and remaining on their toes the entire time. The hip and knee angle traces showed better similarity between CG conditions and the 1-g no-rig condition, but still held prominent differences. Given these facts, it is safe to say there is little in common between the CG conditions and the 1-g no-rig condition as far as gait mechanics adaptation is concerned. Minimal changes were seen among any of the CG conditions, the exception being the CTSD. Across the CG conditions adaptation in the ankle and hip mainly occurred as an increase in ROM. For the knee, the CG showed greater change in shape and timing over the inclines and from each other.

As incline changes, there is a shift in GRF with respect to the location of the hip joint (32). With increases in incline for normal gait, the foot is placed farther out in front of the body at initial contact, increasing the hip moment; just the opposite occurs for declines. The torso is also tilted forward in an attempt to shift the CG forward, thereby reducing the net hip moments; the opposite is true for declines. The increases in lower-body angles for the CG conditions are simply a result of the subjects making changes to accommodate the need for a greater height requirement for gait at an incline, not as a result of compensation to produce more efficient gait. These facts would imply there was little adaptation occurring for the CG conditions as other adaptive methods were unavailable to the subjects as a result of CG rig, gimbal, and POGO restrictions.

5.2.5 Electromyography

For comfortable to fast walking speeds, the erector spinae is active during the swing phase, right before initial contact (33), and for level ambulation; the 1-g no-rig trials for the representative subject followed this trend. On the other hand, all CG rig trials above 1.7 $m \cdot s^{-1}$ only showed muscle activity during the swing phase. This may have been because the subject had a reduced GRF as compared to the 1-g no-rig condition or as a result of the altered gait patterns (lack of heel contact) and; therefore, had a reduced need for spinal stability. As speed increased, the duration of activation decreased, possibly because of an increase in cadence and a decrease in swing motion.

The decline and highest incline for the CG rig configurations had a high percentage of high-intensity contraction during the active segments. Low-level activation was substantially reduced at these inclines. The erector spinae may have been contracting at a high intensity and long duration to maintain balance. Some differences were seen among different CG rig conditions, but none was uniformly consistent across conditions.

Analysis of the erector spinae data proved useful in the understanding of treadmill data. This muscle has a primary role as a core stabilizer during ambulation. Upon changing the CG, it was hypothesized that

the erector spinae response would adapt accordingly by increasing activity, but such a change was not seen for the analyzed subject. The addition of the CG rig before offloading the subject largely influenced activation of the erector spinae.

5.2.6 Subjective ratings

Subjective rating trends followed the metabolic data trends with respect to the varied CG conditions. RPE was clearly rated differently in and out of the CG rig, which is consistent with other data showing different RPE ratings in and out of the MK III suit. This finding indicates that while RPE alone may be highly correlated with metabolic rate, it may only be specific to certain test conditions, and any model expecting to use RPE to predict metabolic rate should be limited to certain conditions or employ an additional factor describing different conditions for which the data were collected.

The 1-g data were not included when modeling VO_2 based on subjective ratings, thus leaving only the varied CG conditions. VO_2 was predicted from the subjects' RPE and GCPS. Mixed-effect regression analysis was used to model VO_2 from RPE and GCPS scores, including subject-level grouping to accommodate for the dependence in the data (ie, repeated observations within subjects) and a random intercept term to allow subjects to vary randomly on the y-intercept of the model. The model residuals appeared normally distributed with constant variance over the range of the outcome, suggesting that the transformed data are appropriately analyzed with these techniques.

The model revealed that both RPE and GCPS predictors made significant variance contributions to VO_2 in this multivariate context ($P < .05$), with the highest relative contribution observed for the RPE predictor. RPE scores were positively correlated with VO_2 and GCPS scores were negatively associated with VO_2 in this model. Model-predicted and -observed VO_2 values are shown in Figure 87. The variation in VO_2 seen per unit of RPE was notably improved by the model.

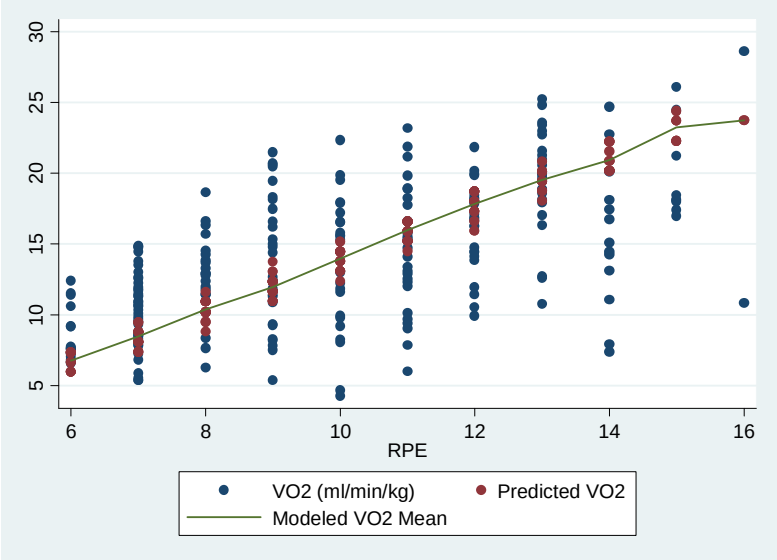

Figure 87. Model-predicted VO_2 (red) and -observed VO_2 (blue) with respect to RPE.

While these effects are statistically significant to traditionally held scientific standards, the reader is reminded that they are based on a very small sample of $n = 6$ astronauts. We remain cautious about making inferences to the larger astronaut population or outside of level-ground ambulation until these results can be replicated in future work.

Another interesting finding from the ambulation data was that subjective RPE and GCPS ratings tended to either stay the same or increase slightly by one unit on the rating scale from a measurement taken at the 30-s mark to the measurement taken at the 150-s mark of a 180-s trial. For RPE during

ambulation trials, 68% of the ratings stayed the same and 26% increased by one. For GCPS during ambulation trials, 82% of the ratings stayed the same and 12% increased by one. As would be expected, GCPS ratings were less affected by trial duration. While this may be a good indication of what generally happens with these ratings, these findings are only applicable to ambulation data. More research will be needed to determine whether RPE can be applied to different types of tasks, higher-intensity tasks, and tasks of less than 30-s duration.

5.3 Exploration Tasks

Three different types of exploration tasks were performed: a rock pickup, shoveling, and kneel-and-recover. It is important to note that as all of these tasks were performed in a fashion intended to be similar to previous and concurrent studies, they differ somewhat from how they would be performed during an actual EVA. Bags filled with lead shot, which were used as "rocks," were picked up and shoveled off of a significantly elevated surface rather than the ground. The kneel-and-recover task did require the subject to bring his knee down to the ground, but it is unlikely this task would be performed alone but, rather, would be a portion of a task involving picking something up off the ground or using a tool close to the ground. Future tests should attempt to perform EVA tasks in the most realistic way possible first and then modify this with an alternate performance method only if it was not possible to complete the task. With this method, data on both realistic EVA tasks and modified EVA tasks will be available from which to draw conclusions and develop forward work and recommendations.

5.3.1 Strategy

The varying movement strategies adopted by subjects to complete exploration tasks did not allow for customary biomechanical analyses to be performed. Therefore, a qualitative analysis of adopted strategy was employed to characterize the performance of these tasks. This approach was incorporated to provide meaningful interpretation of exploration task data, given the difficulty inherent in generalizing kinematic analyses of variable adopted movement strategies to a population. This analysis was also used to provide an initial, observation-based assessment of CG rig and gimbal components, and to determine whether these components had any confounding effects on task performance.

For the rock pickup task, all subjects used their right hand to pick up the rock when performing the task under 1-g, no-rig conditions. However, not all trials performed under offloaded conditions involved the use of the right hand, suggesting the movement pattern selected under these conditions was affected by restrictions placed on the subjects by parts of the offloading system components. This finding was further confirmed by observation of movement coordination between the upper and lower body to perform the rock pickup task. Under offloaded conditions, when picking up the rock with the left hand, subjects never bent down to their left. Similarly, when picking up the rock with the right hand, subjects never bent down to their right. One possible explanation for this finding pertains to the need for subjects to maintain balance to complete the task. Based on the 1-g baseline findings for this task, we could assume that the CG rig used in the offloaded conditions introduced extra, artificial inertial factors that may have affected subjects' balance and; therefore, their movement strategy.

All rock pickup trials in the current test performed under 1-g, no-rig conditions corresponded to stable foot placement by subjects. However, half of the trials performed in the CTSD CG condition and nearly 60% of the trials performed in the 1-g (Perfect) condition led to unstable foot placement by subjects. Again, this may be attributed to balance being affected by the CG rig and gimbal structures offloading the subjects.

During the kneel-and-recover task, subjects either stood up from the kneeling position or jumped up. Kneel-and-recover, under 1-g conditions, typically does not involve rapid, explosive jumping up to the standing position mainly due to the considerable amount of muscular effort that would be required to perform such a maneuver. It is possible that on the lunar surface, astronauts may be able to more easily jump up than stand up from a kneeling position. However, the to-be-determined ROM requirements of a planetary suit, as well as the demands and objectives of the specific lunar sortie task, will play large roles

in the crewmembers' adopted strategy and overall task performance. While all 1-g, no-rig trials involved standing up from the kneeling position, approximately 25% of trials performed with the "Backpack" and "CTSD" conditions and over 30% of the trials performed with the POGO CG involved subjects jumping up from the kneeling position. This may be the result of assistance provided by the offloading system (ie, for these CGs, subjects often felt pulled backward), thus potentially making it easier for subjects to take advantage of the system and jump up. If the CG configuration were to have kept a subject's COM forward enough, it may have been easier for the subject to stand up.

Performance of the shoveling task resulted in varying interactions between the upper and lower extremity segments across subjects, and whole-body coordination was required to complete the task. The observation of foot placement on the force platforms throughout each trial helped to provide a qualitative assessment of stability during task performance. Stable foot placement on the force plates was observed for all 1-g, no-rig trials and approximately 85% of the "Perfect-rig offloaded." This may be because while the CG rig was offloaded, subjects tended to keep a 1-g footprint on the ground.

Over 50% of trials for both the CTSD and the POGO conditions had observed unstable foot placement by subjects. Several movement strategies were employed by subjects to complete the shoveling task; these varying strategies may also have been the reason for observations of unstable foot placement in certain trials. For instance, subjects varied the position and orientation of their hands on the shovel handle, effectively altering their approach to the task. This may have been a result of the difficulty experienced when trying to shovel bean bags from an elevated platform, the long length of the shovel handle, and/or the subjects attempting to keep the end of the shovel handle from interacting with the CG rig when performing the task. This often led to subjects pushing the bag off the elevated platform rather than actually scooping the rock and moving it. These factors may have also led to subjects altering their movement strategy, including movement of the shovel platform, and interaction (ie, contact) of the CG rig and the gimbal structure.

5.3.2 Stability

Although the CTSD CG resulted in the most time spent outside of the BOS, on average it had a smaller area of support. This smaller area of support may have been why the time outside the BOS was high for this condition. However, as discussed in previous sections of this report, this result may not be solely due to CG placement. Subject strength and method play an important role in the ability to control the COP. As seen with Subject 1, who had the fewest occurrences of COP outside the BOS, the distance the COP traveled was comparable to that of the other subjects, but the area of support was much larger. Further, Subject 4 recorded the greatest amount of time the COP was outside the BOS for configuration CTSD CG, but had the least amount of total COP travel. Thus, individual differences contribute a great amount to the results for stability and should be considered in future tests.

Several factors may have worked to confound the stability analysis results. As mentioned previously, many subjects did not adhere to the rock pickup protocol. One subject dropped down to pick the rock up but just dropped it while standing instead of bending to set it down. Some subjects chose to step onto the force plates while also reaching forward for the rock, thus confounding the data. Stricter subject adherence to the testing protocol will only improve the quality of the results.

When subjects were in the gimbal and suspended by the POGO, only one subject tried to continue bending at the waist. Other subjects used a lunge technique, did not move the upper torso at all, or used the POGO uplift to gain assistance with dropping or leaning in to get the rock. Constructing or using test hardware that will allow subjects all the degrees of freedom afforded to them with no hardware attached may improve the results and inferences for this analysis.

On average, the shoveling task had much less percentage of time outside the BOS as compared to the rock pickup. This is contrary to what would be expected. Shoveling requires more complex movements of coordinating upper and lower body. Each subject experienced difficulty with different configurations. There was no clear trend across configurations. Only Subject 3 performed each configuration consistently, but the

rotation of the gimbal falling forward and the rig getting caught on the gimbal for only the Perfect CG configuration confounded the results.

No CG configuration clearly appeared to have greater stability than the other configurations. For both the rock pickup and the shoveling tasks, too much variability was noted among the subjects and across the conditions to make any viable comparisons. Further, there were no observable trends for either task in any of the tested CG conditions. It is believed this lack of finding is mostly due to the confounding interactions among the POGO, gimbal, CG rig, and subjects previously mentioned. Subject strength, or lack thereof, may also have played a role in the variability of the results.

5.3.3 Subjective ratings

Subjective results further supported the negative impacts of the CTSD CG on human performance, but this finding was more likely due to system CG misalignment with the gimbal axes of rotation than to system CG variation from the subject CG.

Beyond using the subjective ratings to compare different configurations, one surprising finding was the large amount of variation within the ratings at a given condition – most notably with the Backpack, CTSD, and POGO CGs. This highlights the great degree of variability present in the astronaut population. Future EVA systems tests should include a larger sample size and not assume a reasonably homogenous astronaut population. Further, subjects should be characterized with respect to anthropometry, strength, and fitness so these measures can be considered during posttest analyses and explanations of results.

5.4 Postural Stability

While we set out to answer the question of which CG configuration(s) might least influence postural stability control, it was also necessary, to interpret our results, to determine whether the POGO system and/or offload affected postural stability control during the experiments. We also needed to determine how the POGO system affected the subject BW from condition to condition. We found that the weight was fairly well controlled throughout the experiments (Figure 77), that both the POGO system and the offload level affected postural stability, and that at least one CG configuration was very disruptive to postural stability control.

The test conditions employed were derived from the measurements routinely used in clinical assessment of balance disorders (34) as well as in assessment of postflight recovery of neurological function in astronauts (35) (36) (37) (38). SOT 1 was selected as the best-case postural stability control condition, with full sensory system availability and no challenging environmental conditions. SOT 4 challenged the subjects' posture control systems by distorting somatosensory inputs in ways similar to those a crewmember might experience while standing (or walking) in a thick layer of regolith on the lunar surface. The perturbation trials examined the subjects' abilities to respond to sudden external challenges to postural stability in the forward (TD) or backward (TU) direction. Such perturbations could occur on the lunar surface by a sudden shift in the regolith or by being bumped by another crewmember.

The postural stability performance measures employed included the EQ score (34), which is a standard clinical measure that allows comparison of performance results with a large extant database of normal test subject performance measured by JSC Neurosciences Laboratory personnel over the past 20 yr, and TTC, a more robust measure that has become more widely used in the past 5 to 10 yr (39). EQ score is somewhat limited in that it is based on peak postural sway displacements over a 20-s period. TTC improves on this by adding information concerning sway velocity and extending analyses to the entire 100-s duration of the trial. We analyzed the TTC time series in terms comparable to the EQ score, to the worst-case (minimum) value of TTC over the trial, and by integrating the total time during the trial the TTC was less than 10 s (an arbitrary cutoff value). EQ score and TTC_{min} point to how close the subject came to losing balance during a trial (which could have been a singular event), while iTTC is a measure related to the total amount of time the subject was at risk of losing balance during the trial, and should be related to the amount of metabolic effort the subject had to put in to maintain upright stability during the trial.

We were unable to perform our planned statistical analysis because of the small number of subjects tested and relatively high variability of dependent measure data. Thus, we recommend that future studies strive to recruit more test subjects. Nevertheless, qualitative assessments of these data provide some valuable insights into the general effects of the CG configurations under evaluation and the independent effects of the POGO system and the offload profile.

It appears from the EQ score data that postural stability during quiet stance improved when the subject donned the POGO gimbal system and the system was activated to offload the weight of the gimbal structure (Figure 78, 1-g vs. 1-g [Perfect]). This putative stability improvement was not observed for the two TTC indices because of increased variability (Figure 79 and Figure 80, 1-g vs. 1-g [Perfect]), suggesting that the POGO system more greatly affected sway displacements than sway velocities. Possible reasons for this putative stability improvement include: (a) an increased test subject vigilance caused by the perceived threat of falling while wearing the heavy, unwieldy gimbal system; (b) a mechanical stabilizing effect of the POGO system support device; and/or (c) new orientation information provided by the POGO force vector, perhaps similar to the posture-stabilizing effect of light touch (40). For sudden postural perturbations, the POGO system appeared to improve the worst-case stability (TTC_{min}, Figure 81) but degraded the overall postural stability performance (iTTC; (Figure 82).

It appears from the SOT 1 quiet stance data that increasing the offload from body weight to one-sixth of body weight plus gimbal and CG rig weight degraded postural stability control (Figure 78 through Figure 80, top, 1-g [Perfect] vs. Perfect), possibly related to an unappreciated decrease in the gain requirement for the control-system generating motor responses to counter postural balance errors detected by the visual, vestibular, and somatosensory systems or, alternatively, to a reduction in the sensitivity of somatosensory detectors. However, as postural stability control was not affected in a similar way during the SOT 4 trials (Figure 78 to Figure 80, top, 1-g [Perfect] vs. Perfect), in which somatosensory cues were purposefully distorted by the CDP system, it seems more likely that the reduced loading affected the sensory information available from the somatosensory system. If this is true, this could have significant implications to postural stability during lunar (and other hypogravity) EVA activities. For this reason, we recommend that this finding be investigated further, and suggest that the best next step would be to use similar CDP paradigms to examine the postural stability control of test subjects exposed to intermittent hypogravity at different g-levels (0.17-g, 0.33-g, 0.5-g, etc.) during parabolic flight campaigns.

It appears that the CTSD configuration substantially degrades postural stability during quiet stance and in response to sudden unexpected postural perturbations. Some subjects, when wearing the CTSD configuration, lost balance or refused to attempt each test condition examined in this study. No other CG configuration stood out as having particularly positive or negative effects on postural stability control, although one subject refused to attempt the quiet stance tasks while in the POGO configuration, and at least one subject lost balance multiple times during TU rotations while in the Backpack configuration. Thus, the Perfect CG appears to have least affected the postural stability of the CG configurations tested.

5.5 Study Limitations

There were a number of limitations with this test. Given the biomechanical, physiological, and capability and strategy observations, analyses suggest that some subjects may have been using the inherent POGO system mechanics to reduce their physical workload while ambulating. Data also suggest that the system (POGO, gimbal, and CG rig) may have greatly altered the gait mechanics of the subjects and restricted their normal ROMs. The added inertia of the POGO pneumatic cylinder, gimbal, and CG rig were large enough to impede the subjects while they were performing tasks. As a result, there is a significant need for an improved offload system, including improvements to the gimbal and CG rig, that would minimize altered inertial effects.

The POGO system also was found to have its own dynamics that influenced subjects during ambulation. These influences were observed as a lack of rigid attachment of the CG rig to the subject while ambulating. The POGO system was shown to lag slightly behind the subject during ambulation trials, creating a dynamic out-of-phase condition between the subject and the rest of the system. These

two system characteristics created collisions between the subject and the CG rig, resulting in abnormal system CG variation during ambulation trials. Abnormalities of this type are assumed to have influenced the kinetic, kinematic, and physiologic data collected.

Another limitation was that CG locations were modeled based on a standard subject (182.9 cm, 81.6 kg), which meant that as the tested subjects differed from this standard subject, the actual location of the system CG was affected. System CG locations varied by subject, but did not vary enough such that any one categorical CG location crossed into another CG category (Figure 12). Although each system CG differed slightly from the model-calculated system CG, each was still within a 2-cm radius of the model-calculated system CG.

Of the four tested CG locations, the CTSD configuration led to increased metabolic rate, decreased postural stability, and confounded some of the biomechanical markers. Posttest analyses indicated this CG configuration was not properly aligned with the gimbal axes of rotation, thereby placing subjects in a difficult position for which many could not properly compensate. Subjects felt as if they were being pulled down and backwards and this feeling was consistent with the analysis placing the CTSD system CG notably aft of the gimbal axes of rotation (Figure 13).

Although many IST team members agree with the previous theory, that the CTSD CG condition led to poor performance because the system CG was misaligned with gimbal axes of rotation, there was a contrasting point of view expressed by the Anthropometry and Biomechanics Facility (ABF). Based on the ABF's biomechanical analysis, minimal variation was seen among the different CG locations. The ABF asserts that this may be because the gimbal rotational axes were collocated with the system CG locations. The ABF's hypothesis is that, as the system was offloaded by 83% of the total system 1-g weight, the gimbal axes became the major pivot point for the human torso, thus reducing the differences that would be felt by the subject. It is the ABF's position that, due to this alignment, the full difference in inertia from the changing CG locations was not realized.

A significant issue with attempting to collocate the gimbal axes of rotations with the subject's major pivot point, ie, the hips, would be that the system CG would then be aft and above the gimbal axes of rotation, which could lead to many of the same problems seen with the CTSD CG. Without further testing using an improved offload system and gimbal that minimize added rotational and translational inertia, it will be impossible to determine the separate effects of gimbal/CG misalignment.

5.6 Lessons Learned

It is clear that studying varied CG locations by using overhead suspension has both limitations and unanswered questions. These include where to properly align the gimbal axes of rotation (subject hips or system CG), how to add enough mass to vary CG without overwhelming the moments of inertia and compromising normal human movement, and how to account for two potential sources of stability (ie, feet and overhead lift vector). To properly evaluate varied CG using overhead suspension, several improvements will need to be made. These include the following:

1. Decreasing the overall mass and moment of inertia of the gimbal support structure and additional CG rig components
2. Designing a gimbal that would provide adjustability needed to either collocate the gimbal axes of rotation with the subject's hips or with the system CG
3. Designing a CG rig that does not require long horizontal arms that impede the subject's workspace
4. Providing translational freedom in both the X and Y axes
5. Reducing mass and moment of inertia in the overhead lift system
6. Providing active control of the overhead lift column in both the X and Y translational axes

Exploration tasks were not performed in as EVA-like a manner as possible. This was due to the long horizontal arms of the CG rig and a desire to use similar methodology on other tests (2). All future tests

should attempt to perform an assessment in the most EVA-similar manner possible and then only make a modification if necessary while providing the rationale for the modification.

Initially, it was thought that changing among all four CG configurations would be too difficult within the same test session. Although this was somewhat more burdensome, it was possible and would have allowed all level-ambulation trials at each CG condition to be performed on 1 day and all incline-ambulation trials at each CG condition to be performed on a different day, rather than mixing level and incline trials and limiting sessions to only two CG configurations on any test day. This would potentially lead to a better ability to subjectively compare and provide feedback among different CG conditions because the tasks would be the same on the same day for all four CG conditions.

6 Summary

6.1 Metabolic Rate

The only CG that resulted in significant metabolic differences was the CTSD configuration. All other varied CG configurations unexpectedly showed almost identical metabolic values. The variation in the CTSD configuration was likely due to system configuration issues and not because it was a poor CG location. Overall, the lack of variability among the other three CG configurations indicates that either there was no notable difference in human performance among these CG configurations or there were factors that compromised the ability to effectively vary CG using an overhead suspension lunar-gravity simulator. Possible solutions to this question were discussed in the Section 5.6.

6.2 Biomechanics

No meaningful changes were seen among the differing CG conditions. Some differences were seen between one of the CG locations and the other three locations, but the data analysis led us to believe the difference was a result of the system dynamics, hardware setup, and testing methodology and not a direct result of the system CG location in relation to the subject's CG.

6.3 Subjective Ratings

Results among CG conditions for ambulation were very similar to the metabolic results and led to similar conclusions. Findings of greater importance were the high degree of variability for subjective ratings among subjects for the exploration tasks and postural control tests. This highlights the need to test a greater number of subjects and to thoroughly characterize the subject pool so that aspects of anthropometry, strength, and/or fitness can be analyzed to determine whether these underlying subject characteristics significantly affect a subject's performance.

In addition to the standard end-of-trial assessment of RPE and GCPS, subjects were also assessed at the 30-s mark shortly after each trial began. Results indicated that GCPS had less variability between the early and end-of-trial measurements, with 82% of trials showing no change. RPE experienced more variability, but still 68% of trials did not change from the initial to the end-of-trial rating. The vast majority of the RPE and GCPS results that did change increased by one unit (26% for RPE, 12% for GCPS). Although this is not conclusive, it does show promise for using both of these ratings in non-steady-state tasks, especially in environments that preclude metabolic measurement.

RPE was rated differently in the 1-g, no-rig setting than in all other settings involving the CG rig. This is a similar finding to how suited and unsuited subjects rate RPE differently (5) (1). In a model using RPE and GCPS to predict metabolic rate, both were significant predictors with RPE driving the model and GCPS providing the fine-tuning that has been a consistent finding with other studies (5) (1).

6.4 Postural Control

The POGO system provides a reasonable ground-based analog for testing postural stability during reduced-gravity loading; however, its mechanical couplings limit observations to a single plane of motion (in this case, sagittal), and its upward force vector may exercise a mechanical and/or physiologic (haptic) stabilizing influence on balance control that could reduce apparent instabilities, particularly in body sway displacement.

Postural stability appeared to be degraded during the simulated reduced-gravity loading conditions tested in this experiment, and the performance patterns suggest that somatosensory information may be degraded in hypogravity environments. This finding has significant implications regarding the fall incidence observed during Apollo surface operations and those fall incidences that should be anticipated during future exploration missions, regardless of suit design constraints. We recommend that follow-up experiments be performed, probably during parabolic flight, to verify these findings without the potential mechanical confounds of the POGO system.

Comparisons among the four CG configurations tested show that the CTSD CG created far greater disruptions to postural stability than any of the other CGs, likely due to the misalignment issues rather than implying that an EVA suit having this CG configuration would result in more falls and higher metabolic effort than one having any of the other CG configurations tested. Differences among the other CG configurations were more difficult to discern; however, the Perfect configuration appeared to have the smallest effect on postural stability as assessed by this experiment.

The small number of subjects tested and the relatively high variability of dependent measures limited our ability to perform statistical analyses. Thus, these conclusions are based on subjective interpretation of our results, and further study would be required to provide conclusions that may assist in finalizing an optimal CG design location.

7 Works Cited

1. Norcross JR, Clowers KG, Clark T, Harvill L, Morency RM, Stroud LC, et al. Metabolic Costs and Biomechanics of Level Ambulation in a Planetary Suit. NASA/TP–2010–216115. Washington DC; 2010.

2. Norcross JR, Clowers KG, Clark T, Harvill L, Morency RM, Stroud LC, et al. Metabolic Costs and Biomechanics of Inclined Ambulation and Exploration Tasks in a Planetary Suit. NASA/TP–2010-216215. Washington DC; 2010.

3. Jadwick J, Rullman K, Skytland N, Gernhardt M. Influence of Center of Gravity on Human Performance in Partial Gravity. *Aviat Space Environ Med*. 2008; 79(3):p. Abstract 365.

4. Martin PE, Nelson RC. The effect of carried loads on the walking patterns of men and women. *Ergonomics*. 1986; 29:1191–1202.

5. Norcross JR, Lee LR, Clowers KG, Morency RM, Desantis L, De Witt JK, et al. Feasibility of Performing a Suited 10-km Ambulation - Final Report of the EVA Walkback Test (EWT). NASA/TP–2009–214796. Washington DC; 2009.

6. Chappell SP, Norcross JR, Gernhardt ML, Clowers KG, Cowley MS, Clark T, et al. Final Report of the Integrated Parabolic Flight Test: Effects of Varying Gravity, Center of Gravity, and Mass on the Movement Biomechanics and Operator Compensation of Ambulation and Exploration Tasks. NASA/TP–In Publication. Washington DC; 2010.

7. Wu G, Siegler S, Allard P, Kirtley C, Leardini A, Rosenbaum D, et al. ISB recommendation on definitions of joint coordiante system of various joints for the reporting of human joint motion -

Part 1: ankle, hip, and spine. International Society of Biomechanics. *J Biomechanics*. 2002; 35:543–548.

8. Borg GA. Psychophysical bases of perceived exertion. *Med Sci Sports Exerc*. 1982; 14(5):377–381.
9. Corlett EN, Bishop RPA. A technique for assessing postural discomfort. *Ergonomics*. 1976; 19(2):47–51.
10. Bedford T. The warmth factor in comfort at work. MRC Industrial Health Board Report No. 76. MRC Industrial Health Board Report. London:; 1936.
11. Wikipedia. [Online].; 2009 [cited 2009 12 17]. Available from: http://en.wikipedia.org/wiki/Horse-collar_tackle.
12. Tagliabue P. Rule 12, Section 2, Article 1 (d). In Upson L, editor. 2006 Official Playing Rules of the National Football League. USA: National Football League; 2006. p. 80.
13. Keller TS, Weisberger AM, Ray JL, Hasan SS, Shiavi RG, Spengler DM. Relationship between vertical ground reaction force and speed during walking, slow jogging, and running. *Clin Biomechan* (Bristol, Avon). 1996; 11:253–259.
14. Perry JE. Gait Analysis: Normal and Pathological Function. New York: McGraw-Hill Inc.; 1992.
15. Kuo AD, Donelan JM, Ruina A. Energetic consequences of walking like an inverted pendulum: step-to-step transitions. *Exercise and Sport Science Reviews*. 2005; 33:88–97.
16. Gordon KE, Ferris DP, Kuo AD. Metabolic and mechanical energy costs of reducing vertical center of mass movement during gait. *Archives of Physical Medicine and Rehabilitation*. 2009; 90:136–144.
17. Ortega JD, Farley CT. Minimizing center of mass vertical movement increases metabolic cost in walking. *J Appl Physiol.* 2005; 99:2099–2107.
18. Bonato P, D'Alessio T, Knaflitz M. A statistical method for the measurement of muscle activation intervals from surface myoelectric signal during gait. *IEEE Transactions on Biomedical Engineering*. 1998; 45:287–99.
19. Redfern MS, Hughes RE, Chaffin CB. High-pass filtering to remove electrocardiographic interference from torso EMG recordings. *Clin Biomech*. 1993; 8:44–48.
20. Ivanenko YP, Poppele RE, Lacquaniti F. Five basic muscle activation patterns account for muscle activity during human locomotion. *J Physiol.* 2004; 556:267–82.
21. McIntosh AS, Beatty KT, Dwan LN, Vickers DR. Gait Dyanmics on an inclined walkway. *J Biomech.* 2006; 39:2491–2502.
22. Holt KG, Wagenaar RC, LaFiandra ME, Kubo M, Obusek JP. Increased musculoskeletal stiffness during load carriage at increasing walking speeds maintains constant vertical excursion of the body center of mass. *J Biomech*. 2003; 36:465–71.
23. Alton F, Baldey L, Caplan S, Morrissey MC. A kinematic comparison of overground and treadmill walking. Clinical Biomechanics (Briston, Avon). 2003; 13: p. 434–440.

24. Gage JR, DeLuca PA, Renshaw TS. Gait analysis: principle and applications with emphasis on its use in cerebral palsy. Instr Course Lect. 1996; 45: p. 491–507.

25. LaFiandra ME, Wagenaar RC, Holt KG, Obusek JP. The effect of walking speed and adding a backpack on trunk dynamics during treadmill walking. In Command M, editor. U.A.M.R.; 2002. p. 32.

26. Threlkeld AJ, Cooper LD, Monger BP, Craven AN, Haupt HG. Temporospatial and kinematic gait alterations during treadmill walking with body weight suspension. *Gait and Posture*. 2003; 17: 235–43.

27. Finch L, Barbeau H, Arsenault B. Influence of body weight support on normal human gait: development of a gait retraining strategy. *Physical Therapy*. 1991; 71:842–55; Discussion 855-6.

28. Taylor CR. Force development during sustained locomotion: a determinant of gait, speed and metabolic power. *J Experi Biol*. 1985; 115:253–62.

29. Novacheck TF. The biomechanics of running. *Gait and Posture*. 1998; 7:77–95.

30. Schache AG, Bennell KL, Blanch PD, Wrigley TV. The coordinated movement of the lumbo-pelvic-hip complex during running: a literature review. *Gait and Posture*. 1999; 10:30–47.

31. Andriachhi TP, Andersson GB, Fermier RW, Stern D, Galante JO. A study of lower-limb mechanics during stair-climbing. *J Bone Joint Surg Am*. 1980; 62:749–57.

32. Roberts TJ, Belliveau RA. Sources of mechanical power for uphill running in humans. *J Experi Biol*. 2005; 208:1963–70.

33. Waters RL, Morris JM. Electrical activity of muscles of the trunk during walking. *J Anat.* 1972; 111:191–9.

34. Nashner LM. Computerized dynamic posturography: Clinical Applications. In Jacobsen GP, Newman CW, Kartush JM, editors. Handbook of Balance Function Testing. Chicago, IL: Mosby-Year Book Inc.; 1993. p. 308–34.

35. Black FO, Paloski WH, Doxey-Gasway DD, Reschke MF. Vestibular plasticity following orbital spaceflight: Recovery from postflight postural instability. *Acta Oto Laryngologica Supplemen*t. 1995; 2:450–4.

36. Paloski WH. Vestibulospinal adaptation to microgravity. *Otolaryngol Head Neck Surg*. 1998; 118(3 Pt 2):S3944.

37. Paloski WH, Black FO, Metter EJ. Postflight balance control recovery in an elderly astronaut: A case report. *Otol Neurotol*. 2004; 25(1):53–6.

38. Paloski WH, Reschke MF, Black FO. Recovery of postural equilibrium control following space flight (DSO 605). In Sawin CF, Taylor GR, Smith WL, editors. Extended Duration Orbiter Medical Project. Final Report. National Aeronautics and Space Administration; NASA/SP–199-534. Houston, TX; 1999. Section 5.4.1–5.4.16

39. Forth KE, Metter EJ, Paloski WH. Age associated differences in postural equilibrium control: A comparison between EQ score and minimum time to contact (TTCmin). *Gait and Posture*. 2007; 25(1):56–62.

40. Jeka JJ, Lackner JR. Fingertip contact influences human posture control. *Experimental Brain Research*. 1994; 100(3):495–502.

Appendix A: Biomechanics Definitions and Reference Frames

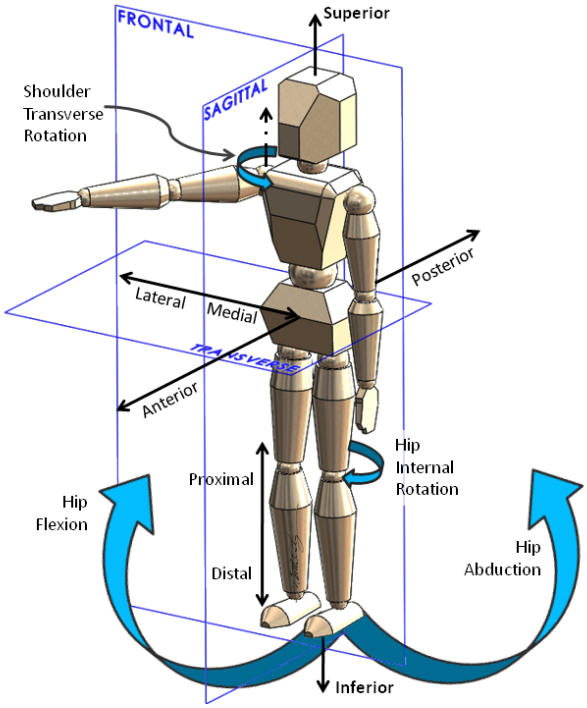

Figure A-1. Commonly used biomechanics nomenclature of the body planes, the types of joint motion, and the body-based directions.

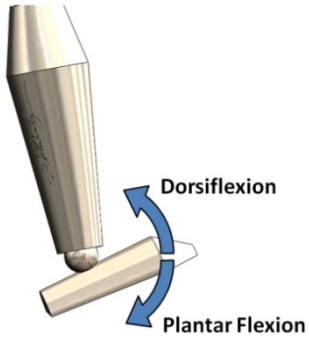

Figure A-2. Designations for the ankle joint directional rotations.

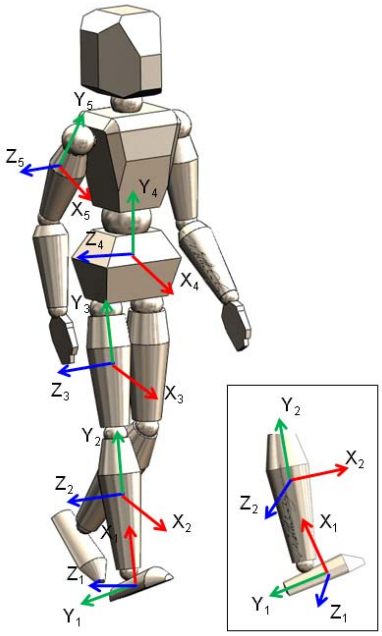

Figure A-3. Convention for local reference frames as prescribed by the International Society of Biomechanics and used by the ABF (4). The Y-axis usually lies along the long axis of the segment.

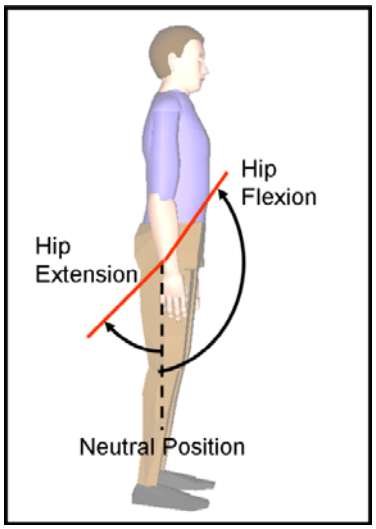

Figure A-4. Flexion is termed as the decrease in the relative angle between two segments. Flexion/dorsiflexion of a joint will always be a positive rotation in this report.

Appendix B: Subjective Ratings Scales

B.1 Gravity Compensation and Performance Scale

1	**Excellent** – easier than 1-g
2	**Good** – equivalent to 1-g
3	**Fair** – minimal compensation for desired performance
4	**Minor** – moderate compensation for desired performance
5	**Moderately objectionable** – considerable compensation for adequate performance
6	**Very objectionable** – extensive compensation for adequate performance
7	**Major deficiencies** – considerable compensation for control, performance compromised
8	**Major deficiencies** – intense compensation, performance compromised
9	**Major deficiencies** – adequate performance not attainable with maximum tolerable compensation
10	**Major deficiencies** – unable to perform task

B.2 Borg Rating of Perceived Exertion Scale (RPE)

6	No exertion at all
7	Extremely light
8	
9	Very light
10	
11	Light
12	
13	Somewhat hard
14	
15	Hard (heavy)
16	
17	Very hard
18	
19	Extremely hard
20	Maximal exertion

B.3 Corlett and Bishop Discomfort Scale

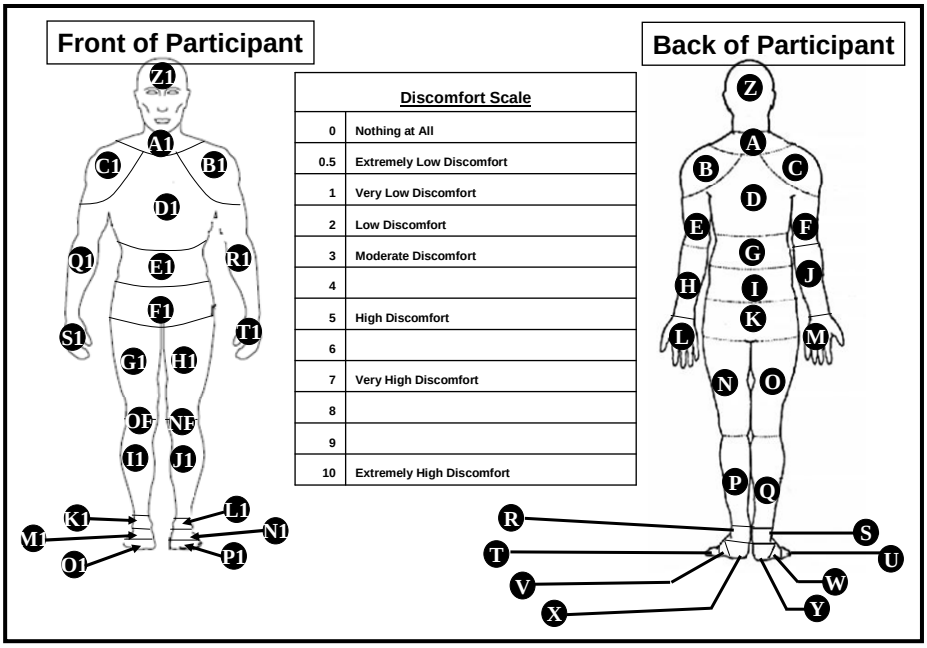

B.4 Bedford Thermal Scale

-3	Much Too Cool
-2	Too Cool
-1	Comfortably Cool
0	Comfortable
1	Comfortably Warm
2	Too Warm
3	Much Too Warm

B.5 Thermal Preference

-2	Much warmer
-1	A Bit Warmer
0	No Change
1	A Bit Cooler
2	Much Cooler

Appendix C: Treadmill Relative Velocity

In normal, stationary reference frame environments, vertical and horizontal velocities determine the distance traveled (Figure C-1). On a treadmill the reference frame is moving; so to an external observer, the trajectory will be elongated as a function of the reference frame velocity (Figure C-2). Equations (C1) and (C2) are the basic equations used for trajectory motion for a ballistic body.

For vertical motion in the *y* direction:

$$y = v_{0y}t - \frac{1}{2}gt^2 \tag{C1}$$

For horizontal motion in the *x* direction:

$$x = v_{0x}t \tag{C2}$$

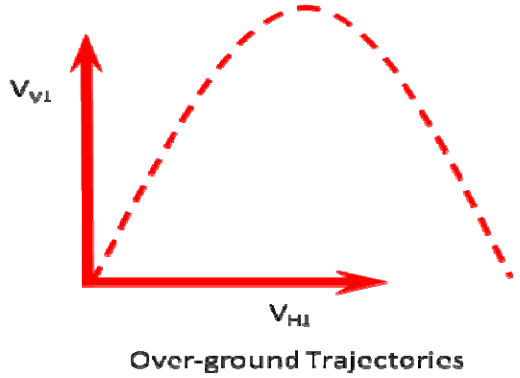

Figure C-1. Visual representation of trajectory motion with a stationary reference frame.

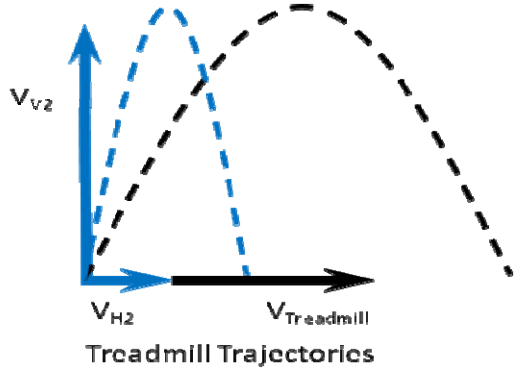

Figure C-2. Visual representation of a trajectory with and without a moving reference frame. The blue line represents the relative trajectory from the ballistic velocities as seen from the moving coordinate system; the black line represents the trajectory as seen by an outside observer.

Appendix D: List of Variables for Common Equations and Relationships

D.1 Linear Motion

Position: x

Velocity: v

Acceleration: a

Mass: m

Force: ma

Work: Fd

Kinetic energy: $\frac{1}{2} mv^2$

Power: Fv

D.2 Rotational Motion

Angular position: θ

Angular velocity: ω

Angular acceleration: α

Moment of inertia: I

Moment/torque: $I\alpha, \tau$

Work: $\tau\theta$

Kinetic energy: $\frac{1}{2} I\omega^2$

Power: $\tau\omega$

Per the NASA Constellation Interoperability Standards (CxP 70022-04) document, the units expressed in this report are in the standard SI units. The following conversions to English units are given:

Mass:	1 kg	=	2.204 lbm
Force:	1 N	=	0.225 lb
Speed:	1 m/s	=	2.237 mph
Pressure:	1 kPa	=	0.145 psi

Appendix E: Additional Electromyography Graphs

E.1 Changing Speed Conditions

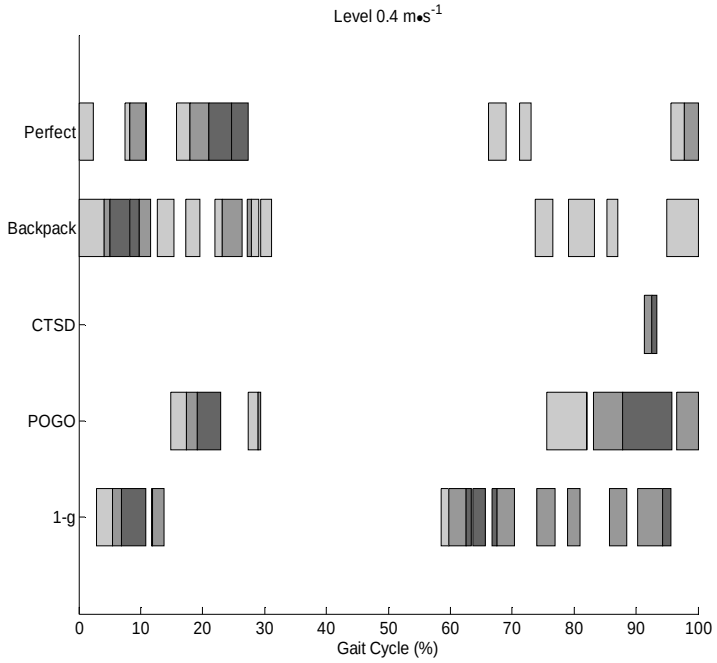

Figure E-1. Muscle activation of the erector spinae at 0.4•m·s^{-1} for all CG configurations and with no rig at 1-g.

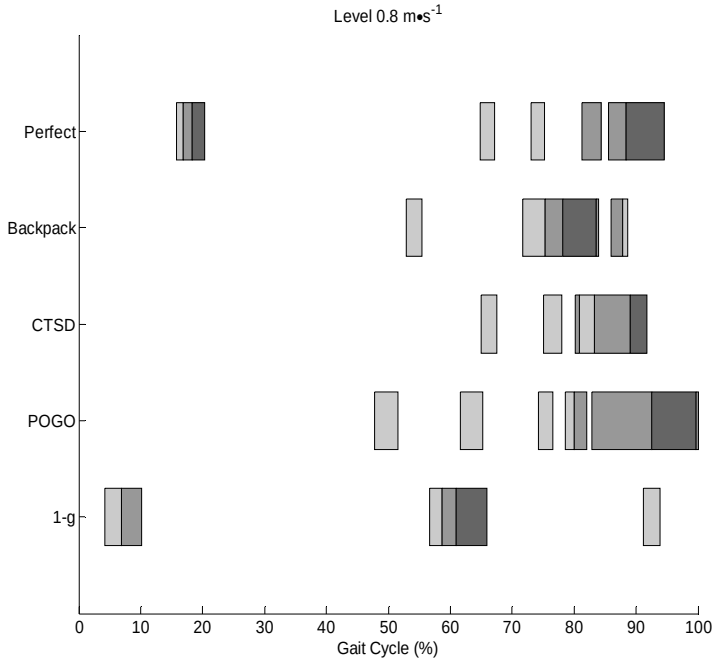

Figure E-2. Muscle activation of the erector spinae at 0.8•m·s^{-1} for all CG configurations and with no rig at 1-g.

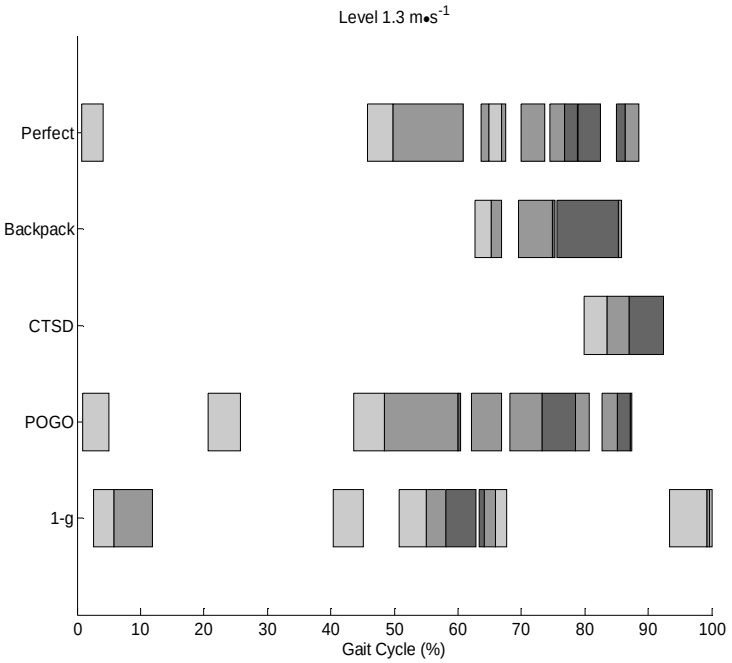

Figure E-3. Muscle activation of the erector spinae at 1.3•m·s^{-1} for all CG configurations and with no rig at 1-g.

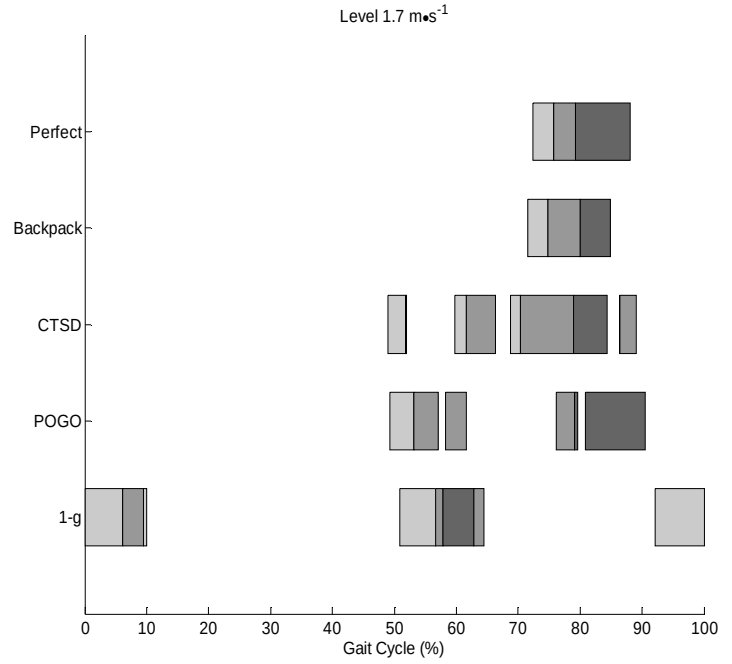

Figure E-4. Muscle activation of the erector spinae at 1.7 m•s^{-1} for all CG configurations and with no rig at 1-g.

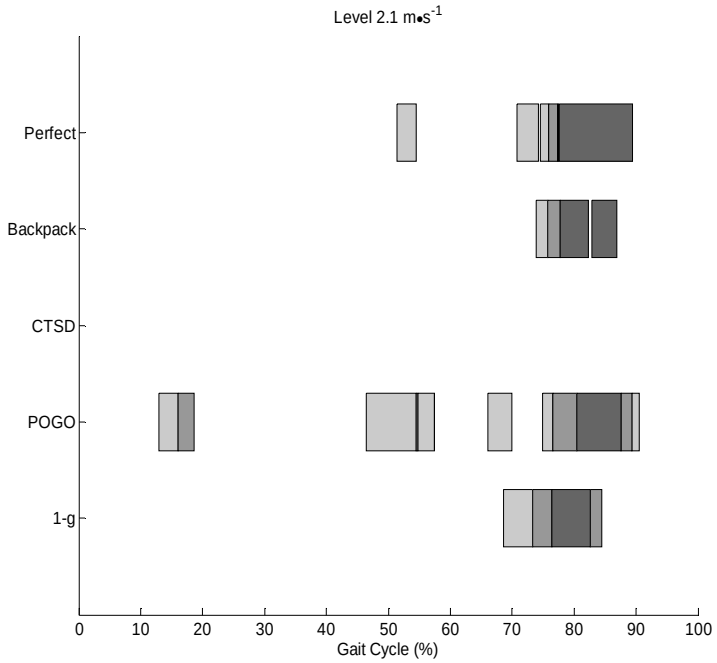

Figure E-5. Muscle activation of the erector spinae at 2.1 m•s^{-1} for all CG configurations and with no rig at 1-g.

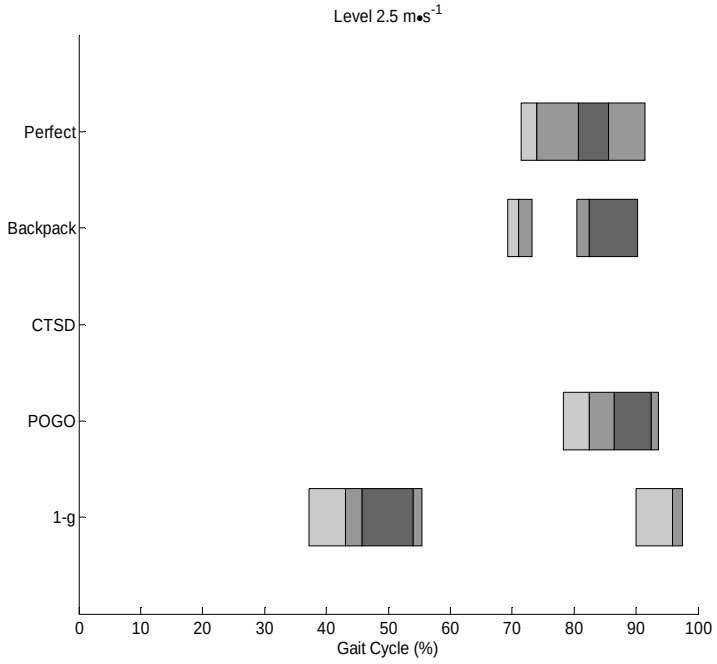

Figure E-6. Muscle activation of the erector spinae at 2.5•m·s^{-1} for all CG configurations and with no rig at 1-g.

E.2 Changing Incline Conditions

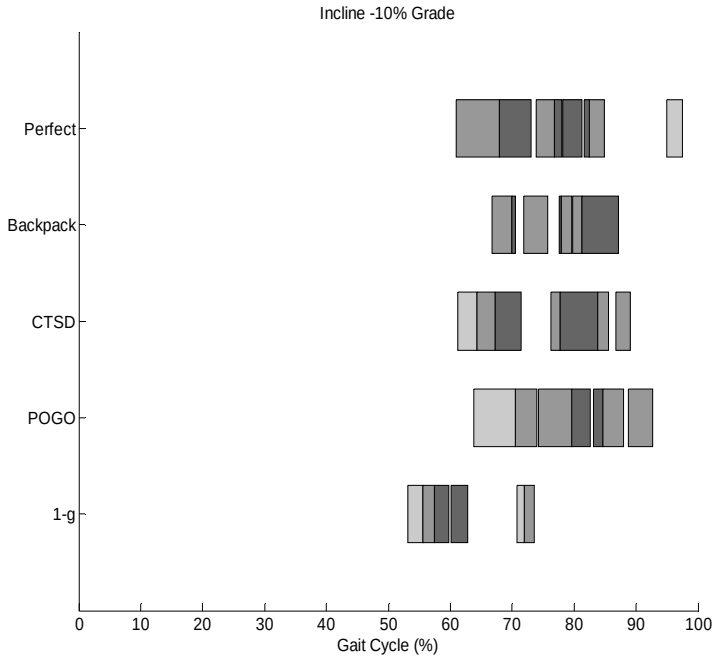

Figure E-7. Muscle activation of the erector spinae at -10% grade for all CG configurations and with no rig at 1-g.

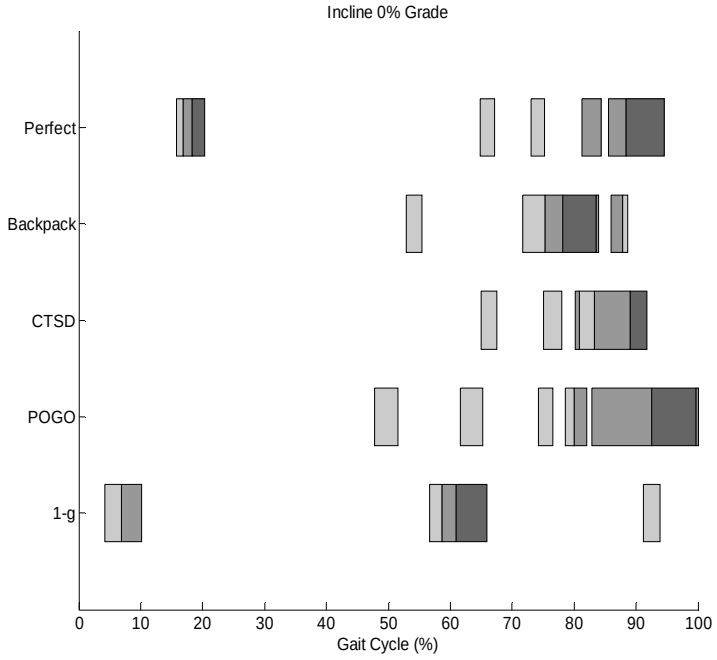

Figure E-8. Muscle activation of the erector spinae at 0% grade for all CG configurations and with no rig at 1-g.

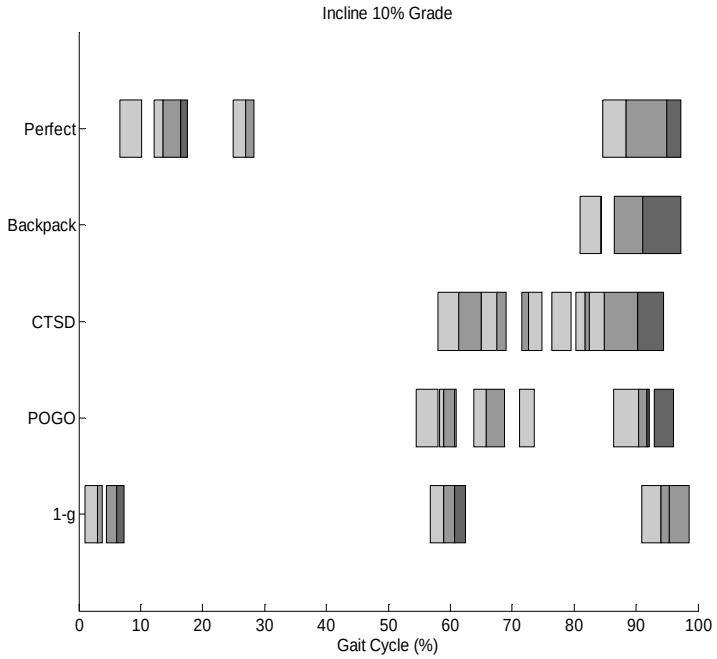

Figure E-9. Muscle activation of the erector spinae at 10% grade for all CG configurations and with no rig at 1-g.

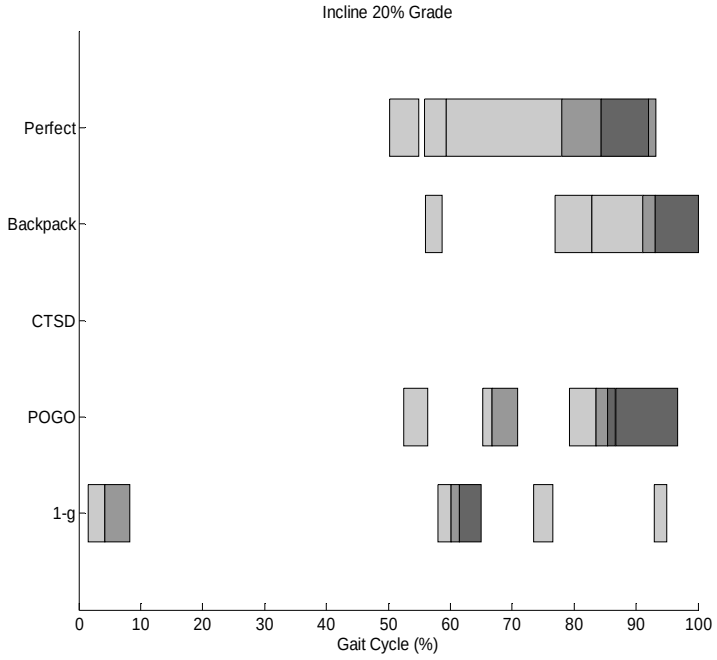

Figure E-10. Muscle activation of the erector spinae at 20% grade for all CG configurations and with no rig at 1-g.

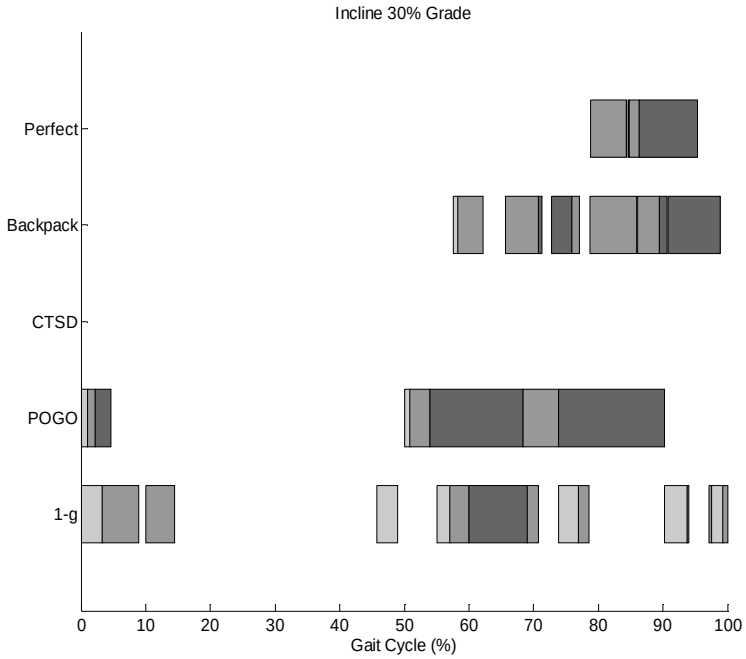

Figure E-11. Muscle activation of the erector spinae at 30% grade for all CG configurations and with no rig at 1-g.

Appendix F: Test Termination Criteria

F.1 Test Termination Criteria for All Submaximal Testing

- Subject request to stop at any time
- Subject's HR or measured VO_2 at level > 85% VO_2pk or 85% of age predicted HR max (if no recent VO_2pk test on file) for 2 min or more
- If subject reports discomfort rating > 7 (on Corlett and Bishop 10-point discomfort scale) for two consecutive recording periods, subject will be asked to terminate test
- Subject reports discomfort rating of 10
- Failure of POGO hardware and/or treadmill system

F.2 Test Termination Criteria for Postural Stability

- Subject request to stop at any time
- Syncope or significant dizziness
- Subject reports persistent pain or discomfort
- Injury due to a fall

Appendix G: Integrated Suit Test-3 Test Conductor Checklist

G.1 Constellation Program Extravehicular Activity Systems Test 3 – Shirtsleeve Test Session 1 Checklist

Setup

□ 1) Ensure subject's clothes and shoes are ready
□ 2) Determine and record the randomized order to be used for the day's trials (EVA Physiology, Systems and Performance [EPSP] Project)
□ 3) Prepare data sheets for test session (EPSP)
□ 4) Ensure medical monitor is identified (EPSP)
□ 5) Prepare and calibrate met cart (Exercise Physiology Laboratory [EXL])
□ 6) Prepare and calibrate near-infrared spectroscopy (NIRS) system (EXL)
□ 7) Prepare and calibrate motion capture system for subject (ABF)
□ 8) Prepare and calibrate GRF system (ABF)
□ 9) Prepare shirtsleeve rig for initial condition (EPSP)

Pretest Preparation

□ 1) Have subject read and sign informed consent form, with test conductor answering questions
□ 2) Ask subject to enter the changing area
□ 3) Provide subject clothing and heart rate strap – explain donning order
□ 4) Instrument subject with EMG system and remaining clothes
□ 5) Ask subject to don the form-fitting suit and shoes for motion capture
□ 6) Weigh subject
□ 7) Describe the test procedure and familiarize the subject with the shirtsleeve rig
□ 8) Go over GCPS, RPE, and thermal ratings with subject (Usability Testing and Analysis Facility [UTAF])

Pretest Briefing

□ 1) Hand out data/cover sheet with test order and objectives
□ 2) Review motion capture field
□ 3) Review hard hat area
□ 4) Medical monitor identified and contact information posted
□ 5) Test termination criteria reviewed and posted
□ 6) Emergency egress procedures reviewed and personnel identified

Trial 1 Preparation – Level Treadmill

□ 1) Instrument subject with reflective markers for motion capture
□ 2) Instrument subject with NIRS
□ 3) Instrument subject with COSMED
□ 5) Assist subject onto center of treadmill
□ 6) Have subject stand still for approximately 10 s for static shot and weight capture
□ 7) Check EMG system (ABF)

Trial 1 Steps – Level Treadmill

- □ 1) Ensure all teams are ready and subject's metabolic rate is being captured
- □ 2) Inform test subject that the treadmill is starting and increase to 0.9 mph
- □ 3) Based on COSMED clock, start actual data collection on the minute or half-minute
- □ 4) UTAF to record RPE and GCPS at 30 s
- □ 5) ABF to record kinetic/kinematic data for 30 strides immediately after UTAF
- □ 6) UTAF to record RPE, GCPS, discomfort, and thermal comfort within last 30 s of 3 min
- □ 7) Increase speed to 1.9 mph and repeat steps 4–6
- □ 8) Increase speed to 2.8 mph and repeat steps 4–6
- □ 9) Increase speed to 3.7 mph and repeat steps 4–6
- □ 10) Increase speed to 4.6 mph and repeat steps 4–6
- □ 11) Increase speed to 5.6 mph and repeat steps 4–6
- □ 12) Inform test subject that the treadmill is stopping and stop treadmill
- □ 13) Help subject off treadmill and provide subject a seat
- □ 14) Offer subject water, as needed

Trial 2 Preparation – Incline/Decline Treadmill

- □ 1) Check and re-instrument subject with reflective markers, as needed
- □ 2) Check NIRS
- □ 3) Instrument subject with COSMED
- □ 4) Assist subject onto center of treadmill
- □ 5) Have subject stand still for approximately 10 s for static shot and weight capture
- □ 6) Help subject off treadmill and adjust to -10%
- □ 7) Check EMG system (ABF)

Trial 2 Steps – Incline/Decline Treadmill

- □ 1) ABF measures treadmill orientation data at -10%
- □ 2) Assist subject onto center of treadmill
- □ 3) Ensure all teams are ready and subject's metabolic rate is being captured
- □ 4) Inform test subject that the treadmill is starting and increase to 1.9 mph
- □ 5) Based on the COSMED clock, start actual data collection on the minute or half-minute
- □ 6) UTAF to record RPE and GCPS at 30 s
- □ 7) ABF to record kinetic/kinematic data for 30 strides immediately after UTAF
- □ 8) UTAF to record RPE, GCPS, discomfort, and thermal comfort within last 30 s of 3 min
- □ 9) At 3 min, stop treadmill and help subject off treadmill
- □ 10) Increase incline to 10% and repeat steps 1–9
- □ 11) Increase incline to 20% and repeat steps 1–9
- □ 12) Increase incline to 30% and repeat steps 1–9
- □ 13) Remove COSMED and recalibrate, also download COSMED data
- □ 14) Return treadmill to 0%
- □ 15) Offer subject water, as needed

Trial 3 Preparation – Level Treadmill

- □ 1) Offload CG rig to neutral
- □ 2) Assist subject in getting into the shirtsleeve rig harness while attached to the Pogo
- □ 3) Instrument subject with reflective markers for motion capture
- □ 4) Instrument subject with NIRS
- □ 5) Instrument subject with COSMED
- □ 6) Offload subject to approximate target weight
- □ 7) Subject stands on scale
- □ 8) Adjust to target weight and record weight
- □ 9) Assist subject onto center of treadmill
- □ 10) Have subject stand still for approximately 10 s for static shot and weight capture
- □ 11) Check EMG system (ABF)

Trial 3 Steps – Level Treadmill

- □ 1) Ensure all teams are ready and subject's metabolic rate is being captured
- □ 2) Inform test subject that the treadmill is starting and increase to 0.9 mph
- □ 3) Based on COSMED clock, start actual data collection on the minute or half-minute
- □ 4) UTAF to record RPE and GCPS at 30 s
- □ 5) ABF to record kinetic/kinematic data for 30 strides immediately after UTAF
- □ 6) UTAF to record RPE, GCPS, discomfort, and thermal comfort within last 30 s of 3 min
- □ 7) Increase speed to 1.9 mph and repeat steps 4–6
- □ 8) Increase speed to 2.8 mph and repeat steps 4–6
- □ 9) Increase speed to 3.7 mph and repeat steps 4–6
- □ 10) Increase speed to 4.6 mph and repeat steps 4–6
- □ 11) Increase speed to 5.6 mph and repeat steps 4–6
- □ 12) Inform test subject that the treadmill is stopping and stop treadmill
- □ 13) Help subject off treadmill and provide a seat
- □ 14) Reduce offload to CG rig neutral
- □ 15) Remove COSMED and download data

Trial 4 Preparation – Incline/Decline Treadmill

- □ 1) Check and re-instrument subject with reflective markers, as needed
- □ 2) Check NIRS
- □ 3) Instrument subject with COSMED
- □ 4) Offload subject to approximate target weight
- □ 5) Subject stands on scale
- □ 6) Adjust to target weight and record weight
- □ 7) Assist subject onto center of treadmill
- □ 8) Have subject stand still for approximately 10 s for static shot and weight capture
- □ 9) Help subject off treadmill and adjust to -10%
- □ 10) Check EMG system (ABF)

Trial 4 Steps – Incline/Decline Treadmill

- □ 1) ABF measures treadmill orientation data at -10%
- □ 2) Assist subject onto center of treadmill
- □ 3) Ensure all teams are ready and subject's metabolic rate is being captured
- □ 4) Inform test subject that the treadmill is starting and increase to 1.9 mph
- □ 5) Based on the COSMED clock, start actual data collection on the minute or half-minute
- □ 6) UTAF to record RPE and GCPS at 30 s
- □ 7) ABF to record kinetic/kinematic data for 30 strides immediately after UTAF
- □ 8) UTAF to record RPE, GCPS, discomfort, and thermal comfort within last 30 s of 3 min
- □ 9) At 3 min, stop treadmill and help subject off treadmill
- □ 10) Increase incline to 10% and repeat steps 1–9
- □ 11) Increase incline to 20% and repeat steps 1–9
- □ 12) Increase incline to 30% and repeat steps 1–9
- □ 13) Reduce offload to CG rig neutral and provide a seat
- □ 14) Remove COSMED and download COSMED data
- □ 15) Return treadmill to 0%

Trial 5 Preparation – Level Treadmill

- □ 1) Adjust CG rig to new CG setting, as described in test randomization order
- □ 2) Check and re-instrument subject with reflective markers, as needed
- □ 3) Check NIRS
- □ 4) Instrument subject with COSMED
- □ 5) Offload subject to approximate target weight
- □ 6) Subject stands on scale
- □ 7) Adjust to target weight and record weight
- □ 8) Assist subject onto center of treadmill
- □ 9) Have subject stand still for approximately 10 s for static shot and weight capture
- □ 11) Check EMG system (ABF)

Trial 5 Steps – Level Treadmill

- □ 1) Assist subject onto center of treadmill
- □ 2) Ensure all teams are ready and subject's metabolic rate is being captured
- □ 3) Inform test subject that the treadmill is starting and increase to 1.9 mph
- □ 4) Based on the COSMED clock, start actual data collection on the minute or half-minute
- □ 5) UTAF to record RPE and GCPS at 30 s
- □ 6) ABF to record kinetic/kinematic data for 30 strides immediately after UTAF
- □ 7) UTAF to record RPE, GCPS, discomfort, and thermal comfort within last 30 s of 3 min
- □ 8) Increase speed to 1.9 mph and repeat steps 6–8
- □ 9) Increase speed to 2.8 mph and repeat steps 6–8
- □ 10) Increase speed to 3.7 mph and repeat steps 6–8
- □ 11) Increase speed to 4.6 mph and repeat steps 6–8

□ 12) Increase speed to 5.6 mph and repeat steps 6–8
□ 13) Inform test subject that the treadmill is stopping and stop treadmill
□ 14) Help subject off treadmill
□ 15) Reduce offload to CG rig neutral and provide subject a seat
□ 16) Remove COSMED and download COSMED data

Trial 6 Preparation – Incline/Decline Treadmill

□ 1) Check and re-instrument subject with reflective markers, as needed
□ 2) Check NIRS
□ 3) Instrument subject with COSMED
□ 4) Offload subject to approximate target weight
□ 5) Subject stands on scale
□ 6) Adjust to target weight and record weight
□ 7) Assist subject onto center of treadmill
□ 8) Have subject stand still for approximately 10 s for static shot and weight capture
□ 9) Help subject off treadmill and adjust to -10%
□ 10) Check EMG system (ABF)

Trial 6 Steps – Incline/Decline Treadmill

□ 1) ABF measures treadmill orientation data at -10%
□ 2) Assist subject onto center of treadmill
□ 3) Ensure all teams are ready and subject's metabolic rate is being captured
□ 4) Inform test subject that the treadmill is starting and increase to 1.9 mph
□ 5) Based on the COSMED clock, start actual data collection on the minute or half-minute
□ 6) UTAF to record RPE and GCPS at 30 s
□ 7) ABF to record kinetic/kinematic data for 30 strides immediately after UTAF
□ 8) UTAF to record RPE, GCPS, discomfort, and thermal comfort within last 30 s of 3 min
□ 9) At 3 min, stop treadmill and help subject off treadmill
□ 10) Increase incline to 10% and repeat steps 1–9
□ 11) Increase incline to 20% and repeat steps 1–9
□ 12) Increase incline to 30% and repeat steps 1–9
□ 13) Reduce offload to CG rig neutral and provide subject a seat
□ 14) Remove COSMED and download COSMED data
□ 15) Return treadmill to 0%

Test Completion and Cleanup

□ 1) Collect and properly secure metabolic cart data for subject
□ 2) Collect and properly secure motion capture data for subject
□ 3) Collect and properly secure GRF data for subject
□ 4) Collect and properly secure POGO data for subject
□ 5) Clean met cart equipment, including sterilization of nose clip and mouthpiece
□ 6) Clean and power down all equipment, as necessary

G.2 Constellation Program Extravehicular Activity Systems Test 3 – Shirtsleeve Test Session 2 Checklist

Setup

□ 1) Ensure subject's clothes and shoes are ready
□ 2) Determine and record the randomized order to be used for the day's trials (EPSP)
□ 3) Prepare data sheets for test session (EPSP)
□ 4) Ensure medical monitor is identified (EPSP)
□ 5) Prepare and calibrate met cart (EXL)
□ 6) Prepare and calibrate motion capture system for subject (ABF)
□ 7) Prepare and calibrate GRF system (ABF)
□ 8) Prepare shirtsleeve rig for initial condition (EPSP)

Pretest Preparation

□ 1) Have subject read and sign informed consent form, with test conductor answering questions
□ 2) Ask subject to enter the changing area and record his/her naked BW
□ 3) Provide subject clothing and heart rate strap – explain donning order
□ 4) Instrument subject with EMG system and remaining clothes
□ 5) Ask subject to don the form-fitting suit for motion capture
□ 6) Describe the test procedure and familiarize the subject with the shirtsleeve rig

Pretest Briefing

□ 1) Hand out data/cover sheet with test order and objectives
□ 2) Review motion capture field
□ 3) Review hard hat area
□ 4) Medical monitor identified and contact information posted
□ 5) Test termination criteria reviewed and posted
□ 6) Emergency egress procedures reviewed and personnel identified

Trial 1 Preparation – Level Treadmill

□ 1) Offload CG rig to neutral
□ 2) Assist subject in getting into the shirtsleeve rig harness while attached to the Pogo
□ 3) Instrument subject with reflective markers for motion capture
□ 4) Instrument subject with NIRS
□ 5) Instrument subject with COSMED
□ 6) Offload subject to approximate target weight
□ 7) Subject stands on scale
□ 8) Adjust to target weight and record weight
□ 9) Assist subject onto center of treadmill
□ 10) Have subject stand still for approximately 10 s for static shot and weight capture
□ 11) Check EMG system (ABF)

Trial 1 Steps – Level Treadmill

□ 1) Ensure all teams are ready and subject's metabolic rate is being captured
□ 2) Inform test subject that the treadmill is starting and increase to 0.9 mph
□ 3) Based on COSMED clock, start actual data collection on the minute or half-minute
□ 4) UTAF to record RPE and GCPS at 30 s
□ 5) ABF to record kinetic/kinematic data for 30 strides immediately after UTAF
□ 6) UTAF to record RPE, GCPS, discomfort, and thermal comfort within last 30 s of 3 min
□ 7) Increase speed to 1.9 mph and repeat steps 4–6
□ 8) Increase speed to 2.8 mph and repeat steps 4–6
□ 9) Increase speed to 3.7 mph and repeat steps 4–6
□ 10) Increase speed to 4.6 mph and repeat steps 4–6
□ 11) Increase speed to 5.6 mph and repeat steps 4–6
□ 12) Inform test subject that the treadmill is stopping and stop treadmill
□ 13) Help subject off treadmill and provide subject a seat
□ 14) Reduce offload to CG rig neutral
□ 15) Remove COSMED and download data

Trial 2 Preparation – Incline/Decline Treadmill

□ 1) Check and re-instrument subject with reflective markers, as needed
□ 2) Check NIRS
□ 3) Instrument subject with COSMED
□ 4) Offload subject to approximate target weight
□ 5) Subject stands on scale
□ 6) Adjust to target weight and record weight
□ 7) Assist subject onto center of treadmill
□ 8) Have subject stand still for approximately 10 s for static shot and weight capture
□ 9) Help subject off treadmill and adjust to -10%
□ 10) Check EMG system (ABF)

Trial 2 Steps – Incline/Decline Treadmill

□ 1) ABF measures treadmill orientation data at -10%
□ 2) Assist subject onto center of treadmill
□ 3) Ensure all teams are ready and subject's metabolic rate is being captured
□ 4) Inform test subject that the treadmill is starting and increase to 1.9 mph
□ 5) Based on the COSMED clock, start actual data collection on the minute or half-minute
□ 6) UTAF to record RPE and GCPS at 30 s
□ 7) ABF to record kinetic/kinematic data for 30 strides immediately after UTAF
□ 8) UTAF to record RPE, GCPS, discomfort, and thermal comfort within last 30 s of 3 min
□ 9) At 3 min, stop treadmill and help subject off of treadmill
□ 10) Increase incline to 10% and repeat steps 1–9
□ 11) Increase incline to 20% and repeat steps 1–9

□ 12) Increase incline to 30% and repeat steps 1–9
□ 13) Reduce offload to CG rig neutral and provide subject a seat
□ 14) Remove COSMED and download COSMED data
□ 15) Return treadmill to 0%

Trial 3 Preparation – Level Treadmill

□ 1) Adjust CG rig to new CG setting, as described in test randomization order
□ 2) Check and re-instrument subject with reflective markers, as needed
□ 3) Check NIRS
□ 4) Instrument subject with COSMED
□ 5) Offload subject to approximate target weight
□ 6) Subject stands on scale
□ 7) Adjust to target weight and record weight
□ 8) Assist subject onto center of treadmill
□ 9) Have subject stand still for approximately 10 s for static shot and weight capture
□ 11) Check EMG system (ABF)

Trial 3 Steps – Level Treadmill

□ 1) Assist subject onto center of treadmill
□ 2) Ensure all teams are ready and subject's metabolic rate is being captured
□ 3) Inform test subject that the treadmill is starting and increase to 1.9 mph
□ 4) Based on the COSMED clock, start actual data collection on the minute or half-minute
□ 5) UTAF to record RPE and GCPS at 30 s
□ 6) ABF to record kinetic/kinematic data for 30 strides immediately after UTAF
□ 7) UTAF to record RPE, GCPS, discomfort, and thermal comfort within last 30 s of 3 min
□ 8) Increase speed to 1.9 mph and repeat steps 6–8
□ 9) Increase speed to 2.8 mph and repeat steps 6–8
□ 10) Increase speed to 3.7 mph and repeat steps 6–8
□ 11) Increase speed to 4.6 mph and repeat steps 6–8
□ 12) Increase speed to 5.6 mph and repeat steps 6–8
□ 13) Inform test subject that the treadmill is stopping and stop treadmill
□ 14) Help subject off of treadmill
□ 15) Reduce offload to CG rig neutral and provide subject a seat
□ 16) Remove COSMED and download COSMED data

Trial 4 Preparation – Incline/Decline Treadmill

□ 1) Check and re-instrument subject with reflective markers, as needed
□ 2) Check NIRS
□ 3) Instrument subject with COSMED
□ 4) Offload subject to approximate target weight
□ 5) Subject stands on scale

- □ 6) Adjust to target weight and record weight
- □ 7) Assist subject onto center of treadmill
- □ 8) Have subject stand still for approximately 10 s for static shot and weight capture
- □ 9) Help subject off treadmill and adjust to -10%
- □ 10) Check EMG system (ABF)

Trial 4 Steps – Incline/Decline Treadmill

- □ 1) ABF measures treadmill orientation data at -10%
- □ 2) Assist subject onto center of treadmill
- □ 3) Ensure all teams are ready and subject's metabolic rate is being captured
- □ 4) Inform test subject that the treadmill is starting and increase to 1.9 mph
- □ 5) Based on the COSMED clock, start actual data collection on the minute or half-minute
- □ 6) UTAF to record RPE and GCPS at 30 s
- □ 7) ABF to record kinetic/kinematic data for 30 strides immediately after UTAF
- □ 8) UTAF to record RPE, GCPS, discomfort, and thermal comfort within last 30 s of 3 min
- □ 9) At 3 min, stop treadmill and help subject off treadmill
- □ 10) Increase incline to 10% and repeat steps 1–9
- □ 11) Increase incline to 20% and repeat steps 1–9
- □ 12) Increase incline to 30% and repeat steps 1–9
- □ 13) Reduce offload to CG rig neutral and provide subject a seat
- □ 14) Remove COSMED and download COSMED data
- □ 15) Return treadmill to 0%

Test Completion and Cleanup

- □ 1) Collect and properly secure metabolic cart data for subject
- □ 2) Collect and properly secure motion capture data for subject
- □ 3) Collect and properly secure GRF data for subject
- □ 4) Collect and properly secure Pogo data for subject
- □ 5) Clean met cart equipment, including sterilization of nose clip and mouthpiece
- □ 6) Clean and power down all equipment, as necessary

G.3 Constellation Program Extravehicular Activity Systems Test 3 – Postural Stability and Exploration Task Checklist

Setup

□ 1) Ensure subject's clothes and shoes are ready
□ 2) Determine and record the randomized order to be used for the day's trials (EPSP)
□ 3) Prepare data sheets for test session (EPSP)
□ 4) Ensure medical monitor is identified (EPSP)
□ 5) Prepare and calibrate postural stability system (Neurosciences)
□ 6) Prepare and calibrate motion capture system for subject (ABF)
□ 7) Prepare and calibrate GRF system (ABF)
□ 8) Prepare shirtsleeve rig for initial condition (EPSP)
□ 9) Prepare exploration task hardware (EPSP)

Pretest Preparation

□ 1) Describe the test procedure and familiarize subject with the shirtsleeve rig
□ 2) Ask subject to enter the changing area
□ 3) Provide subject clothing and heart rate strap – explain donning order
□ 4) Weigh and record subject weight

Pretest Briefing

□ 1) Hand out data/cover sheet with test order and objectives
□ 2) Review motion capture field
□ 3) Review hard hat area
□ 4) Medical monitor identified and contact information posted
□ 5) Test termination criteria reviewed and posted
□ 6) Emergency egress procedures reviewed and personnel identified

Trial 1 Preparation – Postural Stability and Exploration Tasks

□ 1) Instrument subject with reflective markers for motion capture
□ 2) Assist subject onto posture platform with proper foot placement

Trial 1 Steps – Postural Stability and Exploration Tasks

□ 1) Inform test subject that the postural test is starting and complete 100-s SOT 1 baseline trial
□ 2) UTAF to record RPE and GCPS at trial completion
□ 3) Inform test subject that the postural test is starting and complete 100-s SOT 4 baseline trial
□ 4) UTAF to record RPE and GCPS at trial completion
□ 5) Inform test subject that the postural test is starting and complete 6×10-s TU/TD trials
□ 6) UTAF to record RPE and GCPS at trial completion
□ 7) Move subject to rock pickup area
□ 8) On the ABF's signal, subject completes 3× rock pick up task
□ 9) UTAF to record RPE and GCPS at trial completion
□ 10) Switch shovel platform in for rock pickup
□ 11) On the ABF's signal, subject completes 3× shoveling task

□ 12) UTAF to record RPE and GCPS at trial completion and then move subject to open area
□ 13) On the ABF's signal, subject completes 3× kneel-and-recover task
□ 14) UTAF to record RPE and GCPS at trial completion
□ 15) Subject rests

Trial 2–6 Preparation – Postural Stability and Exploration Tasks

□ 1) Help subject don adjustable CG rig
□ 2) Instrument subject with reflective markers for motion capture
□ 3) Adjust subject to correct offload
□ 4) Assist subject onto posture platform with proper foot placement

Trial 2 Steps – Postural Stability and Exploration Tasks

□ 1) Inform test subject that the postural test is starting and complete 100-s SOT 1 baseline trial
□ 2) UTAF to record RPE and GCPS at trial completion
□ 3) Inform test subject that the postural test is starting and complete 100-s SOT 4 baseline trial
□ 4) UTAF to record RPE and GCPS at trial completion
□ 5) Inform test subject that the postural test is starting and complete 6×10-s TU/TD trials
□ 6) UTAF to record RPE and GCPS at trial completion
□ 7) Move subject to rock pickup area
□ 8) On the ABF's signal, subject completes 3× rock pickup task
□ 9) UTAF to record RPE and GCPS at trial completion
□ 10) Switch shovel platform in for rock pickup
□ 11) On the ABF's signal, subject completes 3× shoveling task
□ 12) UTAF to record RPE and GCPS at trial completion and then move subject to open area
□ 13) On the ABF's signal, subject completes 3× kneel-and-recover task
□ 14) UTAF to record RPE and GCPS at trial completion
□ 15) Subject rests and offload is removed
□ 16) CG rig is adjusted and subject is assisted onto posture platform with proper foot placement
□ 17) Steps 1–16 are repeated until all configurations are tested

REPORT DOCUMENTATION PAGE	Form Approved OMB No. 0704-0188

Public reporting burden for this collection of information is estimated to average 1 hour per response, including the time for reviewing instructions, searching existing data sources, gathering and maintaining the data needed, and completing and reviewing the collection of information. Send comments regarding this burden estimate or any other aspect of this collection of information, including suggestions for reducing this burden, to Washington Headquarters Services, Directorate for Information Operations and Reports, 1215 Jefferson Davis Highway, Suite 1204, Arlington, VA 22202-4302, and to the Office of Management and Budget, Paperwork Reduction Project (0704-0188), Washington, DC 20503.

1. AGENCY USE ONLY *(Leave Blank)*	2. REPORT DATE	3. REPORT TYPE AND DATES COVERED
	July 2010	TM-2010-216127

4. TITLE AND SUBTITLE
Effects of Changing Center of Gravity on Shirtsleeve Human Performance in Reduced Gravity

5. FUNDING NUMBERS

6. AUTHOR(S)
Jason R. Norcross*, Kurt G. Clowers†, Tim Clark†, Matthew S. Cowley**, Lauren Harvill**, Stephen P. Chappell*, Leah C. Stroud††, Lena Desantis**, William H. Polaski***, Richard M. Morency†††, Jessica R. Vos†††, Michael L. Gernhardt†††

7. PERFORMING ORGANIZATION NAME(S) AND ADDRESS(ES)

Lyndon B. Johnson Space Center
Houston, Texas 77058

8. PERFORMING ORGANIZATION REPORT NUMBERS
S-1072

9. SPONSORING/MONITORING AGENCY NAME(S) AND ADDRESS(ES)

National Aeronautics and Space Administration
Washington, DC 20546-0001

10. SPONSORING/MONITORING AGENCY REPORT NUMBER
TM-2010-216127

11. SUPPLEMENTARY NOTES
*Wyle Integrated Science & Engineering Group, Houston; †MEI Technologies, Inc., Houston; **Lockheed Martin, Houston; ††Rice University, Houston; ***University of Houston, Houston; NASA Johnson Space Center, Houston

12a. DISTRIBUTION/AVAILABILITY STATEMENT

Unclassified/Unlimited
Available from the NASA Center for AeroSpace Information (CASI)
7115 Standard
Hanover, MD 21076-1320 Category: 54

12b. DISTRIBUTION CODE

13. ABSTRACT *(Maximum 200 words)*

This test evaluated the effects of varying center-of-gravity (CG) locations on unsuited (ie, shirtsleeve) human performance. Although different performance results were noted, data analysis indicates many of these performance differences may have resulted from system dynamics, hardware setup, and/or testing methodology. Three of the configurations unexpectedly had almost identical metabolic values. This lack of variability indicates that either there were no notable differences in human performance among them or other factors may have compromised our ability to effectively vary CG using an overhead suspension lunar gravity simulator. Metabolic and subjective results among CG conditions for ambulation were very similar, leading to the same conclusions. Although the Space Vehicle Mockup Facility's partial-gravity simulator "POGO" provided a reasonable ground-based analog for testing postural stability during reduced-gravity loading, mechanical couplings limit observations to a single plane of motion (sagittal), and its upward force vector may have a mechanical and/or physiologic (haptic) stabilizing influence on balance control that could reduce apparent instabilities. Postural stability appeared to be degraded during the simulated reduced-gravity loading conditions tested in this experiment. We therefore recommend that follow-up experiments be performed, probably during parabolic flight, to verify these findings without the potential mechanical-based confounding factors of the POGO system.

14. SUBJECT TERMS	15. NUMBER OF PAGES	16. PRICE CODE
center of gravity; human performance; metabolism; gravitational fields; lunar gravitation; environment simulation; stability tests; posture, human body	134	

17. SECURITY CLASSIFICATION OF REPORT	18. SECURITY CLASSIFICATION OF THIS PAGE	19. SECURITY CLASSIFICATION OF ABSTRACT	20. LIMITATION OF ABSTRACT
Unclassified	Unclassified	Unclassified	Unlimited